REDOX CHEMISTRY OF 8-OXOPURINE NUCLEOSIDES AND OLIGONUCLEOTIDES AND THEIR POTENTIAL ROLE AS PRIMORDIAL REDOX COENZYMES

by

Khiem Van Nguyen

A dissertation submitted to the faculty of
The University of Utah
in partial fulfillment of the requirements for the degree of

Doctor of Philosophy

Department of Chemistry

The University of Utah

December 2012

The University of Utah Graduate School

STATEMENT OF DISSERTATION APPROVAL

The dissertation of **Khiem Van Nguyen**

has been approved by the following supervisory committee members:

Cynthia J. Burrows	, Chair	**07/27/2012** Date Approved
Kenneth J. Woycechowsky	, Member	**07/27/2012** Date Approved
Jennifer M. Heemstra	, Member	**07/27/2012** Date Approved
Jack Simons	, Member	**07/27/2012** Date Approved
Kuberan Balagurunathan	, Member	**07/27/2012** Date Approved

and by **Henry S. White** , Chair of the Department of **Chemistry**

and by Charles A. Wight, Dean of The Graduate School.

ABSTRACT

The RNA world hypothesis about the origin of life enjoys wide acceptance. The fact that RNA is capable of catalyzing a wide range of chemical reactions supports a RNA-based primitive metabolism. Redox reactions are very important to metabolism, and at the present time, protein enzymes need the assistance of redox coenzymes such as flavin and nicotinamide to promote these processes. In our current work, we investigate the potential role of 8-oxopurine nucleosides including 8-oxo-7,8-dihydroguanosine (OG) and ribofuranosyl uric acid (RU) as primordial redox coenzymes that could help RNA in redox reactions to support primitive metabolism.

More specifically, we propose that 8-oxopurine nucleosides could function as primitive flavins in repairing cyclobutane pyrimidine dimers (CPD) that are photodamaged lesions of nucleic acids and are currently repaired by a flavin-dependent photolyase enzyme. In support of this, we incorporated OG proximal to a CPD in double-stranded oligonucleotides and investigated the repair of the CPD when OG is selectively photoexcited. Our results showed that OG is able to mediate the CPD repair following a flavin-type mechansim. The repair efficiency is dependent upon base pair context as well as the 5' *vs.* 3' orientation and the strand location. The photorepair activity of OG can operate on versatile environments including directly stacking on to a CPD in the same strand and base pairing with one or the other bases of these lesions.

In addition, CPD repair can also be mediated by OG-containing dinucleotides that are closer mimics of flavin adenine dinucleotide. This finding further supports the potential role of OG as a primitive flavin.

Although RU has a slightly lower redox potential than that of OG, it is not as effective as OG in repairing CPD in a nucleoside model. The shorter life time of the photoexcited state of RU than that of OG is probably responsible for this result. Furthermore, the oxidation of RU gives a complicated mixture of products and this might reduce the possibility of using RU as a multiple turnover catalyst. Nevertheless, these studies present an unusual example of one form of DNA damage, oxidation, functioning to repair another, photodimerization, and may provide insight into the origins of prebiotic redox processes.

For my family

TABLE OF CONTENTS

LIST OF FIGURES

LIST OF TABLES

LIST OF ABBREVIATIONS

A	adenine
Ac_3RU	2’,3’,5’-tri-O-acetyl-9-β-D-ribofuranosyl uric acid
Alla	allantoin
$Alla^{ox}$	oxidized allantoin
AMP	adenosine-5’-monophosphate
C	cytosine
CPD	cyclobutane pyrimidine dimers
dA	2’-deoxyadenosine
DMAP	4-dimethylaminopyridine
DMF	dimethylformamide
DNA	deoxyribonucleic acid
d(OA)	8-oxoguanine adenine dideoxyribonucleotide
EDTA	ethylenediamminetetraacetic acid
EET	excess electron transfer
ESI	electrospray ionization
ET	electron transfer
F	tetrahydrofuran analog
FAD	flavin adenine dinucleotide (oxidized form)
$FADH_2$	flavin adenine dinucleotide (reduced form)
Fapy-G	2,6-diamino-4-hydroxy-5-N-methylformamidopyrimidine

G	guanine
Gh	guanidinohydantoin
Gh^{ox}	oxidized guanidinohydantoin
GlcN6P	glucosamine-6-phosphate
GMP	guanosine-5'-monophosphate
HICA	5-carboxyl-5-hydroxyhydantoin ribonucleoside
HPLC	high performance liquid chromatography
IDA	initial Darwinian ancestors
LC	liquid chromatography
LUCA	last universal common ancestors
Lys	lysine
MB	methylene blue
MTHF	methylenetetrahydrofolate
MS	mass spectrometry
NAC	N-acetylcysteine
NAD^+	nicotinamide adenine dinucleotide (oxidized form)
NADH	nicotinamide adenine dinucleotide (reduced form)
NHE	normal hydrogen electrode
NMR	nuclear magnetic resonance
$^1O_2$	singlet oxygen
$O_2^{-\cdot}$	superoxide radical anion
OA	oxaluric acid
$OADH_2$	8-oxoguanine adenine diribonucleotide
OG	8-oxo-7,8-dihydroguanine
OGMP	8-oxoguanosine-5'-monophosphate

PCET	proton-coupled electron transfer
RB	rose bengal
Rf	riboflavin
RNA	ribonucleic acid
RNP	ribonucleoprotein
ROS	reactive oxygen species
RP-HPLC	reversed phase high performance liquid chromatography
RU	9-β-D-ribofuranosyl uric acid
Sp	spirodihydantoin
ssDNA	single-stranded DNA
TEAA	triethylammonium acetate
TFAA	trifluoroacetic anhydride
TFA	trifluoroacetic acid
THF	tetrahydrofuran
TOF	time of flight
T=T	[*cis,syn*] thymine dimer
U	uracil
UA	uric acid
UPLC	ultra performance liquid chromatography
U=U	[*cis,syn*] uracil dimer
UV	ultraviolet
UVB	ultraviolet B
UV-VIS	ultraviolet-visible

ACKNOWLEDGEMENTS

I am indebted to many people whose generous and valuable assistance makes this dissertation possible.

First, I would like to thank my advisor, Dr. Cynthia Burrows, for giving me the opportunity to work in the lab on such wonderful projects. My dissertation work could not be done without her continuous guidance, encouragement and support. I also greatly appreciate her understanding of life outside the lab and all of her valuable advice.

I am grateful to my committee members, Dr. Kenneth Woycechowsky, Dr. Jenifer Heemstra, Dr. Jack Simons and Dr. Kuberan Balagurunathan for supervising my PhD. I would especially like to thank Dr. Kuberan Balagurunathan for the five months I worked in his lab in which I gained a vast amount of research experience.

I would like to express my gratitude to the Burrows group members who created a very friendly and supportive research environment. In particular, I would like to thank Dr. Aaron Fleming for teaching me many experimental techniques that I regularly used in my research projects. I also thank Dr. James Muller for his scientific advice, especially on the uric acid oxidation project.

Furthermore, I would like to thank my friends, Linh Ha, Hoa Nguyen, Anh Vo, Huong Nguyen and Huy Vo for making my time in Utah enjoyable.

I would like to give my heartfelt thanks to my parents Khue Nguyen and Tam Nguyen, and my sister Phuong Nguyen. Their unconditional love, endless support and

sacrifice make this endeavor possible.

To my wife, Trang Pham, who is always with me during the good times and the bad, I am eternally grateful. My PhD journey and my life would be much less meaningful and joyful without her love and encouragement. Finally, to my little son, Khoi Nguyen, who has been a source of my inspiration and motivation, thank you.

CHAPTER 1

INTRODUCTION

Among various theories about the origin of life, the RNA world hypothesis enjoys considerable support from scientists (Figure 1.1). It proposes that ancient life evolved from the replication and catalysis of RNA oligomers (*1, 2*). This idea was first suggested by Crick (*3*), Orgel (*4*) and Woese (*5*); however it was underestimated until the discovery of the catalytic capability of RNA about 30 years ago (*6, 7*). There are now various lines of evidence that support the existence of a primordial RNA world. For example, the current ribosome machine to synthesize proteins actually works based on the catalytic chemistry of RNA and no amino acids are found within 18 Å of the active site (*8-10*). This probably suggests that RNA evolved first and protein was then synthesized by RNA catalysis. RNA likely predated DNA because deoxyribonucleotides are now biosynthesized from the corresponding ribonucleotides by reduction of the 2'-OH group (*11*). Furthermore, the RNA capability of catalyzing a wide range of chemical reactions supports the existence of a primitive RNA-based metabolism (*12-15*). Many studies have advanced our understanding of the primordial RNA world, such as the prebiotic synthesis of activated nucleotides (*16*), the nonenzymatic oligomerization and self-replication of RNA (*17*), and the confinement of RNA into protocells with primitive membranes (*18*).

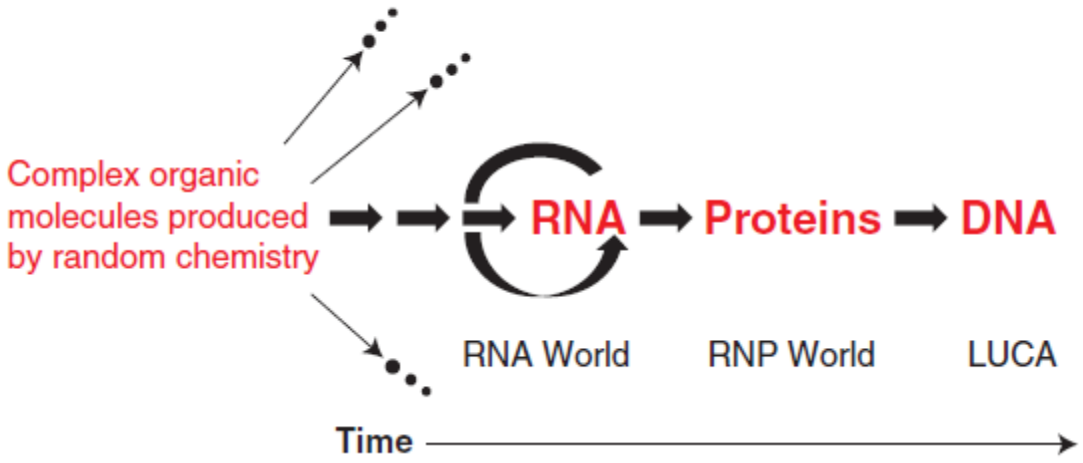

Figure 1.1[*]. An RNA world model. After a long selection process, RNA with self-replication properties has been preserved in its modern descendants. Functional proteins have come only after RNA was available to catalyze peptide ligation or amino acid polymerization. DNA took over the role of the genome about one billion years ago. LUCA (Last Universal Common Ancestors) already had a DNA genome and carried out biocatalysis using protein, RNP enzymes and ribozymes.

*Reproduced with permission from *Cold. Spring. Harb. Perspect. Biol. doi: 10.1101/cshperspect.a006742*

Ribozyme cofactors

In RNA-based life, RNA catalysis was obviously crucial for maintaining both a primitive metabolism and the self-replication of RNA (*12*). Because the chemical transformations made available by the canonical bases are quite limited, RNA may have needed the assistance of functional cofactors to expand the diversity of its catalysis (*13, 19-22*). An example of a natural ribozyme utilizing a small organic cofactor for catalysis is the *glmS* ribozyme that uses glucosamine-6-phosphate (GlcN6P) to facilitate its self-cleavage (*23, 24*). There are also several cofactor-dependent ribozymes that have been isolated from an RNA pool by *in vitro* evolution. For examples, Tsukiji and coworkers found a NAD^+/NADH-dependent ribozyme that catalyzes the reduction of aldehyde or the oxidation of alcohol (*25, 26*). The Breaker lab discovered a DNAzyme employing L-histidine as a cofactor to promote RNA cleaveage (*27*).

Interestingly, present-day proteins employ nucleotide cofactors such as flavins, nicotinamide, pterins, etc. (Figure 1.2) to catalyze processes outside the chemistry of the canonical amino acids. Because of the presence of "RNA parts" in these cofactors, they were referred as "the fossils of the RNA world" (*28*) and likely evolved from four ribonucleotide bases A, U, G, C or co-evolved as separate nucleotide components. There is also an argument that nucleotides are more suitable cofactors for ribozymes than amino acids in the RNA world (*13*). Recently, Yarus proposed AMP-containing dinucleotide cofactors might be descendants of the Initial Darwinian Ancestors (IDA) (*29*). Therefore, it is likely that primordial ribozymes may have adopted nucleotide cofactors whose structures should be simple enough to be available via prebiotic processes for expanding their catalytic scope to support the primitive metabolism.

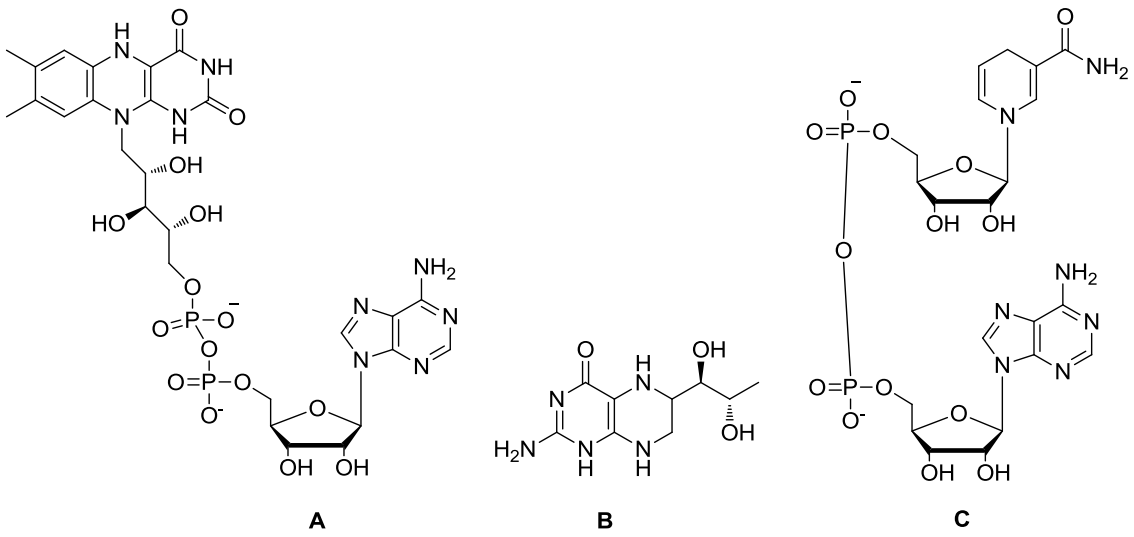

Figure 1.2. Structures of nucleotide coenzymes. (A) Flavin adenine dinucleotide, $FADH_2$. (B) Tetrahydrobiopterin. (C) Nicotinamide adenine dinucleotide, NADH.

8-Oxopurine nucleosides as potential primitive redox cofactors

Early life would require redox reactions to support metabolism; however, our understanding of redox ribozymes is still limited. There is only one example of a ribozyme catalyzing alcohol oxidation or aldehyde reduction in the presence of NAD^+/NADH (*25, 26*), but there are no examples of redox-active ribozymes utilizing RNA oligomers alone. Among the four canonical bases, G is the most redox-active base; however its redox potential (E^0_7 = 1.3V *vs.* NHE) (*30*) is still too high to be effective in catalysis. Instead, nature currently uses G as the starting point to biosynthesize current redox cofactors flavin and pterin with the help of several protein-based enzymes (*31*). Since this process is obviously optimized over million years of evolution, we asked what simple transformations would convert G into a more redox-active heterocycle capable of redox processes in the primitive RNA world?

The simple hydrolysis products of G arising from either N^2 deamination (xanthine) or hydrolytic opening of the imidazole ring (Fapy-G) show only modestly lower reduction potentials, around 1.1V (*32, 33*) (Figure 1.3). In contrast, 8-oxo-7,8-dihydroguanine (OG), the common oxidative damage product of G in DNA and RNA, has a greatly reduced redox potential of 0.74 V, representing a nearly 600 mV reduction in E^o at pH 7; at pH 9, the value is even lower, 0.5 V (*34*). OG is readily formed from G via ionizing radiation or Fenton-like reactions that produce $HO^{\bullet}$, conditions that are plausible on early Earth (*35*). In fact, given the likely complexity of primordial synthesis of G (*36*), OG may have been more plentiful than G. One more deamination step of OG leads to the formation of the even more redox-active molecule uric acid nucleoside (RU) (*37*). Therefore, we hypothesize that 8-oxopurine nucleosides including OG and RU may

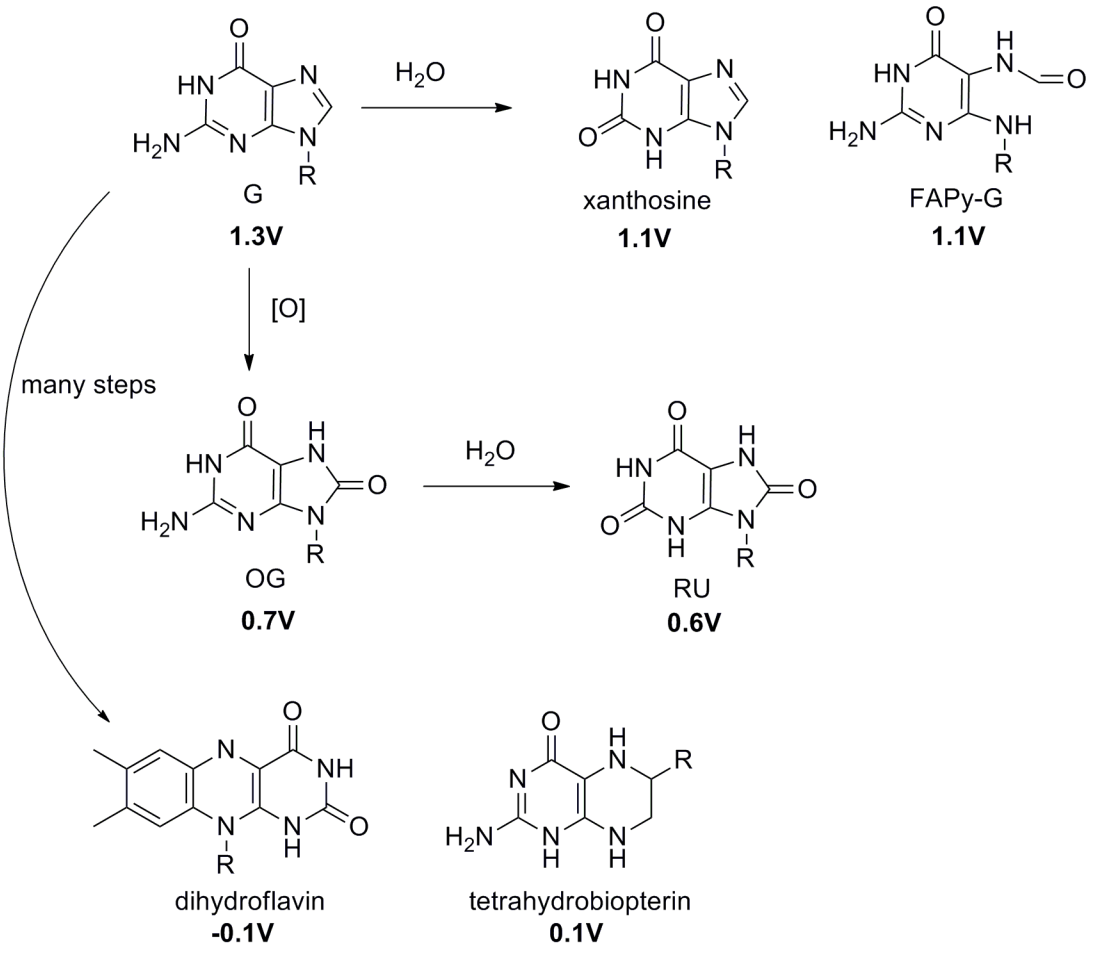

Figure 1.3. Simple chemical transformations of guanosine that yield redox-active ribonucleotides. Guanine can undergo hydrolysis to xanthosine or FAPy-G which both have somewhat lower redox potentials than G. Oxidation to OG leads to a dramatic lowering of the redox potential and further deamination to RU further lowers the potential. For present-day coenzymes (pterins and flavins), several enzyme-catalyzed biosynthetic steps are required that presumably were optimized over millions of years.

have functioned like primitive flavins that assist primordial ribozymes in redox processes.

Our hypothesis is further supported by the similarity in redox chemistry between 8-oxopurine nucleosides and flavins (Figure 1.4). The two-electron oxidation of OG gives an unstable quinonoid intermediate (OG^{ox}) that subsequently adds nucleophiles at C5 and rearranges to a spirodihydantoin (Sp) or guanidinodihydantoin (Gh) depending on the reaction conditions (*38-45*). An analogous quinonoid intermediate RU^{ox} is also proposed as an intermediate in the oxidation of uric acid nucleoside (RU), however it undergoes different rearrangement pathways compared to OG^{ox} (*46-48*). Both redox couples OG^{ox}/OG and RU^{ox}/RU are structurally similar to that of FAD/$FADH_2$ (Figure 1.4). In addition, a side-product of oxidized flavin chemistry is also a spirohydantoin heterocycle that is formed from the rearrangement of the nucleophilic adduct at C4a of flavin (equivalent to C5 of OG^{ox} and RU^{ox}) under strongly basic conditions (Figure 1.5). It is necessary to note that the extensive decomposition of the oxidized forms of 8-oxopurines to form hydantoin products makes them not as ideal redox catalysts as flavins whose oxidized and reduced forms can be readily interconverted. The similarity in redox chemistry between 8-oxopurines and flavins is also shown in the formation of analogous hydroperoxides though under different conditions (Figure 1.5). Flavin hydroperoxides are formed upon exposure of reduced flavins to dioxygen and have been extensively characterized (*38, 49, 50*). The analogous hydroperoxides of OG and RU resulted from reactions of these purines with singlet oxygen or superoxide (*43, 48*). While flavin hydroperoxides were known to be reactive intermediates in flavin- catalyzed oxidation reactions (*51*), only decomposition or rearrangement was observed for hydroperoxides

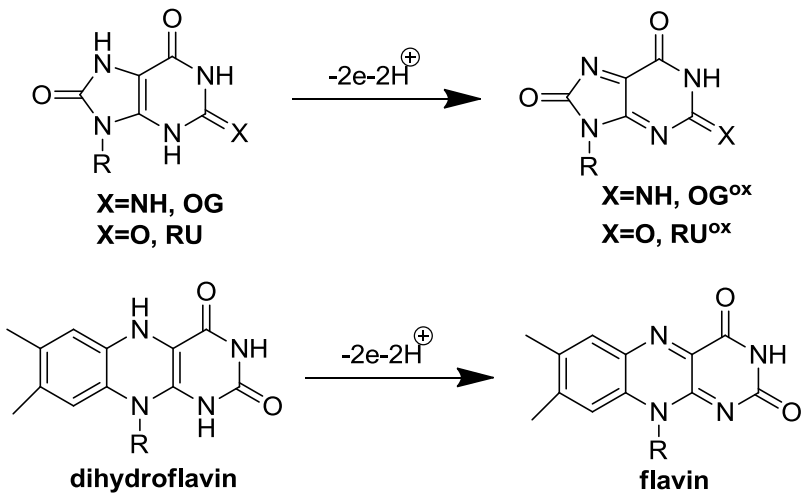

Figure 1.4. Structural similarity of OG, RU and dihydroflavin and their oxidized forms.

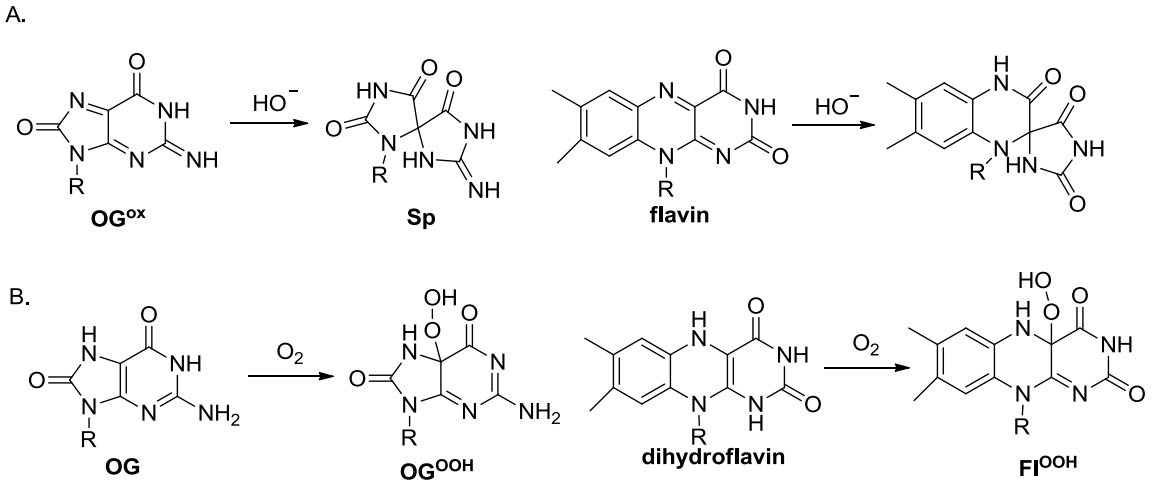

Figure 1.5. (A). Spirocyclic reaarangements of oxidized OG and flavins.
(B). Hydroperoxide formation from dioxygenation of OG or dihydroflavin.

of OG and RU (*48*). Therefore, the potential role of the latter as active specie in oxidation processes catalyzed by OG or RU may need further investigation.

8-Oxopurine nucleosides as substitutes for the flavoenzyme in repairing cyclobutane pyrimidine dimer

To support our hypothesis on the role of 8-oxopurine nucleosides as primitive flavins, we have to find evidence that they can function as flavins in catalyzing electron transfer processes. After extensive searches of flavin-catalyzed reactions, we decided to investigate the possibility of 8-oxopurine nucleosides to promote the repair of cyclobutane pyrimidine dimers (CPD) that are photodamage lesions generated from two adjacent pyrimidine bases upon exposing DNA or RNA to UV light (260-300nm) (Figure 1.6). We chose this process because of several reasons that are outlined below.

First, at the present time, CPD are repaired by flavin-dependent photolyase enzymes in plants and microorganisms (*52, 53*) and the repair mechanism has been extensively studied (Figure 1.6). The flavin cofactor plays a role as an electron donor after being photoexcited or receiving energy from another excited chromophore such as methylenetetrahydrofolate (MTHF) (*52, 53*) . CPD accepts one electron from a flavin to form a highly reactive radical anion that leads to the rapid cleavage of σ bonds and then electron transfer back to the flavin radical (*54-56*). The process regenerates an undamaged TT-containing DNA strand as well as the original flavin cofactor. The role of the protein is as a scaffold to bind CPD in DNA in the correct orientation with respect to the catalytic flavin (*57*). Flavins can also mediate the CPD repair outside the protein environment if they're "forced" to position proximally to CPD in conjugated systems

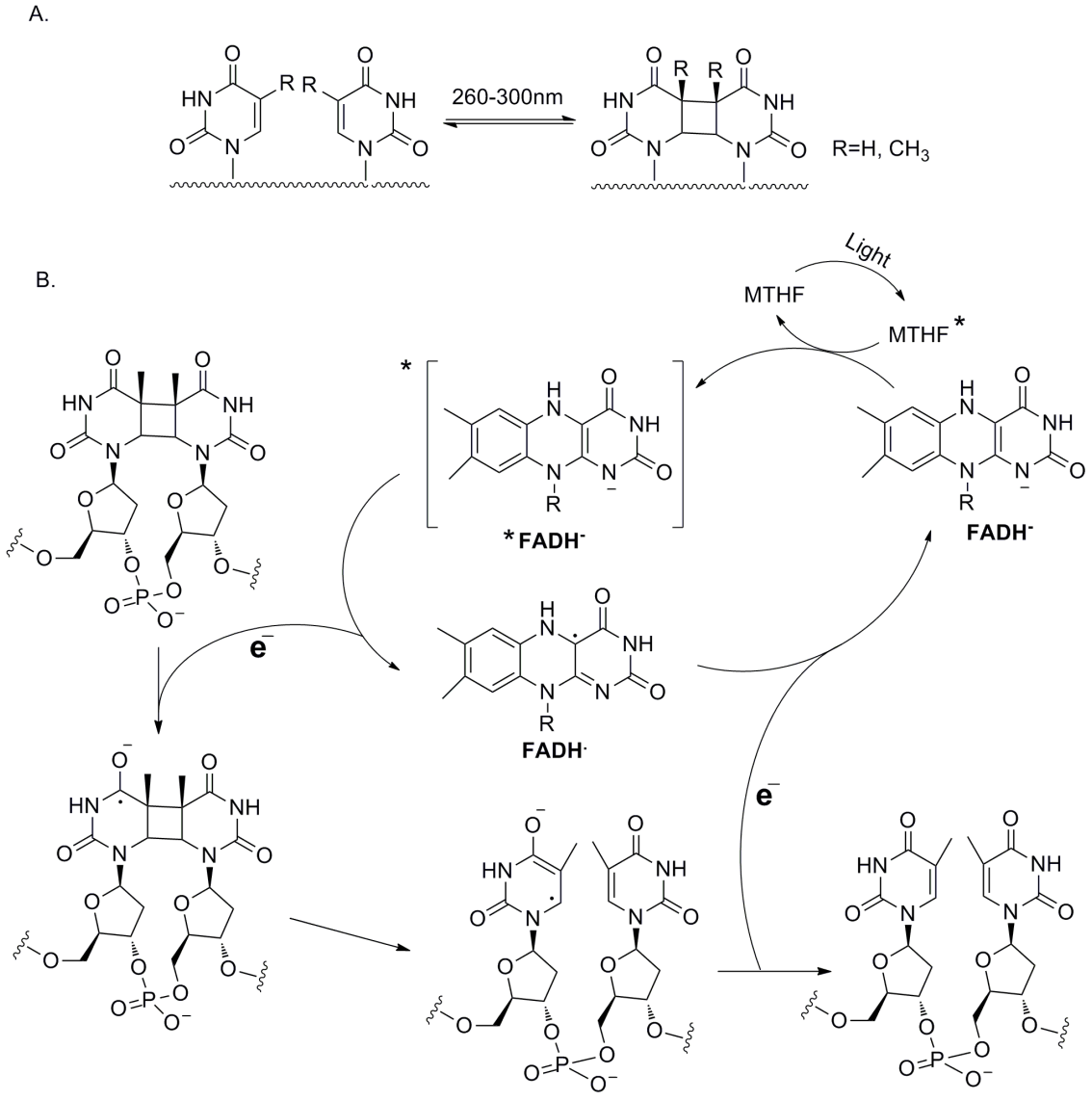

Figure 1.6. (A). Formation of cyclobutane pyrimidine dimers (CPD). (B). Mechanism of photolyase-mediated CPD repair. The excited state of $FADH^-$ transfers an electron to the CPD; after bond cleavage, back electron transfer restores the $FADH^-$ cofactor (Adapted from ref. 52).

(*58-61*) or DNA duplexes (*60, 62-64*), however with lower efficiency.

Secondly, we recognized that 8-oxopurine nucleosides have a longer wavelength absorption band that extends beyond 300nm. This makes it possible to excite the OG or RU bases in the presence of other DNA or RNA bases that normally have no absorbance above 290 nm (Figure 1.7). Because the ground states of OG and RU have a low redox potential, their photoexcited states are likely good electron donors. Therefore, the repair of CPD by photoexcited OG and RU is plausible and potentially follows the same mechanism as the flavin-catalyzed process discussed above (Figure 1.7).

Finally, the repair of CPD might be prebiotically relevant. Solar irradiation on the early Earth must have been powerful source of energy for chemical evolution; however it also causes damage to nucleic acids and potentially led to the formation of CPD (*65-67*). Indeed, studies have been done to understand whether nucleic acid enzymes can repair CPD since there were probably no protein-based enzymes in the primitive world. For example, Sen and coworkers discovered that a DNA enzyme containing a G quartet is able to photorepair a T=T lesion in a complementary strand (*68-70*) (Figure 1.8). This result is inspiring; however the use of the G quartet as a chromophore does not advance our understanding of the emergence of flavin nucleotides. In other work, Rokita and coworkers found that the yield of thymine dimer formation is significantly lower when a G is present at the 5' side of a TT in DNA duplex, and they suggested a self-repair mechanism of inhibiting thymine dimer formation (*71*). However, a recent study showed that the low yield of thymine dimer formation caused by an adjacent G relates to "inhibition" rather than "repair" (*72*). These studies suggest the possibility of repairing CPD by nucleic acid enzymes in the early earth; however, we think these enzymes may

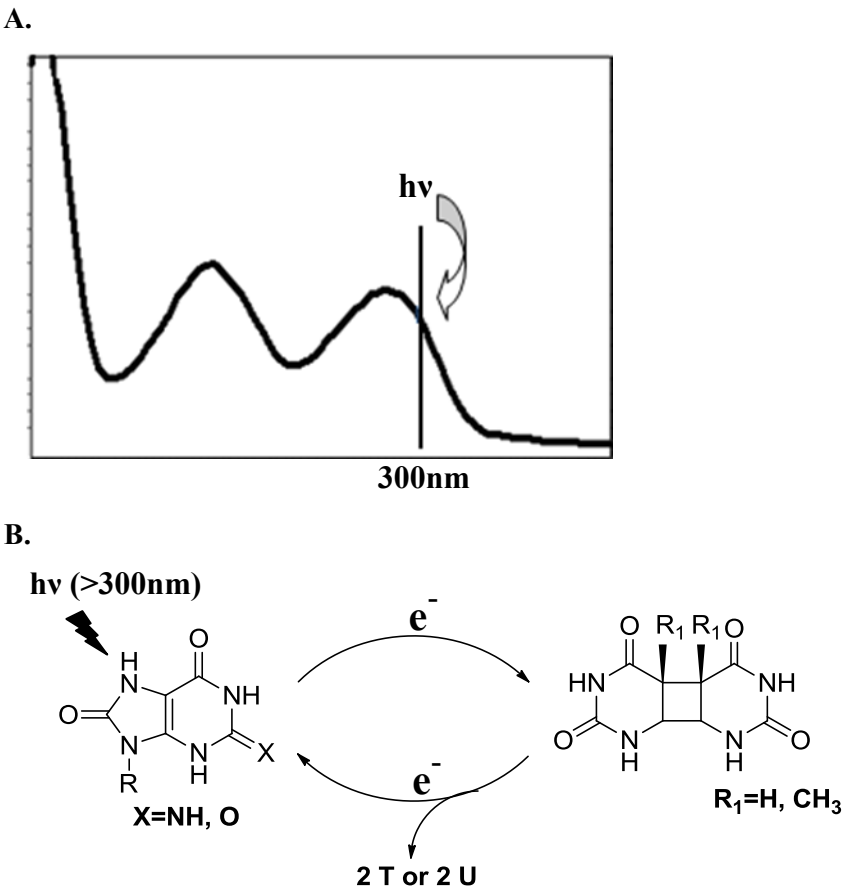

Figure 1.7. (A) UV spectrum of OG. Irradiation at wavelengths > 300 nm photoexcites OG, but not normal bases. (RU has a quite similar UV spectrum to OG). (B) 8-Oxopurine nucleosides are proposed to function as flavins in reparing CPD.

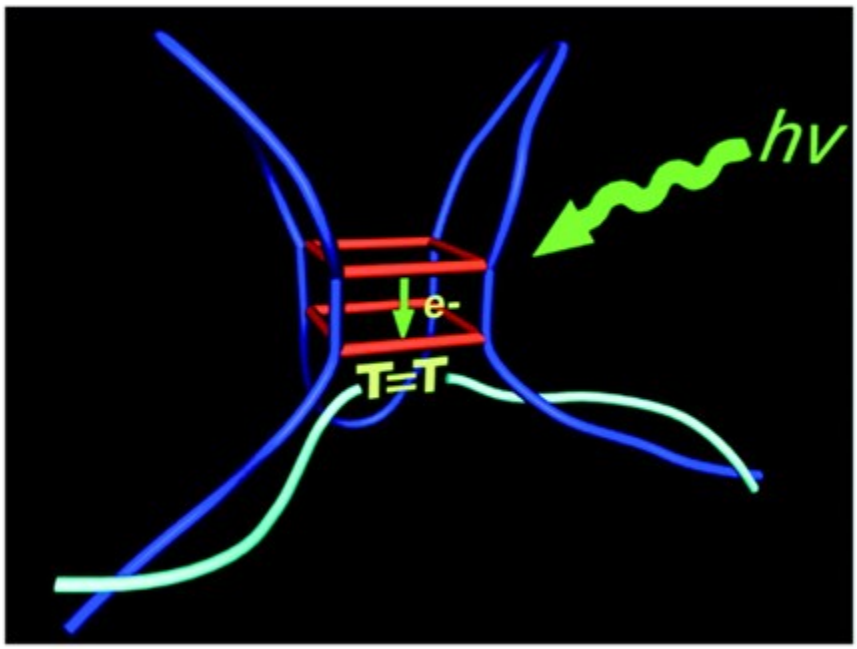

Figure 1.8. Repair of thymine dimer by a DNA enzyme containing a G quartet (Reproduced with permission from ref. 70).

need assistance of primitive cofactors rather than using a G quartet chromophore or unmodified G.

Conclusion

The RNA world hypothesis proposed that RNA acts like both genetic and catalytic materials, and is now widely accepted. My dissertation work is directed toward understanding the potential origin of redox catalysis in the RNA world. We proposed that 8-oxopurine nucleosides (OG and RU) that are simple oxidation products of G may have served as prebiotic versions of redox coenzymes to assist RNA in electron transfer processes. More specifically, we hypothesize that they can function as primitive flavins to repair cyclobutane pyrimidine dimers that are photodamage lesions of nucleic acids caused by UV irradiation. Toward this hypothesis, we first investigate the potential of OG in repairing CPD in various contexts of double-stranded oligonucleotides (Chapter 2 and Chapter 3). Repair of CPD in DNA and RNA by a closer mimic of flavin 5'-5' dinucleotide OA, under plausible prebiotic conditions is studied in Chapter 4. The comparison of CPD repair efficiency between OG and RU is reported in Chapter 5. In the final chapter, we investigate oxidation products of RU by various oxidants to further understand the redox chemistry of this nucleoside.

References

1. Gilbert, W. (1986) Origin of life: The RNA world, *Nature 319*, 618.

2. Cech, T. R. (2011) *RNA worlds: From Life's Origin to Diversity in Gene Regulation*, Cold Spring Harbor Press, New York.

3. Crick, F. H. C. (1968) The origin of the genetic code, *J. Mol. Biol. 38*, 367-379.

4. Orgel, L. E. (1968) Evolution of the genetic apparatus, *J. Mol. Biol. 38*, 381-393.

5. C, W. (1967) *The genetic code*, Harper and Row, New York.

6. Guerrier-Takada, C., Gardiner, K., Marsh, T., Pace, N., and Altman, S. (1983) The RNA moiety of ribonuclease P is the catalytic subunit of the enzyme, *Cell. 35*, 849-857.

7. Kruger, K., Grabowski, P. J., Zaug, A. J., Sands, J., Gottschling, D. E., and Cech, T. R. (1982) Self-splicing RNA: Autoexcision and autocyclization of the ribosomal RNA intervening sequence of tetrahymena, *Cell. 31*, 147-157.

8. Ban, N., Nissen, P., Hansen, J., Moore, P. B., and Steitz, T. A. (2000) The complete atomic structure of the large ribosomal subunit at 2.4 Å resolution, *Science. 289*, 905-920.

9. Wimberly, B. T., Brodersen, D. E., Clemons, W. M., Morgan-Warren, R. J., Carter, A. P., Vonrhein, C., Hartsch, T., and Ramakrishnan, V. (2000) Structure of the 30S ribosomal subunit, *Nature. 407*, 327-339.

10. Yusupov, M. M., Yusupova, G. Z., Baucom, A., Lieberman, K., Earnest, T. N., Cate, J. H. D., and Noller, H. F. (2001) Crystal structure of the ribosome at 5.5 Å resolution, *Science. 292*, 883-896.

11. Cech, T. R. (2011) The RNA worlds in context, *Cold Spring Harbor Perspectives in Biology*, *3,*a006742.

12. Bartel, D. P., and Unrau, P. J. (1999) Constructing an RNA world., *Trends in Cell Biology 9*, M9-M13.

13. Chen, X., Li, N., and Ellington, A. D. (2007) Ribozyme catalysis of metabolism in the RNA world, *Chem. Biodiversity. 4*, 633-655.

14. Joyce, G. F. (2002) The antiquity of RNA-based evolution, *Nature 418*, 214-221.

15. Benner, S. A., Ellington, A. D., and Tauer, A. (1989) Modern metabolism as a palimpsest of the RNA world, *Proc. Natl. Acad. Sci. U S A. 86*, 7054-7058.

16. Powner, M. W., Gerland, B., and Sutherland, J. D. (2009) Synthesis of activated pyrimidine ribonucleotides in prebiotically plausible conditions, *Nature. 459*, 239-242.

17. Robertson, M. P., and Joyce, G. F. (2010) The origins of the RNA world, *Cold Spring Harbor Perspectives in Biology*., a003608.

18. Schrum, J. P., Zhu, T. F., and Szostak, J. W. (2010) The origins of cellular life, *Cold Spring Harbor Perspectives in Biology*., a002212

19. Cochrane, J. C., and Strobel, S. A. (2008) Riboswitch effectors as protein enzyme cofactors, *RNA 14*, 993-1002.

20. Jadhav, V. R., and Yarus, M. (2002) Coenzymes as coribozymes, *Biochimie.84*, 877-888.

21. Breaker, R. R. (2010) Riboswitches and the RNA world, *Cold Spring Harbor Perspectives in Biology*., a003566.

22. Fedor, M. J., and Williamson, J. R. (2005) The catalytic diversity of RNAs, *Nat. Rev. Mol.Cell. Biol. 6*, 399-412.

23. Klein, D. J., and Ferré-D'Amaré, A. R. (2006) Structural basis of glmS ribozyme activation by glucosamine-6-phosphate, *Science 313*, 1752-1756.

24. Winkler, W. C., Nahvi, A., Roth, A., Collins, J. A., and Breaker, R. R. (2004) Control of gene expression by a natural metabolite-responsive ribozyme, *Nature 428*, 281-286.

25. Tsukiji, S., Pattnaik, S. B., and Sugar, H. (2003) An alcohol dehydrogenase ribozyme, *Nat. Struct. Biol. 10*, 713-717.

26. Tsukiji, S., Pattnaik, S. B., and Suga, H. (2004) Reduction of an aldehyde by a NADH/Zn2+-dependent redox active ribozyme, *J. Am. Chem. Soc. 126*, 5044-5045.

27. Roth, A., and Breaker, R. R. (1998) An amino acid as a cofactor for a catalytic polynucleotide, *Proc. Natl. Acad. Sci. 95*, 6027-6031.

28. White, H. B. (1976) Coenzymes as fossils of an earlier metabolic state, *J. Mol. Evol. 7*, 101-104.

29. Yarus, M. (2011) Getting past the RNA world: The initial Darwinian ancestor, *Cold Spring Harb Perspect Biol 3:a003590*.

30. Steenken, S., and Jovanovic, S. V. (1997) How easily oxidizable is DNA? One-electron reduction potentials of adenosine and guanosine radicals in aqueous solution, *J. Am. Chem. Soc. 119*, 617-618.

31. Webb, M. E., Marquet, A., Mendel, R. R., Rebeille, F., and Smith, A. G. (2007) Elucidating biosynthetic pathways for vitamins and cofactors, *Nat. Prod. Rep. 24*, 988-1008.

32. Xue, L., and Greenberg, M. M. (2007) Facile quantification of lesions derived from 2‘-deoxyguanosine in DNA, *J. Am. Chem. Soc. 129*, 7010-7011.

33. Jo, S., Jeong, H., Bae, S. R., and Jeon, S. (2008) Determination of xanthine in the presence of ascorbic and uric acids on the glassy carbon electrode modified with poly(sulfosalicylic acid) nanorods, *Bull. Korean Chem. Soc. 29*, 2407-2412.

34. Steenken, S., Jovanovic, S. V., Bietti, M., and Bernhard, K. (2000) The trap depth (in DNA) of 8-Oxo-7,8-dihydro-2'-deoxyguanosine as derived from electron-transfer equilibria in aqueous solution, *J. Am. Chem. Soc. 122*, 2373-2374.

35. Liang, M.-C., Hartman, H., Kopp, R. E., Kirschvink, J. L., and Yung, Y. L. (2006) Production of hydrogen peroxide in the atmosphere of a Snowball Earth and the origin of oxygenic photosynthesis, *Proc. Natl. Acad. Sci. 103*, 18896-18899.

36. Powner, M. W., Sutherland, J. D., and Szostak, J. W. (2010) Chemoselective multicomponent one-pot assembly of purine precursors in water, *J. Am. Chem. Soc. 132*, 16677-16688.

37. Simic, M. G., and Jovanovic, S. V. (1989) Antioxidation mechanisms of uric acid, *J. Am. Chem. Soc. 111*, 5778-5782.

38. Ye, Y., Muller, J. G., Luo, W., Mayne, C. L., Shallop, A. J., Jones, R. A., and Burrows, C. J. (2003) Formation of 13C-, 15N-, and 18O-Labeled guanidinohydantoin from guanosine oxidation with singlet oxygen. Implications for structure and mechanism, *J. Am. Chem. Soc. 125*, 13926-13927.

39. Luo, W., Muller, J. G., and Burrows, C. J. (2001) The pH-Dependent Role of Superoxide in Riboflavin-Catalyzed Photooxidation of 8-Oxo-7,8-dihydroguanosine, *Org. Lett. 3*, 2801-2804.

40. Luo, W., Muller, J. G., Rachlin, E. M., and Burrows, C. J. (2001) Characterization of hydantoin products from one-electron oxidation of 8-Oxo-7,8-dihydroguanosine in a nucleoside model, *Chem. Res. Toxicol. 14*, 927-938.

41. Henderson, P. T., Delaney, J. C., Muller, J. G., Neeley, W. L., Tannenbaum, S. R., Burrows, C. J., and Essigmann, J. M. (2003) The hydantoin lesions formed

from oxidation of 7,8-dihydro-8-oxoguanine are potent sources of replication errors *in vivo*, *Biochemistry 42*, 9257-9262.

42. Munk, B. H., Burrows, C. J., and Schlegel, H. B. (2008) An exploration of mechanisms for the transformation of 8-Oxoguanine to guanidinohydantoin and spiroiminodihydantoin by density functional theory, *J. Am. Chem. Soc. 130*, 5245-5256.

43. Misiaszek, R., Uvaydov, Y., Crean, C., Geacintov, N. E., and Shafirovich, V. (2005) Combination reactions of superoxide with 8-Oxo-7,8-dihydroguanine radicals in DNA, *J. Biol. Chem. 280*, 6293-6300.

44. Yun, B. H., Lee, Y. A., Kim, S. K., Kuzmin, V., Kolbanovskiy, A., Dedon, P. C., Geacintov, N. E., and Shafirovich, V. (2007) Photosensitized oxidative DNA damage: From hole injection to chemical product formation and strand cleavage, *J. Am. Chem. Soc. 129*, 9321-9332.

45. Crean, C., Lee, Y. A., Yun, B. H., Geacintov, N. E., and Shafirovich, V. (2008) Oxidation of guanine by carbonate radicals derived from photolysis of carbonatotetramminecobalt (III) complexes and the pH dependence of intrastrand DNA cross-links mediated by guanine radical reactions, *ChemBioChem 9*, 1985-1991.

46. Goyal, R., Brajter-Toth, A., Besca, J., and Dryhurst, G. (1983) The electrochemical and perodidase-catalyzed redox chemistry of 9-β-D-ribofuranosyl uric acid, *J. Electroanal. Chem. 144*, 163-190.

47. Tyagi, S. K., and Dryhurst, G. (1987) Electrochemical oxidation of 9-β-D-ribofuranosyluric acid in basic solution, *J. Electroanal. Chem. 223*, 119-141.

48. Nguyen, K. V., Muller, J. G., and Burrows, C. J. (2011) Oxidation of 9-β-D-ribofuranosyl uric acid by one-electron oxidants versus singlet oxygen and its implications for the oxidation of 8-oxo-7,8-dihydroguanosine, *Tet. Lett. 52*, 2176-2180.

49. Kemal, C., and Bruice, T. C. (1976) Simple synthesis of a 4a-hydroperoxy adduct of a 1,5-dihydroflavine: preliminary studies of a model for bacterial luciferase, *Proc. Natl. Acad. Sci. 73*, 995-999.

50. Bruice, T. C. (1980) Mechanisms of flavin catalysis, *Acc. Chem. Res. 13*, 256-262.

51. Massey, V. (1994) Activation of molecular oxygen by flavins and flavoproteins, *J. Biol. Chem. 269*, 22459-22462.

52. Sancar, A. (2003) Structure and function of DNA photolyase and cryptochrome blue-light photoreceptors, *Chem. Rev. 103*, 2203-2238.

53. Müller, M., and Carell, T. (2009) Structural biology of DNA photolyases and cryptochromes, *Curr. Opin. Struct. Biol. 19*, 277-285.

54. Kao, Y.-T., Saxena, C., Wang, L., Sancar, A., and Zhong, D. (2005) Direct observation of thymine dimer repair in DNA by photolyase, *Proc. Natl. Acad. Sci. 102*, 16128-16132.

55. Liu, Z., Tan, C., Guo, X., Kao, Y.-T., Li, J., Wang, L., Sancar, A., and Zhong, D. (2011) Dynamics and mechanism of cyclobutane pyrimidine dimer repair by DNA photolyase, *Proc. Natl. Acad. Sci. 108*, 14831-14836.

56. Thiagarajan, V., Byrdin, M., Eker, A. P., Muller, P., and Brettel, K. (2011) Kinetics of cyclobutane thymine dimer splitting by DNA photolyase directly monitored in the UV, *Proc. Natl. Acad. Sci. 108*, 9402-9407.

57. Mees, A., Klar, T., Gnau, P., Hennecke, U., Eker, A. P. M., Carell, T., and Essen, L.-O. (2004) Crystal structure of a photolyase bound to a CPD-like DNA lesion after in situ repair, *Science 306*, 1789-1793.

58. Butenandt, J., Epple, R., Wallenborn, E.-U., Eker, A. P. M., Gramlich, V., and Carell, T. (2000) A comparative repair study of thymine- and uracil-photodimers with model compounds and a photolyase repair enzyme, *Chem. Eur. J. 6*, 62-72.

59. Heil, K., Pearson, D., and Carell, T. (2011) Chemical investigation of light induced DNA bipyrimidine damage and repair, *Chem. Soc. Rev. 40*, 4271-4278.

60. Manetto, A., Breeger, S., Chatgilialoglu, C., and Carell, T. (2006) Complex sequence dependence by excess-electron transfer through DNA with different strength electron acceptors, *Angew. Chem. Int. Ed. 45*, 318-321.

61. Kao, Y.-T., Song, Q.-H., Saxena, C., Wang, L., and Zhong, D. Dynamics and mechanism of DNA repair in a biomimetic system: Flavin-thymine dimer adduct, *J. Am. Chem. Soc. 134*, 1501-1503.

62. Schwögler, A., Burgdorf, L., and Carell, T. (2000) Self-Repairing DNA based on a reductive electron transfer through the base stack, *Angew. Chem. Int. Ed. 39*, 3918-3920.

63. Fazio, D., Trindler, C., Heil, K., Chatgilialoglu, C., and Carell, T. (2011) Investigation of excess-electron transfer in DNA double-duplex systems allows estimation of absolute excess-electron transfer and CPD cleavage rates, *Chem. Eur. J. 17*, 206-212.

64. Breeger, S., Hennecke, U., and Carell, T. (2004) Excess electron-transfer-based repair of a cis-syn thymine dimer in DNA is not sequence dependent, *J. Am. Chem. Soc. 126*, 1302-1303.

65. Lazcano, A., Guerrero, R., Margulis, L., and Oró, J. (1988) The evolutionary transition from RNA to DNA in early cells, *J. Mol.Evol. 27*, 283-290.

66. Cockell, C. S., and Raven, J. A. (2007) Ozone and life on the Archaean Earth, *Phil. Trans. R. Soc. A. 365*, 1889-1901.

67. Cockell, C. S., and Horneck, G. (2001) The history of the UV radiation climate of the Earth—Theoretical and space-based observations, *Photochem. Photobiol. 73*, 447-451.

68. Chinnapen, D. J. F., and Sen, D. (2007) Towards elucidation of the mechanism of UV1C, a deoxyribozyme with photolyase activity, *J. Mol. Biol. 365*, 1326-1336.

69. Thorne, R. E., Chinnapen, D. J. F., Sekhon, G. S., and Sen, D. (2009) A deoxyribozyme, Sero1C, uses light and serotonin to repair diverse pyrimidine dimers in DNA, *J. Mol. Biol. 388*, 21-29.

70. Chinnapen, D. J.-F., and Sen, D. (2004) A deoxyribozyme that harnesses light to repair thymine dimers in DNA, *Proc. Natl. Acad. Sci. 101*, 65-69.

71. Holman, M. R., Ito, T., and Rokita, S. E. (2006) Self-repair of thymine dimer in duplex DNA, *J. Am. Chem. Soc. 129*, 6-7.

72. Pan, Z., Hariharan, M., Arkin, J. D., Jalilov, A. S., McCullagh, M., Schatz, G. C., and Lewis, F. D. (2011) Electron donor-acceptor interactions with flanking purines influence the efficiency of thymine photodimerization, *J. Am. Chem. Soc. 133*, 20793-20798.

CHAPTER 2

A PREBIOTIC ROLE FOR 8-OXOGUANOSINE AS A FLAVIN MIMIC IN PYRIMIDINE DIMER PHOTOREPAIR

Introduction

The RNA World hypothesis suggests that ancient life evolved from the catalytic chemistry of RNA oligomers (*1*). Numerous *in vitro* selection experiments now demonstrate the concept that RNA can catalyze a wide range of chemical reactions including ligation, hydrolysis, and C-C bond formation (*2, 3*). Early life would have also required redox reactions to support metabolism, but neither the four RNA bases nor the canonical amino acids are very redox active. We therefore hypothesized that prior to the evolution of more sophisticated cofactors such as flavin adenine dinucleotide, a simple and abundant derivative of guanine, namely OG, could have played the role of a redox coenzyme in RNA-based catalysis.

To investigate this hypothesis, we designed experiments that would test the electron-transfer capability of OG as a substitute for the flavoenzyme photolyase. The role of the flavin cofactor in photolyase has been investigated extensively, and there is consensus that the photoexcited state of $FADH^-$ transfers an electron to the cyclobutane thymine dimer (T=T) in bound duplex DNA, resulting in rapid cleavage of the sigma

bonds and back electron transfer to the flavin radical (*4-6*). The process regenerates an undamaged TT-containing DNA strand as well as the original flavin cofactor. In parallel with a lower redox potential than the natural nucleosides, OG also has significant absorbance above 300 nm, a region in which DNA and RNA oligomers have essentially no absorbance. It therefore appeared feasible to photoexcite the OG base specifically in an oligomer using wavelengths >300 nm, and to examine the reversion of the cyclobutane dimer to two undamaged thymidines.

Results and discussion

For ease of synthesis and comparison to other work, initial studies were conducted in DNA oligomers using 8-oxo-7,8-dihydro-2'-deoxyguanosine (designated "O" in sequences) at positions in a 22-mer strand that placed it near a T=T dimer that was either synthesized and purified in an 18-mer strand or installed via the T=T phosphoramidite. The difference in strand length permitted direct analysis of the quantities of T=T-containing strands vs. repaired TT strands in the presence of the longer OG-containing oligomer by denaturing HPLC conducted at 70°C (Figure 2.1). Duplex 1A has an OG:A base pair (Figure 2.2) positioned directly 5' to the T=T site although OG is located in the strand complementary to the dimer. Irradiation of the duplex using a 40W UVB light source (λ_{max}=313 nm) and a polystyrene filter to remove wavelengths <300 nm led to repair of the T=T dimer in a process that showed first order kinetics and a rate constant of ~ $1x10^{-2}$ min^{-1} at 22°C (Figure 2.1). Control experiments in DNA duplexes without OG present resulted in no detectable repair (<5%) indicating the dependence of the repair process on OG.

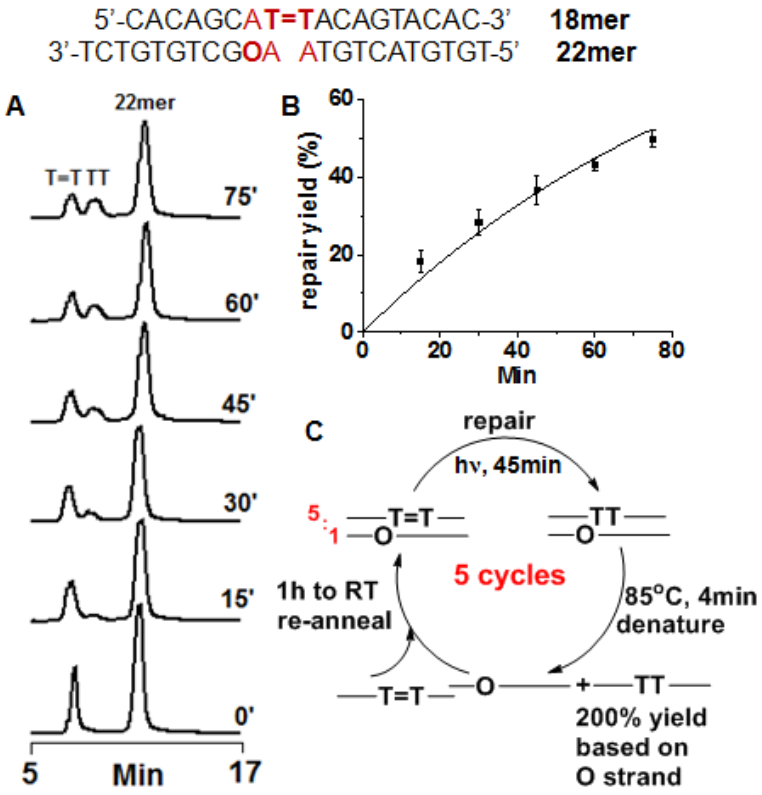

Figure 2.1. Photorepair (λ_{max}=313 nm) of T=T cyclobutane dimer in an 18mer strand of DNA annealed to an O-containing 22mer. (**A**) Denaturing HPLC (70°C) analysis of strands as a function of time. (**B**) Repair demonstrates first-order kinetics. (**C**) Turnover catalysis is shown by repair of a 5.4:1 mixture of T=T and O-containing strands in a light/heat/cool cycle leading to ~200% yield of repair based on OG.

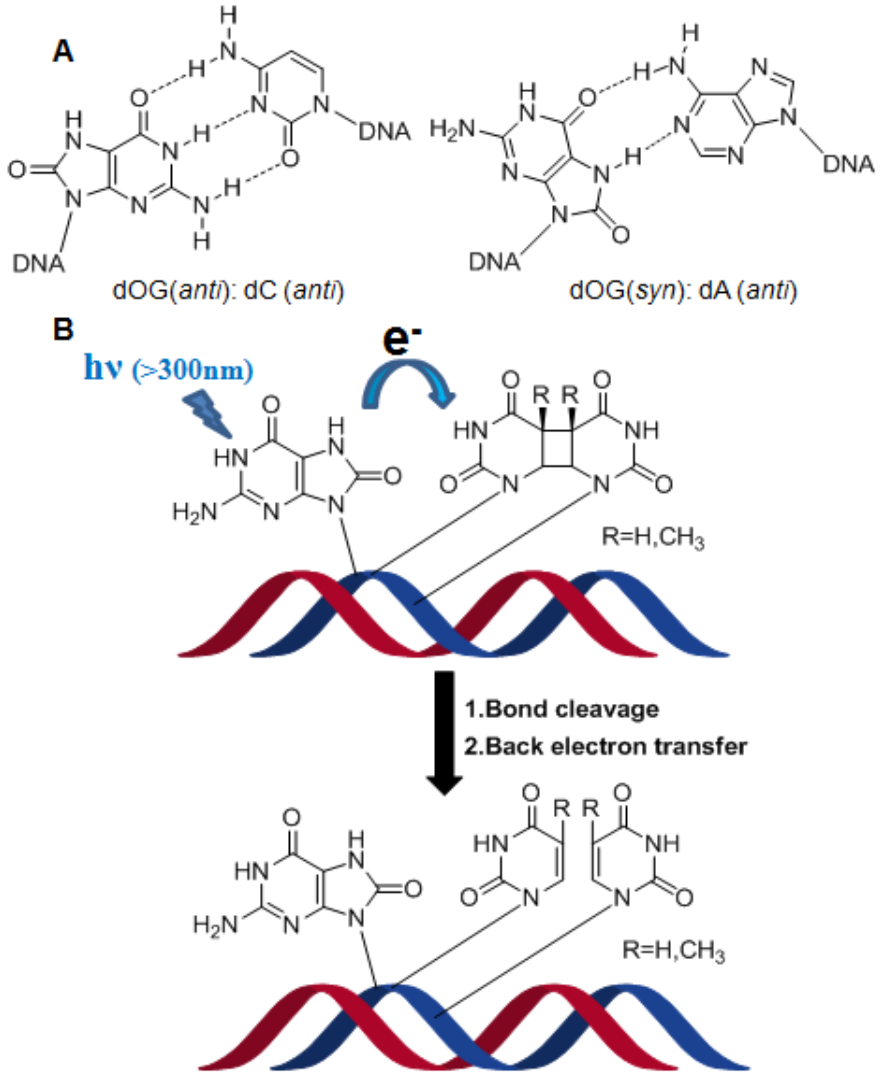

Figure 2.2. Repair of T=T by OG in duplex DNA. (**A**) OG can form a stable Watson-Crick base pair with C or, in the syn conformation, pair with A. (**B**) Studies herein support a photolyase-type mechanism in which the excited state of OG transfers and electron to T=T (or U=U) effecting cleavage of the cyclobutane; back electron transfer regenerates OG and the repaired pyrimidines.

To better understand the catalytic role of OG, the OG-containing strand was isolated after ~ 50% repair and reanalyzed by ion-exchange HPLC. Under these conditions, the oxidation products of OG are readily separable; comparisons with authentic standards indicated that OG remained intact in the DNA strand. Thus, any reactive intermediates formed during photorepair, such as $OG^{+\bullet}$, revert to OG during the course of the reaction. Furthermore, the OG-containing strand showed turnover catalysis. In this experiment, a 5.4:1 ratio of T=T and OG-containing strands was subjected to a reaction cycle of irradiation, thermal denaturation, and re-annealing. Each irradiation period, 45 min, was sufficient to effect approximately 40% repair of the bound strand, and the final yield of repair after 5 cycles was ~200% based on OG (Figure 2.1).

The dependence of the repair process on base pair and sequence context provided insight into the mechanism of repair. OG can form stable base pairs with either C or A, depending upon the anti or syn orientation of the OG base with respect to the glycosidic bond (Figure 2.2), and these base pairs cause very little change in stability or structure of DNA duplexes (*7*). Surprisingly, the OG:A base pair was about three-fold more efficient than the Watson-Crick OG:C base pair in repairing the thymine dimer in both interstrand and intrastrand duplexes (1A vs 1C, 4A vs 4C, Figure 2.3). One explanation of these data is based on the finding that the G:C base pair has a shortened excited state lifetime due to proton-coupled electron transfer (*8-11*). If quenching of the OG* excited state also occurs via the assistance of the relatively acidic N1-H proton transfer to N3 of C, the OG:C base pair would exhibit a reduced excited state lifetime and therefore be less efficient than OG:A in donating an electron to the nearby T=T (Figure 2.2). In addition, computations of ionization potentials predict a lower value for OG:A compared to OG:C (*12*). Internal

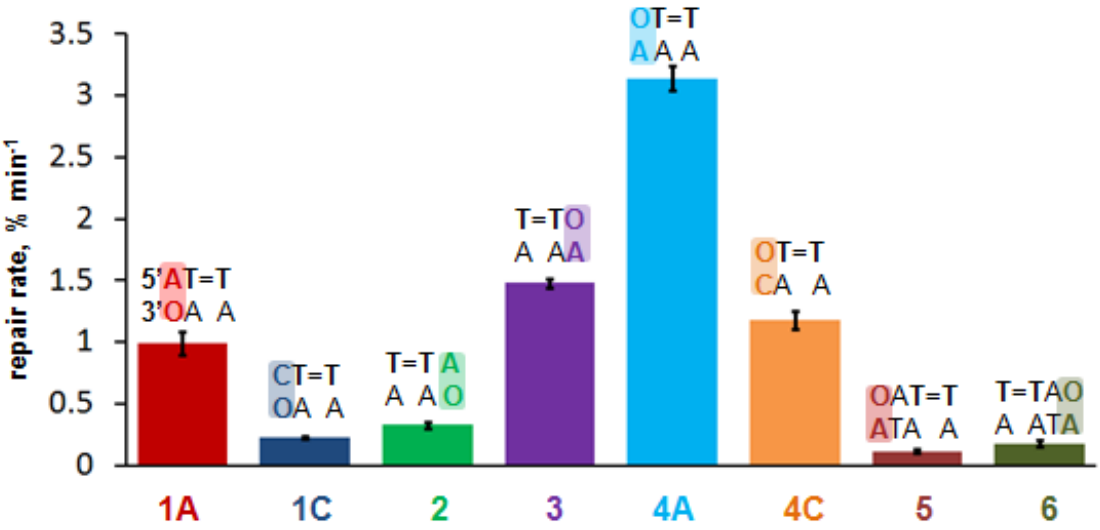

Figure 2.3. Repair rates at 22°C for various sequence contexts for O and T=T. The complete sequence of duplex **1A** is shown in Figure 2.1; see Table 2.2 for others. Repair rates were obtained from fitting the repair yields to the first-order exponential curve. Error bars indicate the standard deviation of at least three experiments.

electron transfer in the OG:A base pair would be less efficient than in an OG:C base pair, because the N7-H of OG is less acidic and because purine bases have lower electron affinity than pyrimidine bases (*8*).

Strand, directional and distal effects on thymine dimer repair by OG were also investigated by changing the location and orientation of the OG:A base pair in the vicinity of the T=T dimer. The highest rate of repair was observed when OG (with A opposite) was located immediately 5' to the T=T lesion and in the same strand (Figure 2.3, duplex 4A vs. 3); in this case, 85% repair was observed in 75 min. The same 5' preference was also exhibited when the orientation of the base pair was reversed, placing OG in the opposite strand (Figure 2.3, 1A vs. 2). These data agree with the observation of Rokita and coworkers who found that formation of T=T in duplex DNA using 254 nm light was inhibited to some extent by the presence of a G nucleotide at the 5' side of the TT sequence (*13*). In addition, we found a 4-5-fold preference for location of the OG nucleotide in the same strand as the lesion, consistent with the higher efficiency of intrastrand electron transfer (Figure 2.3, 4A vs. 1A, 4C vs. 1C, 3 vs. 2) (*14, 15*). The presence of T=T is known to cause disturbance of the duplex DNA and destacking at the thymine dimer site also has an effect on charge migration through duplex DNA (*16*). NMR and crystal structures of thymine dimer-containing DNA show that though the 3' side of T=T still retains good hydrogen bonding, the phosphate backbone changes to the B_{II} conformation upon formation of T=T, which can destack the base at this site (*17, 18*). Therefore, the higher repair efficiency when OG is located at the 5' side of T=T may result from better base stacking at this position, which would in turn facilitate formation of an exciplex between OG as an electron donor and the adjacent T=T acceptor (*19*).

The preference for OG-mediated repair from the immediate 5' side of the T=T dimer was reversed when the repair was attempted from a longer distance. Insertion of an A:T base pair between the OG donor and T=T acceptor yielded sequences 5 and 6 (Figure 2.3), respectively. For these sequences, when OG was present in a 5' orientation with respect to T=T, the presence of the intervening base pair led to a 25-fold reduction in rate, while only an 8-fold reduction in rate was observed from the 3' direction (Figure 2.3, 4A vs. 5, and 3 vs. 6); indeed, duplex 6 is now somewhat more reactive than duplex 5. We propose that the thymine dimer is repaired reductively via electron transfer from OG* to T=T in a manner analogous to flavin-dependent photorepair with the enzyme photolyase. This constitutes an excess electron transfer (EET) mechanism in the DNA duplex, which has been shown to have a 3' to 5' directional preference (*14, 15*) due to the asymmetric overlap of frontier molecular orbitals of the two adjacent bases (*20*). Taken together, the studies of strand, direction and distance effects of OG-catalyzed photorepair of thymine dimers support an electron transfer mechanism of repair, analogous to that of photolyase, with the caveat that the immediate adjacency of the donor-acceptor pair creates a special preference for the 5'-3' orientation because of enhanced exciplex formation resulting from better base stacking.

As reported, EET still occurs in double-stranded DNA containing a structural disturbance (*21*) as well as in single-stranded DNA, although only over a short distance (*22*). Conversely, hole transfer seems not to migrate through single-stranded DNA at all (*23*). Thus, to further support the EET mechanism, we investigated thymine dimer repair by OG in single-stranded DNA in which there was an intervening dA between OG and T=T. The results showed that T=T is moderately repaired, reaching to 19% after 90 min

irradiation in strand 5S. Without OG present, no detectable repair was observed after 150 min of irradiation. The retention of activity of OG in single-stranded DNA further supports the EET mechanism in this system.

The relevancy of OG as a primordial flavin requires that its photorepair activity also operate on uracil dimers in RNA. To this end, we synthesized the cyclobutane photodimer in an RNA sequence analogous to duplex 1A such at a U=U dimer was installed adjacent to an A:O base pair, although the photosynthetic method required that OG be present in the opposite strand where it is threefold less reactive. Table 2.1 compares the yields of T=T vs. U=U photorepair in the 1A sequence context for the DNA:DNA, RNA:DNA, and RNA:RNA duplexes. While less efficient in the A form helices in which base stacking is dramatically altered compared to B form DNA, the photorepair of U=U by OG is still clearly evident.

Conclusion

We have demonstrated that OG, a common base oxidation product in nucleic acids, can trigger cyclobutane pyrimidine dimer repair using wavelengths of light red-shifted from the normal absorption spectrum of DNA or RNA. A related example of such a repair process is the work of Sen and coworkers (*24, 25*) who generated a DNAzyme capable of photorepair of a bound thymine dimer substrate; in that case, a very different motif, a G quartet, appears to be responsible for repair rather than the flavin analogue OG. In addition, Carell and coworkers have demonstrated that the photolyase protein is not necessary for repair of T=T; synthetic incorporation of a flavin into the DNA stack also effects photorepair (*26, 27*).

Table 2.1. Single time point repair yields for cyclobutane pyrimidine dimers in various strand contexts based on the sequence context of duplex **1A**

Entry	Substrate	Irradiation time(min)	Yield(%)
1	$DNA^{T=T}$-DNA^{O}	75	50
2	$RNA^{U=U}$-DNA^{O}	150	40
3	$RNA^{U=U}$-RNA^{O}	150	12

Although more detailed analysis of the photophysical events surrounding this phenomenon are clearly warranted, the context effects on repair kinetics support a catalytic mechanism involving excess electron transfer from OG to the pyrimidine dimer in a fashion analogous to that of the flavin-dependent photolyases. This is an unusual example of one form of DNA damage serving to repair another. While the formation of both OG and T=T are linked in present-day photochemical DNA damage, the relative amounts of these modifications in the prebiotic world are unknown. Nevertheless, conditions favoring OG formation at the same time as cyclobutane pyrimidine dimers could have driven the further evolution of purine nucleotides toward flavin-like activity. The overall similarity of OG and flavin chemistry further suggests that nature may have adopted this close relative of the guanine base as a step towards organic-based redox metabolism, possibly as a component of the IDA, prior to the appearance of modern enzyme cofactors.

Experimental

Oligodeoxynucleotide synthesis and purification. Phosphoramidites for oligodeoxynucleotide synthesis were purchased from Glen Research. Oligodeoxynucleotides were synthesized at the DNA/Peptide Core facility at the University of Utah. The [*cis, syn*] thymine dimer-containing oligodeoxynucleotides were first treated with thiophenol/triethylamine/THF (1/2/2) for 45 min at room temperature to remove the methyl phosphate group (*28, 29*). The solid support was then washed with THF (10x), methanol (5x), acetonitrile (3x) and dried under argon flow. Oligodeoxynucleotides were cleaved and deprotected in sealed glass vials with

concentrated NH_4OH for 16 h at 55 °C in the dark (in the cases of oligodeoxynucleotides containing **OG**, 0.25 M β-mercaptoethanol was added to the deprotection solutions to avoid the oxidation of **OG**). Oligodeoxynucleotides were purified by HPLC on a Dionex DNA Pac PA-100 column with linear gradient of 15% B to 100% B over 30 min (Solvent A: 10% acetonitrile in water; solvent B: 1.5 M sodium acetate, 10% acetonitrile in water, pH 7). Oligodeoxynucleotides were then desalted by dialysis against water for 36 h at 4 °C in the dark. The purity and identity of oligomers were determined by analytical HPLC and mass spectrometry. The [*cis,syn*] thymine dimer-containing oligodeoxynucleotides were quantified by UV-VIS spectroscopy on the Beckman DU 650 spectrometer using extinction coefficient calculated as previously described (*16*). Complete sequences are shown in Table 2.2.

Photorepair of [*cis, syn*] thymine dimer in DNA duplexes. 5 μM of thymine dimer-containing DNA was annealed with 1.3 equiv. of the appropriate complementary strand in a buffer solution containing 20 mM NaPi, 100 mM NaCl, pH 7 by heating at 90 °C for 2 min and cooling to room temperature over 4 h. The DNA duplex was irradiated in polystyrene cuvettes to cut off wavelengths below 300 nm(*24*) at ambient temperature (22 °C) with an FS40 UVB lamp (peak at 313 nm, Homephototherapy, OH, USA). The irradiation mixture was then analyzed by HPLC on Hamilton PRP-1 (5 μm, 250X4.6 mm) column at 70 °C with linear gradient of 10% B to 14% B over 25 min (Solvent A: 50 mM TEAA in water, pH 7; Solvent B: acetonitrile). Detector was set at 260 nm and the flow rate was 0.8 mL/min. Under these conditions, the DNA duplex was denatured and single-stranded DNA oligomers eluted in the following order: the thymine dimer T=T strand (18mer), the repaired TT strand (18mer) and the complementary strand

Table 2.2. Complete sequences studied. Sequences 1-8 are DNA:DNA duplexes. Sequence 5S is single-stranded DNA

	Sequences
1A	5’-CACAGCA**T**=**T**ACAGTACAC-3’ 3’-TCTGTGTCG**O**A ATGTCATGTGT-5’
1C	5’-CACAGCC**T**=**T**ACAGTACAC-3’ 3’-TCTGTGTCG**O**A ATGTCATGTGT-5’
C1	5’-CACAGCA**T**=**T**ACAGTACAC-3’ 3’-TCTGTGTCG**T**A ATGTCATGTGT-5’
C2	5’-CACAGCC**T**=**T**ACAGTACAC-3’ 3’-TCTGTGTCG**G**A ATGTCATGTGT-5’
2	5’-CACAGCA**T**=**T**ACAGTACAC-3’ 3’-TCTGTGTCGTA A**O**GTCATGTGT-5’
3	5’-CACAGCA**T**=**TO**CAGTACAC-3’ 3’-TCTGTGTCGTA AAGTCATGTGT-5’
4A	5’-CACAGC**OT**=**T**ACAGTACAC-3’ 3’-TCTGTGTCGAA ATGTCATGTGT-5’
4C	5’-CACAGC**OT**=**T**ACAGTACAC-3’ 3’-TCTGTGTCGCA ATGTCATGTGT-5’
5	5’-ACAGC**O**A**T**=**T**ACAGTACAC-3’ 3’-TCTTGTCGATA ATGTCATGTGT-5’
6	5’-ACAGC**O**T**T**=**T**ACAGTACAC-3’ 3’-TCTTGTCGAAA ATGTCATGTGT-5’
7	5’-CACAGCA**T**=**T**A**O**CAGTACA-3’ 3’-TCTGTGTCGTA ATAGTCATGTT-5’
8	5’-CACAGCA**T**=**T**T**O**CAGTACA-3’ 3’-TCTGTGTCGTA AAAGTCATGTT-5’
RNA/DNA	5’-CACAGCA**U**=**U**ACAGUACAC-3’ 3’-TCTGTGTCG**O**A ATGTCATGTGT-5’
RNA/RNA	5’-CACAGCA**U**=**U**ACAGUACAC-3’ 3’-UCUGUGUCG**O**A AUGUCAUGUGU-5’
5S	5’-ACAGC**O**A**T**=**T**ACAGTACAC-3’

(22mer). HPLC peaks corresponding to the thymine dimer strand and the repaired strand were integrated. The peak areas were normalized against extinction coefficients of each strand and used to calculate the thymine dimer repair yield. Thymine dimer repair was plotted as function of irradiation time and fit to exponential curve using OriginPro 8.5 software (Originlab). The repair rate (% min^{-1}) was calculated and this value was used to compare the repair efficiency of different DNA duplexes (*14*). The presented data were averaged from three experiments.

Photorepair of [*cis, syn*] uracil dimer. Uracil dimer containing RNA (5'-CACAGCA**U=U**AC AGUACAC-3') was synthesized following a reported procedure (*25*) except using a higher concentration of acetone photosensitizer (10%), and the oligomer was purified by reversed phase HPLC. The preparations of RNA/DNA and RNA/RNA duplexes and irradiation procedure were the same as described above for the DNA duplex. The irradiation mixture was then analyzed by denaturing HPLC on a Hamilton PRP-1 (5 μm, 250x4.6 mm) column at 70 $^{\circ}$C with a linear gradient of 9% B to 13% B over 25 min (Solvent A: 50 mM TEAA in water, pH 7; Solvent B: acetonitrile). The detector was set at 260 nm and the flow rate was 1.0 mL/min. Under these conditions, the uracil dimer strand and the repaired strand coeluted as a broaden peak at 9 min. This peak was isolated and reanalyzed by reversed phase HPLC at room temperature using an Ace C18 column (5 μm, 250x4.6 mm) with a linear gradient of 4% B to 12% B over 30 min (Solvent A: 20 mM CH_3COONH_4, pH 7; Solvent B: acetonitrile). Under these conditions, the uracil dimer strand eluted at 10 min and the repaired strand eluted at 12 min. These peaks were integrated and used to calculate the repair yield.

Photorepair of [*cis, syn*] thymine dimer in single-stranded DNA. The irradiation procedure for single-stranded DNA was the same as described above for the DNA duplex. The irradiation mixture was then analyzed by HPLC on Ace C18 column (5 μm, 250X4.6 mm) with linear gradient of 5% B to 15% B over 25 min (Solvent A: 20 mM CH_3COONH_4, pH 7; Solvent B: acetonitrile). Under these conditions, the thymine dimer strand eluted at 10 min and the repaired strand eluted at 12.5 min.

References

1. Gilbert, W. (1986) Origin of Life: The RNA world, *Nature 319*, 618.

2. Chen, X., Li, N., and Ellington, A. D. (2007) Ribozyme catalysis of metabolism in the RNA world, *Chem. Biodiversity. 4*, 633-655.

3. Joyce, G. F. (2002) The antiquity of RNA-based evolution, *Nature 418*, 214-221.

4. Brettel, K., and Byrdin, M. (2010) Reaction mechanisms of DNA photolyase, *Curr. Op. Struct. Biol. 20*, 693-701.

5. Heil, K., Pearson, D., and Carell, T. (2011) Chemical investigation of light induced DNA bipyrimidine damage and repair, *Chem. Soc. Rev. 40*, 4271-4278.

6. Kao, Y.-T., Saxena, C., Wang, L., Sancar, A., and Zhong, D. (2005) Direct observation of thymine dimer repair in DNA by photolyase, *Proc. Natl. Acad. Sci. 102*, 16128-16132.

7. McAuley-Hecht, K. E., Leonard, G. A., Gibson, N. J., Thomson, J. B., Watson, W. P., Hunter, W. N., and Brown, T. (1994) Crystal structure of a DNA duplex containing 8-hydroxydeoxyguanine-adenine base pairs, *Biochemistry 33*, 10266-10270.

8. Kumar, A., and Sevilla, M. D. (2010) Proton-coupled electron transfer in DNA on formation of radiation-produced ion radicals, *Chem. Rev. 110*, 7002-7023.

9. de La Harpe, K., Crespo-Hernandez, C. E., and Kohler, B. (2009) Deuterium isotope effect on excited-state dynamics in an alternating GC oligonucleotide, *J. Am. Chem. Soc. 131*, 17557-17559.

10. Schwalb, N. K., and Temps, F. (2007) Ultrafast electronic relaxation in guanosine is promoted by hydrogen bonding with cytidine, *J. Am. Chem. Soc. 129*, 9272-9273.

11. Sobolewski, A. L., Domcke, W., and C., H. (2005) Tautomeric selectivity of the excited-state lifetime of guanine/cytosine base pairs: The role of electron-driven proton-transfer processes, *Proc. Natl. Acad. Sci. 102*, 17903-17906.

12. Reynisson, J., and Steenken, S. (2005) The calculated base pairing energy of 8-oxoguanine in the syn-anti conformation with cytosine, thymine, adenine and guanine, *J. Mol. Struct: Theo. Chem. 723*, 29-36.

13. Holman, M. R., Ito, T., and Rokita, S. E. (2006) Self-Repair of thymine dimer in duplex DNA, *J. Am. Chem. Soc. 129*, 6-7.

14. Ito, T., and Rokita, S. E. (2004) Criteria for efficient transport of excess electrons in DNA, *Angew. Chem. Int. Ed 43*, 1839-1842.

15. Tanaka, M., Elias, B., and Barton, J. K. (2010) DNA-mediated electron transfer in naphthalene-modified oligonucleotides, *J. Org. Chem. 75*, 2423-2428.

16. Dandliker, P. J., Nunez, M. E., and Barton, J. K. (1998) Oxidative charge transfer to repair thymine dimers and damage guanine bases in DNA assemblies containing tethered metallointercalators *Biochemistry 37*, 6491-6502.

17. McAteer, K., Jing, Y., Kao, J., Taylor, J. S., and Kennedy, M. A. (1998) Solution-state structure of a DNA dodecamer duplex containing a cis-syn thymine cyclobutane dimer, the major UV photoproduct of DNA, *J. Mol. Biol. 282*, 1013-1032.

18. Park, H., Zhang, K., Ren, Y., Nadji, S., Sinha, N., Taylor, J.-S., and Kang, C. (2002) Crystal structure of a DNA decamer containing a cis-syn thymine dimer, *Proc. Natl. Acad. Sci. 99*, 15965-15970.

19. Crespo-Hernandez, C. E., Cohen, B., and Kohler, B. (2005) Base stacking controls excited-state dynamics in A:T DNA, *Nature 436*, 1141-1144.

20. O'Neill, M. A., and Barton, J. K. (2002) Effects of strand and directional asymmetry on base-base coupling and charge transfer in double-helical DNA, *Proc. Natl. Acad. Sci. 99*, 16543-16550.

21. Ito, T., Kondo, A., Terada, S., and Nishimoto, S.-i. (2006) Photoinduced reductive repair of thymine glycol: Implications for excess electron transfer through DNA containing modified bases, *J. Am. Chem. Soc. 128*, 10934-10942.

22. Ito, T., Kondo, A., Terada, S., and Nishimoto, S.-i. (2007) Flavin-sensitized photoreduction of thymidine glycol, *Bioorg. Med. Chem. Lett. 17*, 6129-6133.

23. O'Neill, M. A., Dohno, C., and Barton, J. K. (2004) Direct chemical evidence for charge transfer between photoexcited 2-aminopurine and guanine in duplex DNA, *J. Am. Chem. Soc. 126*, 1316-1317.

24. Chinnapen, D. J.-F., and Sen, D. (2004) A deoxyribozyme that harnesses light to repair thymine dimers in DNA, *Proc. Natl. Acad. Sci. 101*, 65-69.

25. Chinnapen, D. J. F., and Sen, D. (2007) Towards elucidation of the mechanism of UV1C, a deoxyribozyme with photolyase activity, *J. Mol. Biol. 365*, 1326-1336.

26. Schwögler, A., Burgdorf, L., and Carell, T. (2000) Self-repairing DNA based on a reductive electron transfer through the base stack, *Angew. Chem. Int. Ed. 39*, 3918-3920.

27. Fazio, D., Trindler, C., Heil, K., Chatgilialoglu, C., and Carell, T. (2011) Investigation of excess-electron transfer in DNA double-duplex systems allows estimation of absolute excess-electron transfer and CPD cleavage rates, *Chem. Eur. J. 17*, 206-212.

28. Taylor, J. S., Brockie, I. R., and O'Day, C. L. (1987) A building block for the sequence-specific introduction of cis-syn thymine dimers into oligonucleotides. Solid-phase synthesis of TpT[c,s]pTpT, *J. Am. Chem. Soc. 109*, 6735-6742.

29. Brooks, P. J., Wise, D. S., Berry, D. A., Kosmoski, J. V., Smerdon, M. J., Somers, R. L., Mackie, H., Spoonde, A. Y., Ackerman, E. J., Coleman, K., Tarone, R. E., and Robbins, J. H. (2000) The oxidative DNA lesion 8,5'-(S)-Cyclo-2'-deoxyadenosine is repaired by the nucleotide excision repair pathway and blocks gene expression in mammalian cells, *J. Biol. Chem. 275*, 22355-22362.

CHAPTER 3

EFFECTS OF SEQUENCE CONTEXTS ON THYMINE DIMER REPAIR BY 8-OXOGUANOSINE IN SINGLE-STRANDED AND DOUBLE-STRANDED OLIGONUCLEOTIDES

Introduction

We earlier proposed that RNA could have employed simple derivatives of nucleosides to facilitate electron transfer processes prior to the evolution of modern enzyme redox cofactors such as flavin, pterins and nicontinamide (*1*). We showed that 8-oxoguanosine (OG) can mimic the function of flavins to repair cyclobutane pyrimidine dimers (CPD) when installed into double-stranded DNA or RNA in proximity to these lessons. The repair mechanism is thought to be a photo-induced electron transfer process from OG to CPD. We also found that the repair efficiency has interesting correlations with base pairing, base stacking and the orientation of OG with respect to the CPD (5'-3' vs. 3'-5') (*1*). Therefore, we reasoned that extending the studies to the effects of sequence contexts on CPD repair efficiency may help us better understand the repair mechanism.

In a broader view, the mechanistic aspects of the CPD repair in this system relate to a question of how the photoexcited states of bases relax to the ground states. Indeed, this is an interesting question that has attracted considerable attention of scientists due to its importance to understand mechanisms of DNA photodamage (*2*). As previously

described, electron transfer (ET) leading to the formation of exciplexes is believed to be an important pathway for the deactivation of the photoexcited state of bases in single-stranded or double-stranded DNA (*2-10*). The ground state is then recovered by either charge recombination in the case of intrastrand exciplexes (*2-5, 11*) or proton transfer in the interstrand $G^{+\cdot}$:$C^{-\cdot}$ exciplex (*6, 8-10, 12*). Although the formation of intrastrand exciplexes is widely accepted, the proton-coupled electron transfer (PCET) mechanism for the deactivation of the excited G:C base pair is still controversial (*13*). The unique structure of OG allows it to effectively bind with various bases such as a Watson-Crick base pair with C, a Hoogsten base pair with A and a potential wobble base pair with T (Figure 3.1) (*14, 15*). Therefore, monitoring the CPD repair efficiency in different sequence contexts for OG and CPD might differentiate the two photo-induced electron transfer pathways, through base stacking and base pairing, and help to validate the existence of an interstrand exciplex. In this chapter, we investigate the photorepair activity of OG in different environments of base stacking and base pairing to elucidate photodynamic insights into the repair mechanism.

Results

Base pair effects on the repair of thymine dimer by OG. In the previous report, we proposed that the lower activity of an OG:C base pair as compared to an OG:A base pair in repairing T=T derives from its capability of deactivation by a PCET mechanism (*1*). To further support this argument, we postulate that removal of the base paired with OG will eliminate the PCET mechanism, and therefore may enhance the thymine dimer repair efficiency comparing to the OG:C base pair, even though this modification also

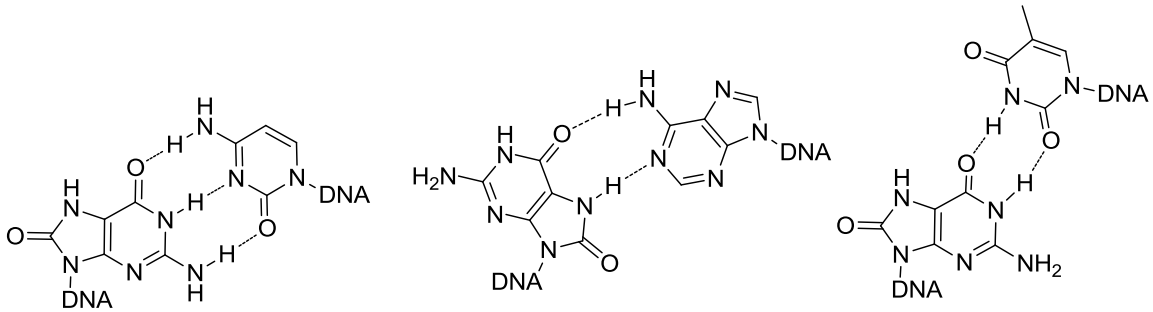

Figure 3.1. Base pairs of OG with different bases

destabilizes the DNA duplex. For this purpose, we constructed DNA duplexes placing OG opposite a tetrahydrofuran analog (F) used as an abasic site mimic. The photolysis experiments of these duplexes were carried out as previously described (*1*) and the irradiation mixtures were analyzed by denaturing HPLC to detect the repaired strand (see experimental section). Integration of HPLC peaks corresponding to the thymine dimer and the repaired strands, and plots of the repair yield *vs.* irradiation time were used to calculate the repair rates that are shown in Figure 3.2.

The repair of thymine dimer was first investigated with DNA duplexes containing OG neighboring to T=T. When OG is at the 5' side of T=T, we observed the activity of an OG:F is 3-fold less than in OG:C base pair (Figure 3.2, 1C vs. 1F). However, the order is reversed when OG was presented at the 3' side of T=T in which an OG:F is about 2-fold more reactive than an OG:C base pair (Figure 3.2, 2C vs. 2F**)**. These results are probably due to the different stacking environments between the two sides of T=T in DNA duplex (*16, 17*). Next, we compared the thymine dimer repair efficiency between OG:C and OG:F in duplexes in which an intervening dA was put in between OG and T=T. In these duplexes, OG does not directly stack onto the T=T, therefore, the intrastrand ET will be greatly reduced while the PCET pathway is not likely affected. The results showed that OG:F duplexes with OG in both sites of T=T (3' and 5') still showed some degree of thymine dimer repair although the reactivity was decreased about 4-fold compared to the corresponding duplexes with OG neighboring to T=T (Figure 3. 2, duplex 2F, 3F). In contrast, no detectable repair of thymine dimer (<5%) was observed in OG:C duplexes after 120 min of irradiation. These results support the plausibility of a PCET mechanism to deactivate the photoexcited state of OG in an OG:C base pair.

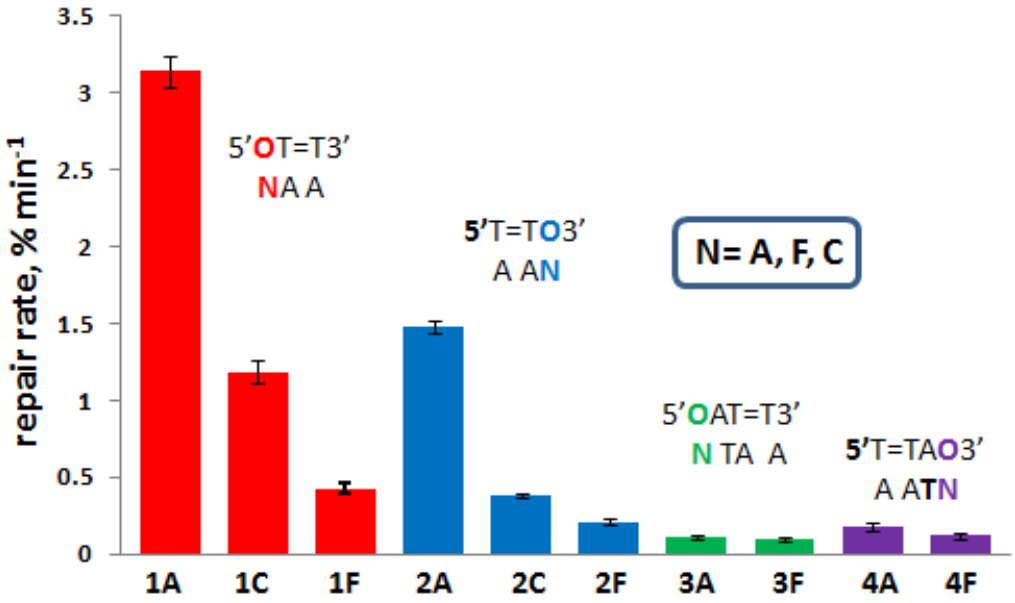

Figure 3.2. Repair rates of T=T in various sequence contexts of DNA duplexes.

Thymine dimer repair in single-stranded DNA (ssDNA). As reported, an exciplex between two neighboring bases can be formed in ssDNA (*2, 3*). Therefore, if the thymine dimer repair is proceeded by formation of an exciplex, it should also be possible in ssDNA. We then investigated the repair efficiency of thymine dimer in OG-containing ssDNA to validate this argument. All the experimental procedures to determine the repair rates of thymine dimer in ssDNA were the same as described above for DNA duplex, except that reversed phase HPLC was used to analyze reaction mixtures (Figure 3.3). The results are shown in Figure 3.4. As expected, the repair efficiency of thymine dimer in ssDNA is generally lower than in the corresponding DNA duplex. In addition, we still observed the 5'-3' preference for the thymine dimer repair efficiency in ssDNA with OG directly flanking T=T (Figure 3.4, duplex 1S vs. 2S). It is also not surprising that insertion of a dA in between 5'-OG and T=T led to a 5-fold decrease in repair efficiency (Figure 4, 1S *vs.* 3S). However, a reversed distance effect in which the activity was slightly increased with an insertion of a dA in between OG and T=T was observed at the 3' side of T=T (2S vs.4S, Figure 3.4).

Repair of thymine dimer by an opposite OG. We have so far demonstrated that OG is capable of mediating the thymine dimer repair via an electron transfer process through base stacking in the DNA duplex as well as in ssDNA. The highest repair efficiency was observed in a duplex with OG presented at the 5' side of T=T and paired with a dA with a quantum yield estimated at 0.01 (see experimental section). Practically, for OG as an RNA repair catalyst, it may be not necessary for the OG to be in the same strand and directly stacked with the lesion T=T. The simplest arrangement one could imagine is that OG is brought close to this lesion by a ribozyme that facilitates the repair

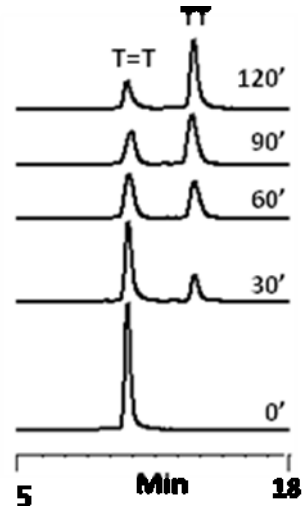

Figure 3.3. Reversed phase HPLC analysis of strand **1S** as a function of irradiation time.

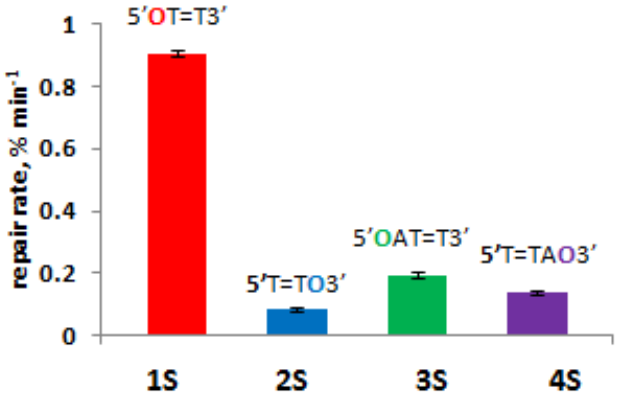

Figure 3.4. Repair rate of T=T in single-stranded DNA

upon irradiation. Therefore, we next investigated thymine dimer repair in DNA duplexes placing OG opposite one or the other T of the dimer. Detection of the repaired strand after photolysis and calculation of repair rates were the same as described above. Surprisingly, OG opposite the 3' T of the dimer (Figure 3.5, duplex 5T) showed an excellent photorepair activity, and it is comparable to the most reactive duplex 1A (Figure 3.5) observed so far. The OG opposite the 5'T (Figure 3.5, duplex 6T) still showed moderate activity but decreases about 8-fold in comparision to the duplex 5T. This result is possibly derived from the difference in the ability to form a base pair between these two Ts of the dimer (*16*).

Repair of uracil dimer in RNA/DNA duplexes by an opposite OG. Since OG is proposed as a ribozyme cofactor in the RNA world, its photorepair activity may also need to operate on uracil dimer (U=U) in RNA. Therefore, we investigated the possibility of this chemistry by constructing the RNA/DNA duplexes in the same sequence contexts as T=T containing DNA/DNA duplexes described above, placing OG opposite one of the Us of the uracil dimer (Table 3.1). After photolysis, the irradiation mixtures of these RNA/DNA duplexes were analyzed by denaturing HPLC to detect the repaired RNA strand. The repair yields are reported in Table 3.1. Similar to the case of the T=T -containing DNA/DNA duplex, we observed better repair activity of OG opposite the 3'U than opposite the 5' U of the dimer. Consistent with our previous study (*1*), the repair efficiency of U=U was less than T=T in the same sequence context, probably due to the change of the helical structure from the B form (DNA/DNA duplex) to the A form (DNA/RNA duplex).

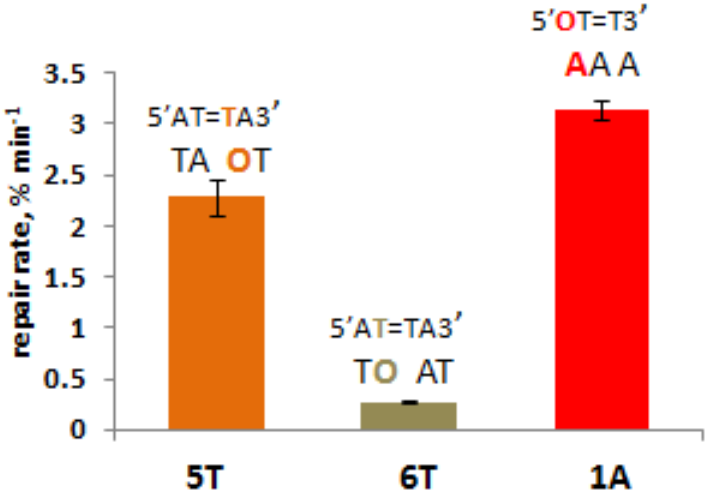

Figure 3.5. Repair rates of T=T in DNA duplexes with OG opposite to one or the other T of the dimer (5T, 6T). 1A is the DNA duplex with the highest T=T repair activity.

Table 3.1. Single time point repair yields for cyclobutane pyrimidine dimers in various sequence contexts based on duplexes 5T and 6T.

Entry	Substrate	Irradiation time (min)	Yield (%)
1	5′-T=T-3′ **O** A	75	20
2	5′-T=T-3′ A **O**	75	82
3	5′-U=U-3′ **O** A	75	<5%
4	5′-U=U-3′ A **O**	75	38

Discussion

In the previous work, we proposed that the repair of thymine dimer by an adjacent OG was first proceeded via the formation of an exciplex $OG^{+}T=T^{-}$ (*1*). The cleavage of a cyclobutane ring, an ultrafast process estimated to occur at picosecond time scale (*18, 19*), might efficiently compete with the charge recombination of an exciplex (~50-180ps) (*3, 11*) and lead to the repair of T=T. Previous studies also suggested that the formation of an exciplex between T and its neighboring purines can prevent the dimerization of TT in DNA (*20*). Although G or A was incapable of repairing thymine dimer in a trinucleotide context via the electron transfer mechanism (*21*), the better electron donor OG in the stacked environments of ssDNA and the DNA duplex efficiently repaired this lesion. In our system, we also found the OG:A base pair was more effective than the OG:C base pair even though the OG:C duplex is slightly more stable (*1*). This observation drove us to an argument that the photoexcited state of OG in the OG:C base pair may also decay via a proton-coupled electron (PCET) mechanism as was proposed for the G:C base pair (Figure 3.6). The results in this chapter further support this argument.

The difference in the thymine dimer repair efficiency between the OG:F and OG:C base pairs (Figure 3.2) suggests that there is a competition of electron transfer through base pairing (OG to C) *vs.* base stacking (OG to T=T). At the 5' side where T=T still retains good stacking with its neighboring base (*16, 17, 22*), the ET through base stacking may be dominant and a higher activity is observed in the more stable duplex (OG:C>OG:F). Stacking at the 3' site of T=T is highly perturbed (*16, 17, 22*); therefore, the photoexcited state of 3'-OG might mainly decay via a PCET mechanism in the OG:C

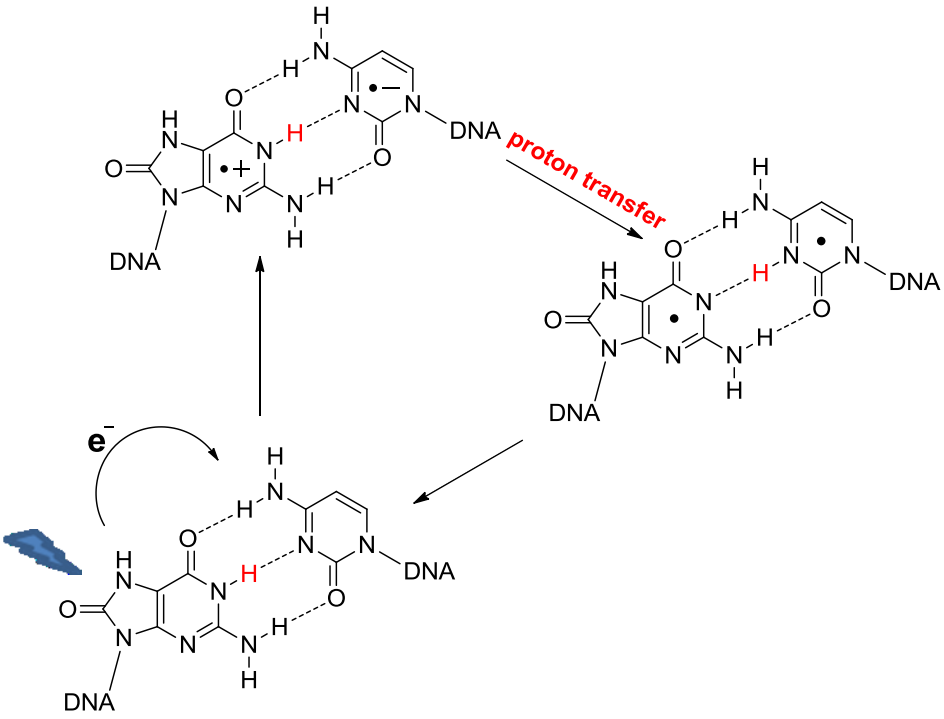

Figure 3.6. A proposed PCET pathway to deactivate the photoexcited state of OG in OG:C base pair

base pair. Because the PCET mechanism could not occur with OG:F, it is more reactive than the OG:C base pair, even though the OG:F duplex is clearly less stable than the OG:C duplex. Furthermore, we always observed a higher activity of OG:F than OG:C when OG does not directly stack to T=T (Figure 3.2), and this does not depend on the location of OG with respect to T=T. These results reasonably suggest that the PCET pathway to deactivate the photoexcited state of OG in OG:C base pair is possible, and it competes with the intrastrand electron transfer from OG to T=T that ultimately leads to the repair of thymine dimer.

In addition, the relative reactivity of OG:F to OG:A also shows interesting aspects. In duplexes with OG directly flanking T=T, OG:A is about 4-7-fold more efficient than OG:F depending on the orientation of OG with respect to T=T (Figure 3.2, 1A vs. 1F, 2A vs. 2F). Obviously, the helical structure at the T=T site is highly disturbed (*16, 17*), therefore, a stable base pair OG:A that is incapable of being deactivated by a PCET mechanism (*1*) may be necessary to maintain efficient repair of the thymine dimer. However, OG:A and OG:F have quite similar reactivity when an A:T base pair was inserted in between OG and T=T (Figure 3.2, 3A vs. 3F, 4A vs. 4F). In these duplexes, we believe an A is possibly a bridge for an electron moving from OG to T=T (*1*). As previously described, the formation of an exciplex between two neighboring bases in oligonucleotides containing A and T was independent of base pairing (*3*). Because the stacking between OG and its adjacent base A is likely similar to the stacking motif of a normal DNA duplex, we thought the formation of an exciplex OG^{+}-A^{-} may not depend on the base paired with OG unless this leads to the PCET deactivation pathway. Therefore, the thymine dimer repair efficiency is quite similar between OG:A and OG:F

duplexes with OG and T=T intervened by a dA.

The capability of OG mediating the repair of thymine dimer in ssDNA further supports a repair mechanism via the formation of an exciplex. Because ssDNA may have a similar base stacking motif as a DNA duplex (*2*), the 5'-3' direction preference for the repair efficiency was still observed in ssDNA (Figure 3.4). When a dA was inserted in between 5'-OG and T=T, we observed the expected trend in which the thymine dimer repair efficiency decreased by 5-fold (Figure 3.4, 1S vs. 3S). In contrast, the same modification at the 3' site of T=T even slightly increases the repair efficiency (Figure 3.4, 2S vs. 4S). Indeed, this opposite trend was observed in the case of hole transfer from 2-aminopurine to a guanine derivative in DNA duplex (*23*). In this case, the decomposition rate of the guanine derivative was used to determine the hole transfer efficiency and the distance effect was inverted because the back electron transfer at a short distance is much faster than the rate of the decomposition reaction (*23*). However, this explanation may not be applied to our system because we still observed the normal distance effect at the 5' side of T=T. Instead, we thought the unusual distance effect at the 3' side of T=T may be caused by the kinked structure at this site. Although ssDNA is considered to have the same stacking motif as duplex DNA, this structure in ssDNA is obviously more dynamic. Therefore, the formation of an exciplex between T=T and its neighboring 3'-OG will greatly be reduced in ssDNA resulting in very low thymine dimer repair efficiency. When a dA is inserted in between 3'-OG and T=T, the formation of the exciplex $OG^{+}A^{-}$ is more feasible, and the repair efficiency may be enhanced. Nevertheless, the fact that the photorepair activity of OG was able to operate in ssDNA suggested that repair was probably proceeded via the formation of an exciplex. In addition, the activity still remains

at longer range (one nucleotide distance) may also indicate an excess electron transfer (EET) mechanism for the repair (*1, 24*).

The finding that OG can efficiently repair CPD in both DNA and RNA contexts when it was opposite to one of the bases of these lesions strengthens the potential role of OG as a RNA coenzyme, because it shows that the photorepair activity of OG can operate in versatile environments. Since the coenzyme OG may not always directly stack next to CPD in the same strand, this finding implies that "OG containing ribozymes" could dock with the dimers and repair these lesions. As shown in an NMR study, G can form a wobble base pair with the 3' T of the dimer T=T and cause only a little conformational distortion compared to the parent T=T:AA duplex (*25, 26*). Having the same pyrimidine ring as G, OG may also have the capability of forming a similar wobble base pair with T (Figure 3.1), even though the carbonyl group at C-8 of OG might also affect the stability of this base pair. Similarly, OG also could form a wobble base pair with U in DNA/RNA duplex. Therefore, the CPD repair in these systems was likely triggered by an internal electron transfer in OG:T or OG:U base pairs (Figure 3.7). In addition, the higher feasibility of the 3' T of the dimer in forming the base pair than the 5' T (*16*) may explain the higher activity of OG when paired with this 3' T.

The next question one would ask is how the electron can transfer in an excited OG:T base pair. As discussed above, we have evidence that electron transfer can occur in the excited OG:C base pair. As for the G:C base pair (*7, 9*), the driving forces for an electron transferring from the photoexcited state of OG to C are probably the high electron affinity of C and a spontaneous proton transfer from a radical cation $OG^{+\cdot}$ to a radical anion $C^{-\cdot}$. This pathway will deactivate the photoexcited state of OG and decrease

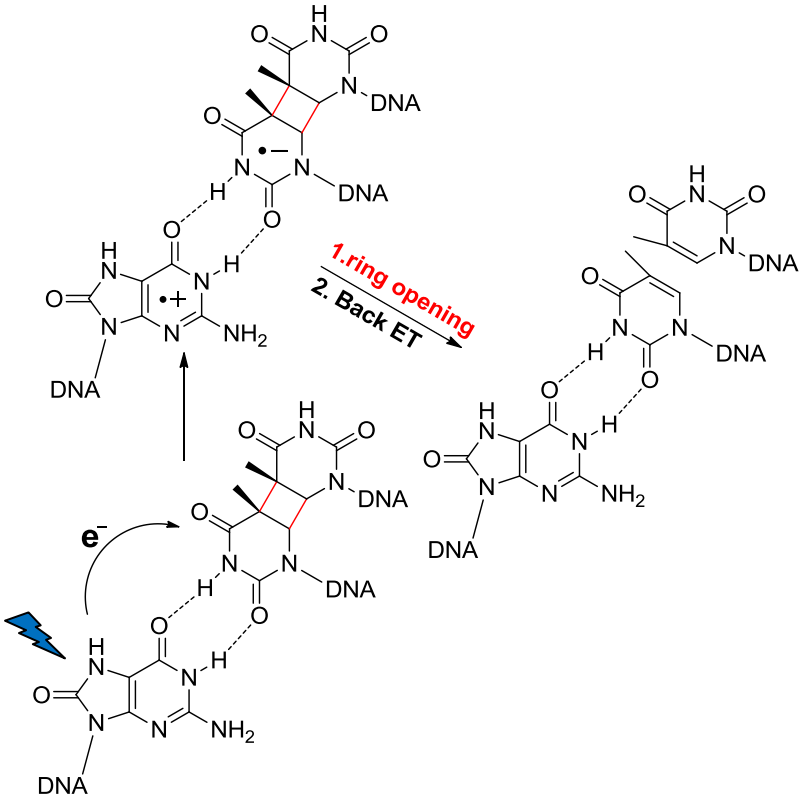

Figure 3.7. Thymine dimer repair is triggered by an internal electron transfer in a wobble OG:T base pair

the thymine dimer repair efficiency. Since T of the T=T dimer is also a good electron acceptor, and the opening of the cyclobutane ring is ultrafast and entropically favorable (*18*), the formation of a charge-transfer species $OG^{+\cdot}$-T=$T^{-\cdot}$ and then the repair of thymine dimer from the radical anion T=$T^{-\cdot}$ are plausible. One could argue that a proton-coupled electron transfer mechanism may also occur in the OG:T base pair and does not lead to the thymine dimer repair. However, we think this pathway would be very inefficient. The reason is that in a wobble OG:T base pair the N1-H of OG forms a hydrogen bond with the oxygen at C6 of T (Figure 3.1) and the proton transfer from the N-H group to an oxyanion is an endothermic process. It is also interesting to note that the internal electron transfer in the G:C base pair was proposed as a deactivation pathway to avoid DNA photodamage in the early stages of the origin of life (*9, 27*). A similar pathway occurring in the OG:T base pair found in our study may contribute to understanding how the photodamage of nucleic acid was repaired during the evolution of life.

Conclusion

In conclusion, we extended studies on the effects of sequence contexts on the repair efficiency of cyclobutane pyrimidine dimer by OG in DNA and RNA to better understand photodynamic insights of the repair mechanism. From findings in these studies, we believe the repair process was triggered by the formation of an intrastrand (via base stacking) or an interstrand (via base pairing) exciplex $OG^{+\cdot}$-$T^{-\cdot}$ The opening of a cyclobutane ring is fast enough to efficiently compete with the charge recombination of these exiplexes and leads to the repair of the dimer. We also have evidence of a PCET pathway to deactivate the photoexcited state of OG in an OG:C base pair, and this results

in the low repair efficiency of this base pair. Although the employment of ultrafast techniques to fully understand mechanistic insights is necessary, these results showed that the photorepair activity of OG could operate in versatile environments of base stacking and base pairing. This provides additional support for our hypothesis of OG as a prebiotic version of the redox coenzyme flavin. Furthermore, the ability of OG to bind with different bases and its property to induce electron transfer upon photoirradiation may make OG a promising probe to study the photodynamics of DNA.

Experimental

All chemicals were purchased from commercial sources and used without further purification unless otherwise stated. DNA containing OG and T=T were synthesized at the DNA/Peptide Core Facility at the University of Utah and purified as previously described (*1*). RNA containing U=U was synthesized from the unmodified RNA by photoirradiation using acetone as a photosensitizer (*1*). The concentration of DNA and RNA was determined by UV-VIS spectroscopy on the Beckman DU 650 spectrometer. Complete sequences studied are shown in Table 3.2.

General procedure for photorepair of CPD by OG. 5 uM of DNA or RNA containing OG and CPD in a buffer solution containing 20 mM NaPi and 100 mM NaCl at pH 7 were irradiated in polystyrene cuvettes to cut off wavelengths below 300 nm (*28*) at ambient temperature (22 °C) with an FS40 UVB lamp (peak at 313 nm). The irradiation mixtures were analyzed by appropriate HPLC methods to calculate the repair yield. Thymine dimer repair yield was then plotted as a function of irradiation time and fit to exponential curve using OriginPro 8.5 software (Originlab). The repair

Table 3.2. Complete sequences studied and their corresponding quantum yields of thymine dimer repair.

	Sequences	$10^3\ \Phi_{repair}$
1A	5′-CACAGC**OT=T**ACAGTACAC-3′ 3′-TCTGTGTCG**A**A ATGTCATGTGT-5′	10
1C	5′-CACAGC**OT=T**ACAGTACAC-3′ 3′-TCTGTGTCG**C**A ATGTCATGTGT-5′	3.8
1F	5′-CACAGC**OT=T**ACAGTACAC-3′ 3′-TCTGTGTCG**F**A ATGTCATGTGT-5′	1.3
2A	5′-CACAGCA**T=TO**CAGTACAC-3′ 3′-TCTGTGTCGTA A**A**GTCATGTGT-5′	4.7
2C	5′-CACAGCA**T=TO**CAGTACAC-3′ 3′-TCTGTGTCGTA A**C**GTCATGTGT-5′	0.7
2F	5′-CACAGCA**T=TO**CAGTACAC-3′ 3′-TCTGTGTCGTA A**F**GTCATGTGT-5′	1.3
3A	5′-ACAGC**O**A**T=T**ACAGTACAC-3′ 3′-TCTTGTCG**A**TA ATGTCATGTGT-5′	0.4
3C	5′-ACAGC**O**A**T=T**ACAGTACAC-3′ 3′-TCTTGTCG**C**TA ATGTCATGTGT-5′	NA*
3F	5′-ACAGC**O**A**T=T**ACAGTACAC-3′ 3′-TCTTGTCG**F**TA ATGTCATGTGT-5′	0.3
4A	5′-CACAGCA**T=T**A**O**CAGTACA-3′ 3′-TCTGTGTCGTA ATAGTCATGTT-5′	0.6
4C	5′-CACAGCA**T=T**A**O**CAGTACA-3′ 3′-TCTGTGTCGTA AT**C**GTCATGTT-5′	NA*
4F	5′-CACAGCA**T=T**A**O**CAGTACA-3′ 3′-TCTGTGTCGTA AT**F**GTCATGTT-5′	0.4
1S	5′-CACAGC**OT=T**ACAGTACAC-3′	2.9
2S	5′-CACAGCA**T=TO**CAGTACAC-3′	0.3
3S	5′-ACAGC**O**A**T=T**ACAGTACAC-3′	0.6
4S	5′-CACAGCA**T=T**A**O**CAGTACA-3′	0.4
5T	5′-CACAGCA**T=T**ACAGTACAC-3′ 3′-TCTGTGTCGTA **O**TGTCATGTGT-5′	7.3
6T	5′-CACAGCA**T=T**ACAGTACAC-3′ 3′-TCTGTGTCGT**O** ATGTCATGTGT-5′	0.9
RNA/DNA	5′-CACAGCA**U=U**ACAGUACAC-3′ 3′-TCTGTGTCGTA **O**TGTCATGTGT-5′	
RNA/DNA	5′-CACAGCA**U=U**ACAGUACAC-3′ 3′-TCTGTGTCGT**O** ATGTCATGTGT-5′	

*repair yields are too low for accurate calculation

rate (% min^{-1}) was calculated and this value was used to compare the repair efficiency of different DNA duplexes (*29*). These values were converted to quantum yields (moles of T=T repaired per min/moles of photons absorbed by OG per min) with an assumption that OG is the only species that absorbed the light at 313nm with an estimated extinction coefficient ε = 2400 $L.mol^{-1}.cm^{-1}$ (Table 3.2). The intensity of incident light was determined by the method of ferrioxalate actinometry (*30*).

References

1. Nguyen, K. V., and Burrows, C. J. (2011) A prebiotic role for 8-Oxoguanosine as a flavin mimic in pyrimidine dimer photorepair, *J. Am. Chem. Soc. 133*, 14586-14589.

2. Middleton, C. T., de La Harpe, K., Su, C., Law, Y. K., Crespo-Hernandez, C. E., and Kohler, B. (2009) DNA Excited-state dynamics: From single bases to the double helix, *Annu. Rev. Phys. Chem. 60*, 217-239.

3. Crespo-Hernandez, C. E., Cohen, B., and Kohler, B. (2005) Base stacking controls excited-state dynamics in A:T DNA, *Nature 436*, 1141-1144.

4. Crespo-Hernandez, C. E., de La Harpe, K., and Kohler, B. (2008) Ground-state recovery following UV excitation is much slower in GC-DNA duplexes and hairpins than in mononucleotides, *J. Am. Chem. Soc. 130*, 10844-10845.

5. Takaya, T., Su, C., de La Harpe, K., Crespo-Hernandez, C. E., and Kohler, B. (2008) UV excitation of single DNA and RNA strands produces high yields of exciplex states between two stacked bases, *Proc. Natl. Acad. Sci., 105*, 10285-10290.

6. de La Harpe, K., Crespo-Hernandez, C. E., and Kohler, B. (2009) Deuterium isotope effect on excited-state dynamics in an alternating GC oligonucleotide, *J. Am. Chem. Soc. 131*, 17557-17559.

7. Kumar, A., and Sevilla, M. D. (2010) Proton-coupled electron transfer in DNA on formation of radiation-produced ion radicals, *Chem. Rev. 110*, 7002-7023.

8. Schwalb, N. K., and Temps, F. (2007) Ultrafast electronic relaxation in guanosine is promoted by hydrogen bonding with cytidine, *J. Am. Chem. Soc. 129*, 9272-9273.

9. Sobolewski, A. L., Domcke, W., and C., H. (2005) Tautomeric selectivity of the excited-state lifetime of guanine/cytosine base pairs: The role of electron-driven proton-transfer processes, *Proc. Natl. Acad. Sci. 102*, 17903-17906.

10. Groenhof, G., Schäfer, L. V., Boggio-Pasqua, M., Goette, M., Grubmüller, H., and Robb, M. A. (2007) Ultrafast deactivation of an excited cytosine-guanine base pair in DNA, *J. Am. Chem. Soc. 129*, 6812-6819.

11. Kwok, W.-M., Ma, C., and Phillips, D. L. (2006) Femtosecond time- and wavelength-resolved fluorescence and absorption spectroscopic study of the excited states of adenosine and an adenine oligomer, *J. Am. Chem. Soc. 128*, 11894-11905.

12. Sobolewski, A. L., and Domcke, W. (2004) Ab initio studies on the photophysics of the guanine-cytosine base pair, *Phys. Chem. Chem. Phys. 6*, 2763-2771.

13. Biemann, L., Kovalenko, S. A., Kleinermanns, K., Mahrwald, R., Markert, M., and Improta, R. Excited state proton transfer is not involved in the ultrafast deactivation of Guanine:Cytosine pair in solution, *J. Am. Chem. Soc. 133*, 19664-19667.

14. McAuley-Hecht, K. E., Leonard, G. A., Gibson, N. J., Thomson, J. B., Watson, W. P., Hunter, W. N., and Brown, T. (1994) Crystal structure of a DNA duplex containing 8-hydroxydeoxyguanine-adenine base pairs, *Biochemistry 33*, 10266-10270.

15. Shibutani, S., Takeshita, M., and Grollman, A. P. (1991) Insertion of specific bases during DNA synthesis past the oxidation-damaged base 8-oxodG, *Nature 349*, 431-434.

16. Park, H., Zhang, K., Ren, Y., Nadji, S., Sinha, N., Taylor, J.-S., and Kang, C. (2002) Crystal structure of a DNA decamer containing a cis-syn thymine dimer, *Proc. Natl. Acad. Sci. 99*, 15965-15970.

17. McAteer, K., Jing, Y., Kao, J., Taylor, J. S., and Kennedy, M. A. (1998) Solution-state structure of a DNA dodecamer duplex containing a cis-syn thymine cyclobutane dimer, the major UV photoproduct of DNA, *J. Mol. Biol. 282*, 1013-1032.

18. Chatgilialoglu, C., Guerra, M., Kaloudis, P., Houée-Lévin, C., Marignier, J. L., Swaminathan, V., and Carell, T. (2007) Ring opening of the cyclobutane in a thymine dimer radical anion, *Chem. Eur. J. 13*, 8979-8984.

19. Liu, Z., Tan, C., Guo, X., Kao, Y.-T., Li, J., Wang, L., Sancar, A., and Zhong, D. (2011) Dynamics and mechanism of cyclobutane pyrimidine dimer repair by DNA photolyase, *Proc. Natl. Acad. Sci. 108*, 14831-14836.

20. Pan, Z., Hariharan, M., Arkin, J. D., Jalilov, A. S., McCullagh, M., Schatz, G. C., and Lewis, F. D. Electron donor-acceptor interactions with flanking purines influence the efficiency of thymine photodimerization (2011), *J. Am. Chem. Soc. 133*, 20793-20798.

21. Pan, Z., Chen, J., Schreier, W. J., Kohler, B., and Lewis, F. D. Thymine dimer photoreversal in purine-containing trinucleotides, *J. Phys. Chem B 116*, 698-704.

22. Cannistraro, V. J., and Taylor, J.-S. (2009) Acceleration of 5-Methylcytosine deamination in cyclobutane dimers by G and tts implications for UV-induced C-to-T mutation hotspots, *J. Mol. Biol., 392*, 1145-1157.

23. O'Neill, M. A., Dohno, C., and Barton, J. K. (2004) Direct chemical evidence for charge transfer between photoexcited 2-aminopurine and guanine in duplex DNA, *J. Am. Chem. Soc. 126*, 1316-1317.

24. Ito, T., Kondo, A., Terada, S., and Nishimoto, S.-i. (2006) Photoinduced reductive repair of thymine glycol: Implications for excess electron transfer through DNA containing modified bases, *J. Am. Chem. Soc. 128*, 10934-10942.

25. Jing, Y., Taylor, J.-S., and Kao, J. F.-L. (1998) Thermodynamic and base-pairing studies of matched and mismatched DNA dodecamer duplexes containing cis-syn, (6-4) and Dewar photoproducts of TT, *Nucl. Acid. Res. 26*, 3845-3853.

26. Lee, J. H., Park, C. J., Shin, J. S., Ikegami, T., Akutsu, H., and Choi, B. S. (2004) NMR structure of the DNA decamer duplex containing double T·G mismatches of *cis-syn* cyclobutane pyrimidine dimer: implications for DNA damage recognition by the XPC-hHR23B complex, *Nucl. Acid. Res. 32*, 2474-2481.

27. Abo-Riziq, A., Grace, L., Nir, E., Kabelac, M., Hobza, P., and de Vries, M. S. (2005) Photochemical selectivity in guanine-cytosine base-pair structures, *Proc. Natl. Acad. Sci. 102*, 20-23.

28. Chinnapen, D. J.-F., and Sen, D. (2004) A deoxyribozyme that harnesses light to repair thymine dimers in DNA, *Proc. Natl. Acad. Sci. 101*, 65-69.

29. Ito, T., and Rokita, S. E. (2004) Criteria for efficient transport of excess electrons in DNA, *Angew. Chem. Int. Ed 43*, 1839-1842.

30. Montalti, M., Credi, A., Prodi, L., and Gandolfi, M. T. (2006) Handbook of photochemistry, Third ed., Taylor & Francis Group.

CHAPTER 4

TOWARD THE STUDY OF PYRIMIDINE DIMER REPAIR BY DINUCLEOTIDES CONTAINING 8-OXOGUANOSINE

Introduction

The existence of a primordial RNA world in which RNA carried out both functions as genetic and catalytic materials is widely accepted. The persistence of nucleotides in most of the modern coenzymes suggests a central role of RNA in early metabolism. In 1976, White first recognized this phenomenon and proposed that these coenzymes are "fossils" of the RNA world and probably evolved from nucleotides (*1*). Recently, Yarus hypothesized a stronger role in evolution for nucleotide coenzymes as modern descendants of Initial Darwinian Ancestors (IDA) (*2*) (Figure 4.1). He thought 5'-5' linked cofactors such as NAD^+ and FAD were primordial replicators prior to the RNA world, because they potentially have stacked structures and might form base pairs with counterpart nucleotides during replication (Figure 4.1). In addition, the 5'-5' link is easily formed from 5'-activated nucleotides and has more chemical resistance than 3'-5' link in term of hydrolysis and is less sensitive to sugar chirality that might make it tolerant of various sugars. 5'-5' replicators with functional nucleotides were later selected to participate in metabolism and then served as cofactors for primordial ribozymes to

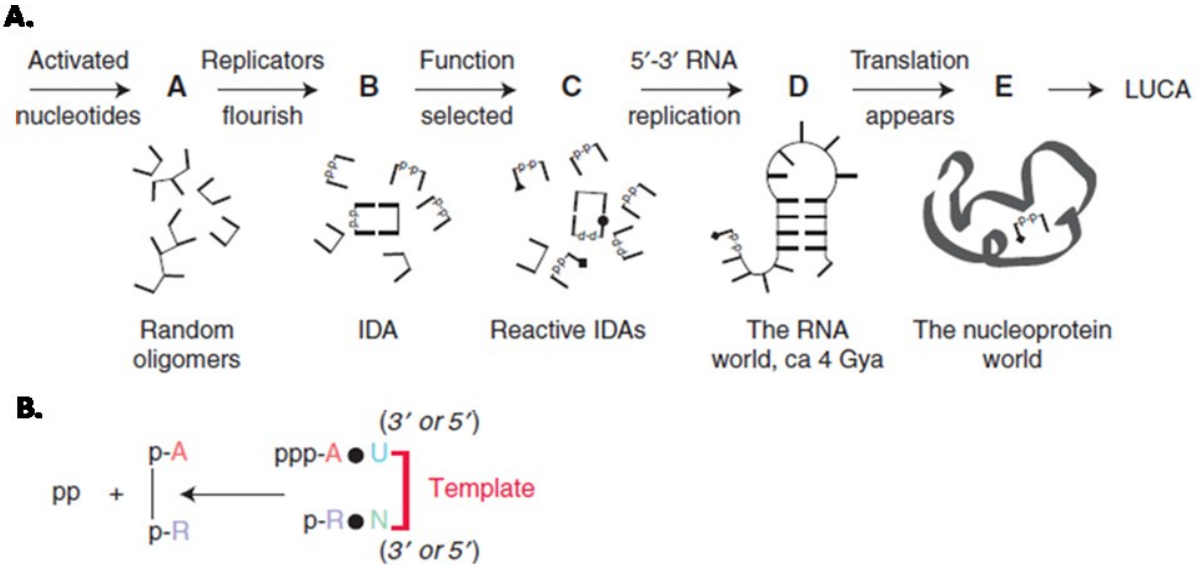

Figure 4.1*. (A) The IDA in context. Roles of 5'-5' dinucleotides in metabolism as primordial replicators and cofactors for ribozymes and ribonucleoproteins. (B) Replication scheme for AMP-containing dinucleotides such as FAD and NAD^+.
*Reproduced with permission from *Cold Spring Harb Perspect Biol*. *doi: 10.1101/cshperspect.a003590*

support the more diverse metabolism in the RNA world. Through evolution, only a few extremely effective 5'-5' dinucleotide cofactors in catalysis such as NAD^+ and FAD were adopted by protein enzymes and are still present today.

Based on experimental observations and theoretical arguments, Yarus hypothesized that dinucleotide cofactors may have served the important roles as replicators in the pre-RNA world and cofactors in the RNA world, for. We proposed that 8-oxoguanosine was a primitive flavin because both OG and flavin heterocycles are "matured" from the canonical base G, however flavin is made via several biosynthetic steps while OG is only one chemical step away from G (Chapter 1). Support for this proposal is that OG can mimic a function of flavin in repairing the photodamage lesions CPDs (Chapter 2 & 3). Following the logic of the Yarus hypothesis, we question is there any role for OG-containing dinucleotides in the origin of life? More specifically, could 5'-5' diphosphate diribonucleotide OA ($OADH_2$), a closer mimic of $FADH_2$ (Figure 4.2), be a component of IDA as a replicator and then enter the RNA world as a primitive redox cofactor? A role for $OADH_2$ as a replicator is reasonable because the unique structure of OG allows it to form base pairs with various bases. Therefore, in this chapter, we will investigate the cofactor chemistry of $OADH_2$ in mediating CPD repair to see if it could have played any role in primitive metabolism. A hint for the possibility of this chemistry comes from a result in Chapter 3 in which OG effectively repairs CPDs when it pairs with the 3' monomer (T or U) of the dimers in 18mer DNA/DNA or DNA/RNA duplexes. We postulate that $OADH_2$ dinucleotide would potentially bind to CPDs, probably via a Watson-Crick base pair A:T(U) and a wobble base pair OG:T(U), under plausible prebiotic conditions of low temperature and high salt concentration and lead to

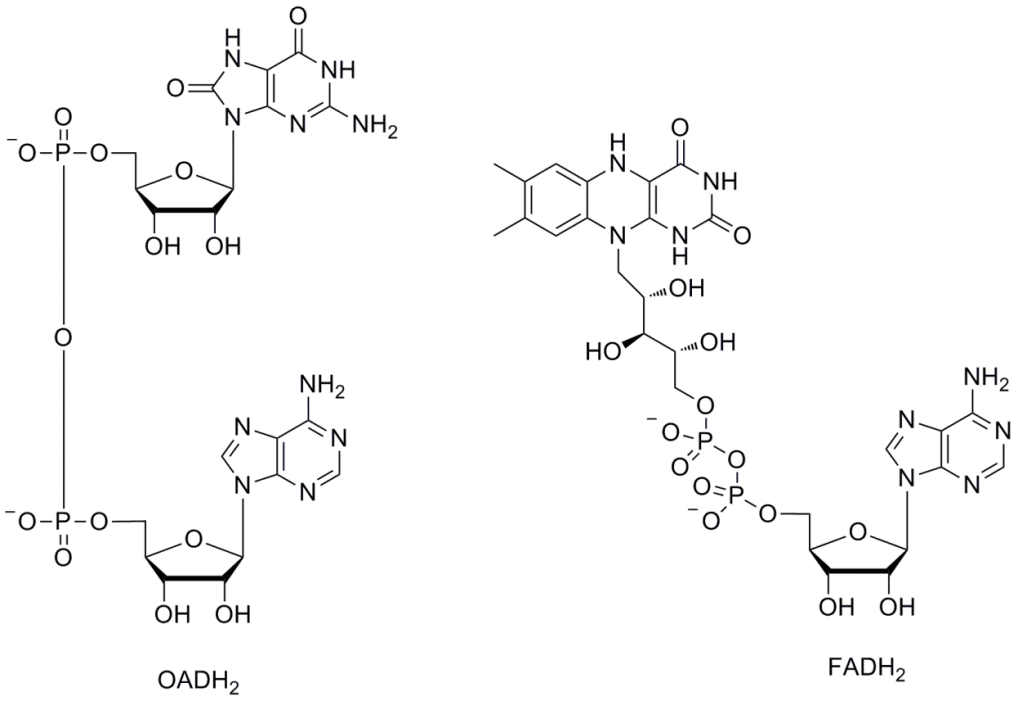

Figure 4.2. Structures of 5'-5' AMP-containing dinucleotides $OADH_2$ and $FADH_2$

CPD repair upon irradiation (Figure 4.3). In this case, $OADH_2$ might be considered a "minimal ribozyme" to repair CPD.

Results and discussion

Effects of temperature and salt concentration on thymine dimer repair by OG. In our proposal of utilizing OG-containing dinuleotides to repair CPDs, temperature and salt concentration are thought to be crucial factors to enhance the binding efficiency between substrates and catalysts. Thus, we first want to know if these two factors have any effect on CPD repair. For this purpose, we designed a 9mer duplex containing an OG paired with the 3' T of a T=T dimer (Figure 4.4). This duplex, with a melting point in the range of 15-20 $^{\circ}$C (by theoretical calculation), is convenient for studying effects of temperature and salt concentration on binding efficiency.

The thymine dimer repair was first investigated at ambient temperature (22 $^{\circ}$C) in which the duplex is assumed to melt (Figure 4.4). The repaired strand was detected by denaturing HPLC and the peaks corresponding to the thymine dimer strand and the repaired strand were integrated to calculate the repair yield. In an experiment carried out in buffer solution containing 100 mM NaCl, about 14% of thymine dimer was repaired after 2 h of irradiation. This value is significantly lower than the repair yield observed in the case of a 18mer duplex under the same conditions (Chapter 3), suggesting the importance of maintaining a stable duplex for effective repair. As expected, the repair yield increased when the salt concentration was increased to 1 M, because high salt concentration favors duplex formation. However, we observed a lower repair yield at 3 M NaCl compared to that at 1 M NaCl. We postulate that at a very high salt concentration,

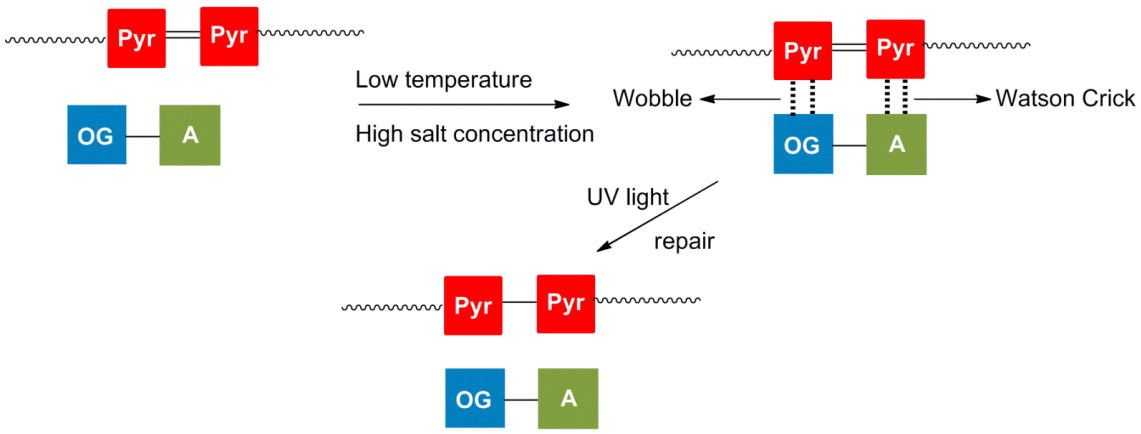

Figure 4.3. A proposed repair pathway of pyrimidine dimers by dinucleotide OA

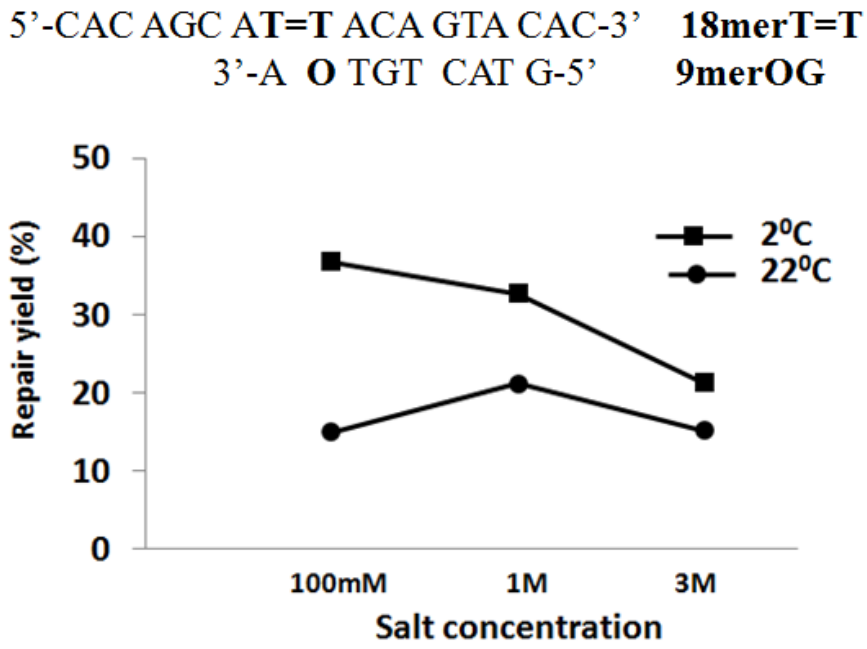

Figure 4.4. Repair yields of thymine dimer in an 18mer DNA strand annealed to a OG-containing 9mer DNA strand after 2 h of irradiation.

DNA might adopt conformations other than B-form and these conformations may be unfavorable structures for electron transfer and therefore reduce the efficiency of thymine dimer repair.

With experiments carried out at 2 $^{\circ}$C, thymine dimer repair yield significantly increases at every salt concentration (Figure 4.4). This result again indicates that a stable duplex is necessary for effective repair of thymine dimer. However, we found that the repair yield was highest at 100 mM salt and decreased when the salt concentration was increased to 1 M or 3 M. Again, we think the change in conformation of the double helix is responsible for this result, and it is possible that this change might require lower salt concentration at low temperature. Nevertheless, we found temperature and salt concentration have significant effect on thymine dimer repair. To get effective repair, these two factors should be optimized to guarantee the T=T substrate and the OG catalyst "immobilized" in a stable duplex at a "correct" conformation of double helix.

Repair of thymine dimer by deoxyribodinucleotide d(OA). The above results suggest that the binding between OG-containing dinucleotides and CPD might be improved by changing the temperature and salt concentration of the buffer solution and make it possible for OG-containing dinucleotides to mediate CPD repair. For ease in synthesis, we first investigated the repair of thymine dimer in a 6mer DNA substrate (6mer T=T) by 5'-3' monophosphate deoxyribodinucleotide d(OA), since d(OA) can be synthesized from commercially available phosphoramidites (Figure 4.5). In addition, OG was placed at the 5' side, because our previous results showed that OG paired with the 3'T of the dimer is more effective in repairing thymine dimer (Chapter 3). The irradiation procedure is described in the experimental section. The irradiation mixture was then

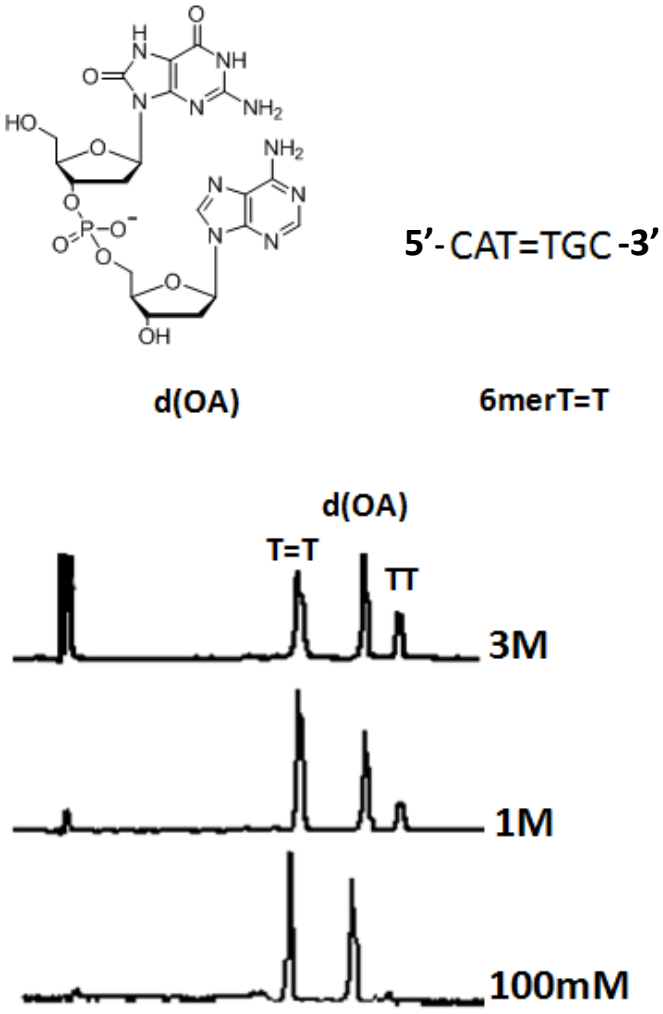

Figure 4.5. HPLC analyses of mixtures containing d(OA) and 6merT=T after 5 h of irradiation at various salt concentrations.

analyzed by reversed phase HPLC to detect the repaired strand and the repair yield was calculated by integration of appropriate HPLC peaks.

At 2 °C, thymine dimer repair yields after 5 h of irradiation were very low (<3%), even at 3 M salt. This result suggested that the binding between d(OA) and T=T is weak and the system seems to have bimolecular characteristic at this temperature (Chapter 5). Therefore, it may be necessary to lower the temperature to enhance the binding of the dinucleotide catalyst to the dimer substrate. In the next set of experiments, we irradiated the sample in a frozen aqueous solution on a dry ice surface (~ -78 °C), which is a condition widely used to study the photochemistry of pyrimidine bases (*3-5*). Analysis of the irradiation mixture by HPLC showed that thymine dimer repair yield significantly increased as compared to that at 2 °C (Figure 4.5). In addition, the repair efficiency was dependent on salt concentration and was better at higher salt concentration. At 3 M NaCl, the thymine dimer repair yield after 5h of irradiation reached about 20%, a much higher yield than that of the bimolecular reaction (Chapter 5). Although this value is still lower than the yield observed in long DNA duplex, it clearly suggested that d(OA) can bind with the T=T site and facilitate the repair.

Repair of pyrimidine dimers by $OADH_2$. Promising results from the repair of T=T by deoxyribodinucleotide d(OA) triggered us to investigate the potential of $OADH_2$ in the same chemistry. Because $OADH_2$ is not commercially available, we first designed a synthetic scheme for this compound following a general procedure to make 5'-5' diphosphate diribonucleotides (*6*) (Figure 4.6). Initially, 8-oxoguanosine-5'-monophosphate (OGMP) was synthesized from guanosine-5'-monophosphate (GMP) by a method developed by Dr. Aaron Fleming in our lab (*7*). OGMP was then coupled with

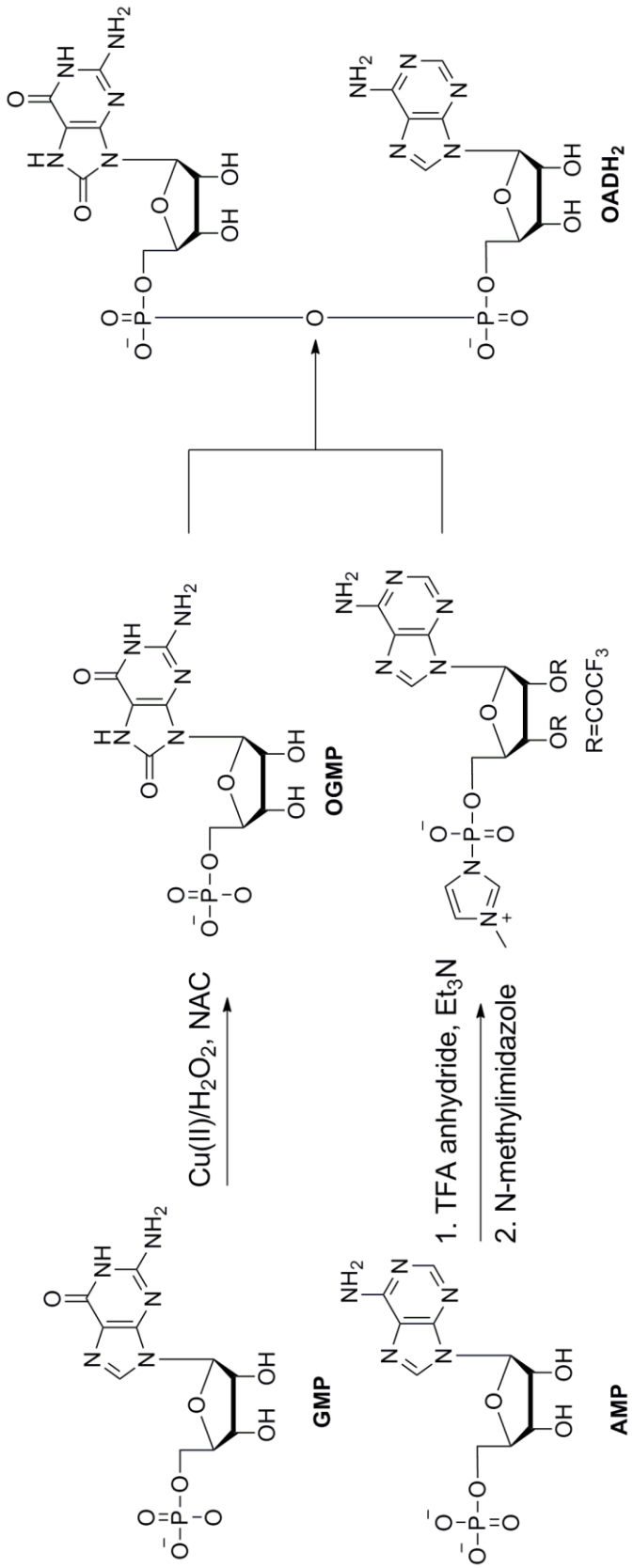

Figure 4.6. A scheme for synthesis of 5'-5' dinucleotide $OADH_2$

an activated adenosine-5'-monophosphate (AMP) that was prepared *in situ* as previously described to form $OADH_2$ with a 10% yield. Optimization of this coupling reaction to get a higher yield of $OADH_2$ is a subject for our future investigation. The identity of $OADH_2$ was confirmed by mass spectrometric analysis and its UV spectrum was identical to the authentic d(OA), therefore no further characterization was carried out.

We next investigated the repair of thymine dimer in a 6mer DNA strand by $OADH_2$ in a frozen aqueous solution containing 3 M NaCl. After 5 h of irradiation, approximately 8% of thymine dimer was repaired (Table 4.1). Apparently, $OADH_2$ is less effective than d(OA) in repairing thymine dimer in DNA within experimental error. At this time, we think this result is caused by the difference in binding ability to T=T between $OADH_2$ and d(OA). The diphosphate link in $OADH_2$ may be too long for effective formation of base pairs between the components of $OADH_2$ and the two T of the T=T dimer. Obviously, additional experimentation is needed to validate this argument. In addition, we also examined the possibility of repairing U=U in a 6mer RNA by d(OA) and $OADH_2$. However, the repair yield was too low (<1%) in both cases to make a quantitative comparison (Table 4.1). Nevertheless, it is evident that $OADH_2$ can bind to the CPDs and facilitate the repair of these lesions. Optimization of reaction conditions may be necessary to improve the repair yield, and this is our goal for next set of experiments.

Conclusion

Inspired by the recent Yarus hypothesis on the role of dinucleotide cofactors in evolution and our findings on mediating CPD repair by OG paired with one monomer of

Table 4.1. Preliminary results on repair yields of pyrimidine dimers by OG-containing dinucleotides after 5 h of irradiation at 3 M salt concentration at -78 °C.

substrates / catalysts	6merT=T	6mer U=U
d(OA)	21%	<1%
$OADH_2$	8%	<1%

the dimers in Chapter 3, we investigated the potential of OG-containing dinucleotides as a minimal ribozyme to repair CPDs in short DNA and RNA oligomers. Our preliminary results showed that these dinucleotides could bind to CPDs at sufficiently low temperature and high salt concentration and mediate repair upon irradiation. We also found that $OADH_2$ has lower photorepair activity than d(OA), probably because the long 5'-5' diphosphate linkage in $OADH_2$ reduces the binding efficiency of this molecule to CPD. Our future work will focus on optimizing reaction conditions to increase the repair yield.

Experimental

Synthesis and purification of d(OA). d(OA) was synthesized from the corresponding phosphoramidites at the University of Utah Core Facility. The dinucleotide was cleaved from the synthetic column by incubating with concentrated ammonium hydroxide solution containing 0.25 M β-mercaptoethanol as an antioxidant at room temperature for 16 h. The solution was then transferred into a vial, incubated at 55 $^{\circ}$C for 17 h to remove base protecting groups, then dried down. The crude material was purified by ion-exchange HPLC on a Dionex DNA Pac PA-100 column with linear gradient of 0% to 2% B over 15 min (solvent A: 10% acetonitrile in water; solvent B: 1.5 M sodium acetate, 10% acetonitrile in water, pH 7). Dinucleotide was desalted by passing through a C18 column with isocratic 8% of B (Solvent A: 0.1% formic acid in water; solvent B: acetonitrile). Concentration of d(OA) was determined by UV spectroscopy.

Synthesis of 6mer DNA containing T=T. A literature procedure was followed (*8*). Briefly, a solution containing 6mer DNA (CATTGC) (150 μM) and acetophenone (5 mM) in water was degassed by bubbling Argon for 30 min and then irradiated by a UVB lamp in a polystyrene cuvette for 2 h. The product (6merT=T) was purified by reversed phase HPLC on a Variant C18 column with linear gradient of 1% to 15% B over 30 min (solvent A: 20 mM ammonium acetate in water, pH 7; solvent B: acetonitrile).

Synthesis of 6mer RNA containing U=U. Uracil dimer containing RNA was synthesized as previously described (*9*). Briefly, a solution containing 6mer RNA (CAUUGC) (150 μM) and acetone (10%) in water was degassed and then irradiated by a UVB lamp in a glass vial for 1.5 h. The product (6merU=U) was purified by reversed phase HPLC on a Variant C18 column with linear gradient of 1%B to 15%B over 30 min (solvent A: 20 mM ammonium acetate in water, pH 7; solvent B: acetonitrile).

Synthesis of OGMP. To a solution of 75 mM NaPi at pH 7 containing GMP (0.72 mg, 2 mM) was added copper (II) acetate (0.18 mg, 1 mM), NAC (3.26 mg, 20 mM), followed by addition of 30% wt H_2O_2 solution (1.03 μL, 10 mM). The reaction mixture was stirred for 1 h at room temperature and quenched with EDTA (10 mM). OGMP was purified from the starting material and other reaction products by reversed phase HPLC on a Variant C18 column using the following method: isocratic 1% B in 10 min, then increase to 15% B over 30 min by a linear gradient (solvent A: 0.1% formic acid in water, solvent B: acetonitrile). The structure of OGMP was confirmed by mass spectrometric analysis ([M-H] calcd: 378.2, found: 378.8). The yield for OGMP formation is 25%.

Synthesis of $OADH_2$. To a suspension of AMP (2 μmol, 0.7 mg) in acetonitrile (10 μL) were added TEA (32.2 μmol, 4.5 μL) and TFAA (32 μmol, 4.5 μL). The reaction mixture was incubated at 0 °C for 30 min under argon and was concentrated under vaccuo. The oily residue was dissolved in 10 μL acetonitrile and 10 μL DMF, followed by addition of TEA (20 μmol, 3 μL), N-methylimidazole (10 μmol, 1 μL) and incubated at 0 °C for 30 min under argon until a bright yellow solution was obtained. This solution was then added to a suspension of triethylamonium salt of OGMP (2.5 μmol, 0.9 mg) in DMF (10 μL). After 2 h, the reaction mixture was quenched by ammonium acetate (250 mM, 1 mL) and washed with CH_2Cl_2 (3 X 1 mL). The $OADH_2$ product was purified by reversed phase HPLC on a Variant C18 column by linear gradient from 1% B to 65% B over 20 min (solvent A: 100 mM TEAA, pH 7; solvent B: acetonitrile) (yield 10%). MS (ESI) [M-H] calcd: 707.4, found: 706.8.

General procedures for photorepair of pyrimidine dimers by OG-containing dinucleotides and analysis of reaction mixtures. Solutions of 20 mM NaPi buffer at pH 7 containing different concentrations of NaCl and OG-containing dinucleotides (15 μM) and thymine dimer or uracil dimer-containing DNA or RNA (10 μM) were frozen in dry ice in polystyrene cuvettes. The frozen solutions were irradiated with an UVB lamp for 5 h. The reaction mixtures were analyzed by reversed phase HPLC on a Variant C18 column with isocratic 1% B in 5 min and then increasing to 15% B over 30 min (solvent A: 20 mM ammonium acetate, solvent B: acetonitrile). The repair yields were calculated from integration of HPLC peaks corresponding to the dimer and the repaired strands.

References

1. White, H. B. (1976) Coenzymes as fossils of an earlier metabolic state, *J. Mol. Evol. 7*, 101-104.

2. Yarus, M. (2011) Getting past the RNA world: The initial Darwinian ancestor, *Cold Spring Harb Perspect Biol 3:a003590*.

3. Füchtbauer, W., and Mazur, P. (1966) Kinetics of the ultraviolet-induced dimerization of thymine in frozen solutions, *Photochem. Photobiol. 5*, 323-335.

4. Varghese, A. J. (1970) Photochemistry of thymidine in ice, *Biochemistry. 9*, 4781-4787.

5. Varghese, A. J. (1971) Photochemistry of uracil and uridine, *Biochemistry 10*, 4283-4290.

6. Mohamady, S., and Taylor, S. D. (2011) General procedure for the synthesis of dinucleoside polyphosphates, *J. Org. Chem. 76*, 6344-6349.

7. Fleming, A. M., Muller, J. G., Ji, I., and Burrows, C. J. (2011) Characterization of 2'-deoxyguanosine oxidation products observed in the Fenton-like system Cu(ii)/H2O2/reductant in nucleoside and oligodeoxynucleotide contexts, *Org. Biomol. Chem. 9*, 3338-3348.

8. Banerjee, S. K., Borden, A., Christensen, R. B., LeClerc, J. E., and Lawrence, C. W. (1990) SOS-dependent replication past a single trans-syn T-T cyclobutane dimer gives a different mutation spectrum and increased error rate compared with replication past this lesion in uninduced cells, *J. Bacteriol. 172*, 2105-2112.

9. Thorne, R. E., Chinnapen, D. J. F., Sekhon, G. S., and Sen, D. (2009) A deoxyribozyme, Sero1C, uses light and serotonin to repair diverse pyrimidine dimers in DNA, *J. Mol. Biol. 388*, 21-29.

CHAPTER 5

PHOTOREPAIR OF CYCLOBUTANE PYRIMIDINE DIMERS BY 8-OXOPURINE NUCLEOSIDES

Introduction

In recent work (*1*) we proposed that a simple derivative of guanosine (G), namely 8-oxo-7,8-dihydroguanosine (OG), may have been a primordial redox cofactor for electron transfer processes. We demonstrated that OG can mimic the function of the flavoenzyme photolyase to repair cyclobutane pyrimidine dimers (CPD) in single- or double-stranded DNA or RNA oligonucleotides by what appears to be a photoinduced electron transfer process. These results support the hypothesis that a simple chemical transformation of a base, such as G to OG or C to 5-hydroxyC, could have launched the evolution of the redox-active cofactors $FADH_2$ or NADH (*2*).

One finding of our previous work was that the distance dependence of CPD photorepair by OG was very steep; the OG base had to be well stacked in the duplex and within a few nucleotides of the CPD for efficient repair (*1*). A key aspect that may be inhibiting repair by photoinduced electron transfer is the separation of charge that occurs when a neutral base such as OG donates an electron to form $CPD^{\bullet -}$ and $OG^{\bullet +}$. We postulated that electron transfer would be more facile if the nucleobase carried a negative charge in its resting state, as does $FADH^-$ in photolyase (*3*). This might be possible by

raising the pH to deprotonate the base, or by selecting a different purine with a lower pK_a, such as uric acid. While the synthesis of the ribonucleoside 9-ribosyluric acid (RU) is straightforward (*4*), the conversion of RU to a phosphoramidite and incorporation into an oligomer are not. Therefore, we elected to study the behavior of monomeric nucleosides toward photorepair of CPDs, realizing that the efficiency of the intermolecular reaction would be much less than that of an intrastrand or intraduplex reaction. In this study, we report the feasibility of repairing the free base CPDs T=T and U=U by 8-oxo-purine nucleosides OG and RU (Figure 5.1) as a function of pH. With respect to prebiotic chemistry, we note that the OG nucleoside is one step removed from the parent G via hydroxylation at C8, while RU could be obtained in one additional step via hydrolytic deamination of the N^2 amino group of OG. Both of these chemical steps would be plausible in the early Earth environment.

Results and discussion

In the present experiments, the 2', 3', and 5' hydroxyl groups of nucleosides were acetylated (*4-6*) to retard their elution times compared to CPDs and free base pyrimidines as monitored by reversed-phase HPLC. Irradiation was carried out in polystyrene cuvettes to cut off wavelengths below 300 nm, thus directing light into the 8-oxopurine chromophore (*1*). Both OG and RU have absorption maxima near 295 nm and absorb significantly above 300 nm, where normal bases and pyrimidine dimers do not. The repair of thymine dimer was first investigated at pH 7, where we found that the presence of an equimolar amount of OG or RU increased the yield of thymine dimer repair approximately four fold compared to background repair, while the parent

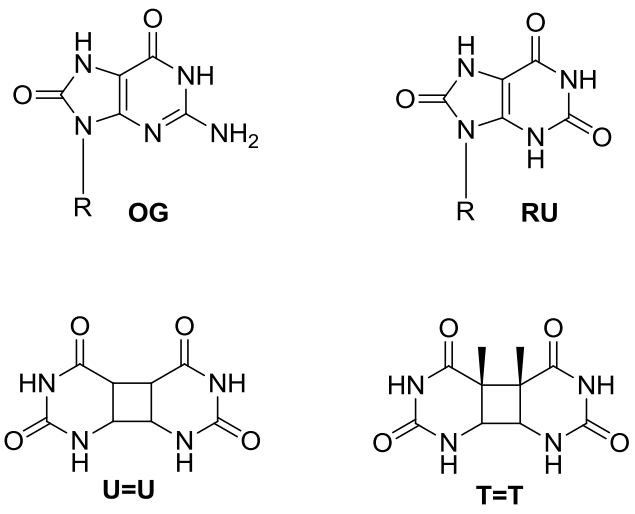

Figure 5.1. Structures of catalysts and substrates (R = 2',3',5'-tri-*O*-acetylribofuranosyl)

nucleoside G did not have any effect (Figure 5.2). Although adjacent guanine bases in DNA have been shown to have an effect on the formation of T=T at shorter wavelengths, the inactivity of G at λ>300 nm is not surprising given that G displays essentially no absorbance above 290 nm (*7, 8*). In addition, we note that no significant decomposition of nucleosides was observed by HPLC during the course of the irradiation, indicating that no permanent oxidation of OG or RU had occurred. The products of such oxidation chemistry have been determined previously (*4, 9*).

We considered three possible mechanisms for the repair process: (1) excited state energy, (2) oxidative electron transfer from T=T to OG, and (3) reductive electron transfer from OG to T=T. The repair of thymine dimer by direct energy transfer from the photoexcited state of OG and RU (mechanism (1)) is excluded because the excited singlet state energy of T=T is much higher than the energy of ~310 nm light used in our experiments (*10*). Although thymine dimer repair may proceed via an oxidative mechanism, particularly in the presence of redox active transition metal complexes (*11-14*), the enhancement of the thymine dimer repair yield by OG and RU is more likely occurring via the reductive mechanism as proposed in our previous study (*1*). In this mechanism, T=T accepts one electron from a photoexcited purine, followed by rapid bond cleavage of the strained cyclobutane ring (Figure 5.3), and finally back electron transfer to the purine. The reductive electron transfer mechanism is supported by the significantly lower redox potential of OG compared to G or other bases and by the observed preference for long-range electron transfer in the 3'-5' direction in studies of duplex DNA (*1*). One can estimate the Gibb free energy (ΔG_{et}) for the electron transfer from the photoexcited OG to T=T at about -1.30 eV or -125 kJ/mol from the a previously

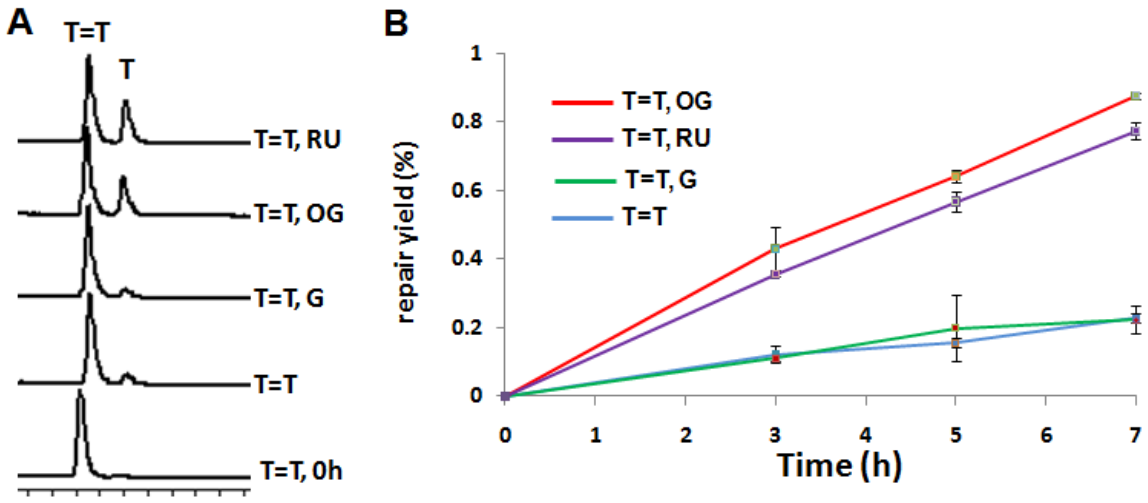

Figure 5.2. (A) HPLC traces analysis of T=T vs. repaired T after 5 h irradiation at pH 7; 2',3',5'-tri-O-acetylnucleosides eluted 20 min later. (B) Plot of T=T repair yield as a function of irradiation time.

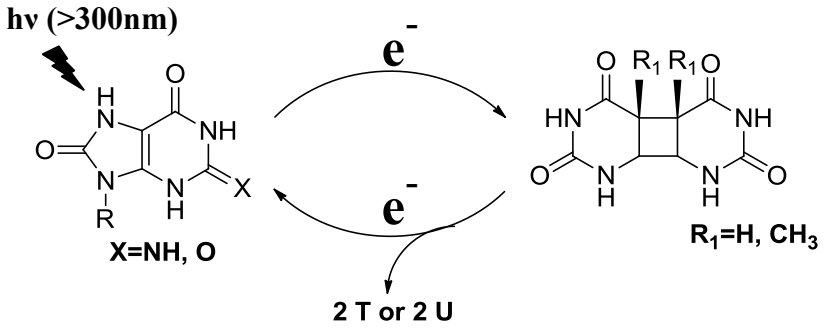

Figure 5.3. Proposed mechanism for the enhancement of CPD repair by 8-oxopurine nucleosides

reported method (*10*). This mechanism has also been well characterized for photolyase and for related model systems (*3, 13, 15-24*).

Mechanistic considerations aside, the absolute repair yield of thymine dimer in these systems is extremely low, only about 1% after 7 h of irradiation. As anticipated, this bimolecular reaction is much less efficient than the case where OG was installed in proximity to the CPD in double-stranded oligonucleotides (*1*). Thus, the "immobilization" of two species, thymine dimer and 8-oxopurine, in an oligomer is important to enhance the repair efficiency.

Nevertheless, the repair yields observed in the initial experiments were sufficiently above background to warrant further study, and we next turned our attention to the uric acid nucleoside. We observed that RU is about equally efficient as OG in repairing thymine dimer at pH 7 (Figure 5.2). This observation was surprising for two reasons: (1) RU has a slightly lower reduction potential, about 200 mV below that of OG (*25, 26*), and it would therefore be a more powerful electron donor, all other factors being equal, and (2) RU exists as an anion at pH 7 which should be a favorable condition for excited state electron donation (*27*). Thus, the finding that RU is not any more effective than OG at intermolecular photorepair was unanticipated. This observation led us to investigate the dependence of thymine dimer repair yield on pH for both RU and OG.

The background photorepair rate of T=T (no purines present) is almost independent of pH in the range from 5 to 9 (Figure 5.4). It is also not surprising that the repair yield only slightly increased from pH 7 to pH 9 in the presence of RU, because with $pK_a \sim 6$ (*27*), RU exists in an anionic form across this pH range. However, we also did not observe a significant increase of thymine dimer repair yield by RU in the pH

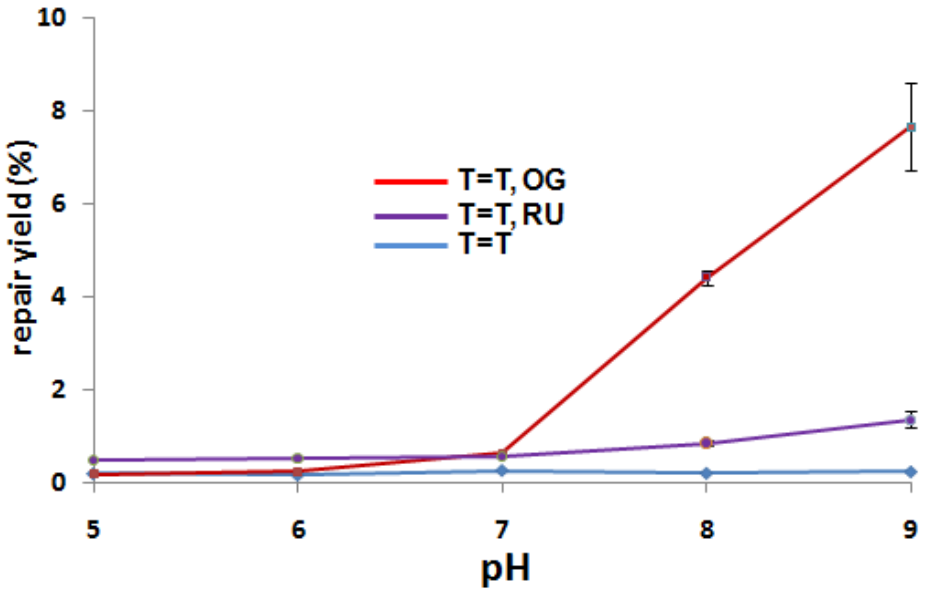

Figure 5.4. Yield of thymine dimer repair after 5 h as a function of pH for various additives; red: OG, violet: RU, blue: none.

range from 5 to 7, for which RU is supposed to change from a neutral to an anionic form. This could indicate that despite a favorable redox potential, the excited state lifetimes of RU and RU^- are both too short to permit effective intermolecular electron transfer. In contrast to RU, the activity of OG dramatically increased from pH 7 to pH 9 (Figure 5.4), which is in good agreement with its pK_a of 8.6 (*28*). At pH 9, the repair yield of T=T by OG reached to about 8%, which is a 30-fold increase compared to background repair.

The instability of 8-oxopurine nucleosides at higher pH precluded investigation of repair at pH>9. Despite that limitation, the pH dependence observed further supports a reductive mechanism for thymine dimer repair by OG and agrees with previous work showing that flavins in an anionic form repair thymine dimer more efficiently (*3, 20*). The difference in activity between OG and RU may also imply that the purine redox potential is not the only factor determining the thymine dimer repair efficiency. Indeed, previous studies showed that not all flavin derivatives are able to repair thymine dimer, and their different photoexcited state lifetimes were thought responsible for this phenomenon (*21, 29*). In studies of duplex vs. monomer systems, base stacking and base pairing are important factors in determining the excited state lifetimes, and are therefore expected to play significant roles in the ability of base chromophores to undergo collisional charge transfer with CPDs (*30-32*). Clearly, additional photophysical studies will be necessary to fully understand the complex factors contributing to the lower efficiency of RU compared to OG in repairing thymine dimer at high pH.

Repair of uracil dimer, a common type of CPD found in RNA, by 8-oxopurine nucleosides was also investigated. A previous study demonstrated that repair of thymine dimer was faster than uracil dimer when mediated by the enzyme photolyase because of a

strain effect induced by the two cis methyl groups (*33*). However, a more recent report produced an opposite result in a model system in which uracil dimer was repaired faster than thymine dimer in flavin-conjugated model compounds, and an explanation was based on stereoelectronic effects (*34*). In previous work (*1*), our laboratory observed slower repair for a CPD in an A-form helix (U=U in RNA/DNA or RNA/RNA duplexes) compared to a CPD in a B-form helix (T=T in a DNA/DNA duplex) by OG. We attributed this to the difference in base stacking between the two helical forms; an adjacent OG-containing base pair stacks poorly on a U=U lesion in A-form RNA. Here, by using a nucleoside repair model, we are able to compare the repair efficiency of OG between these two types of CPD in an identical environment, absent base stacking.

At pH 7, we observed the repair of U=U increased by threefold in the presence of an equimolar amount of OG (Table 5.1). In addition, the repair yield was not significantly different with that of thymine dimer. Unexpectedly, we found the background repair of U=U was somewhat pH dependent compared to T=T, and it reached to 5% at pH 9 (Table 5.1, entry 3). We cannot explain this unusual observation at the present time. In any case, the presence of OG still increased the repair yield for U=U about twofold. From these data, it is reasonable to conclude that OG enhances the intrinsic repair yield of uracil dimer with similar efficiency to that of thymine dimer in the absence of a specific helical environment.

Conclusions

In conclusion, we showed that the 8-oxopurine nucleosides OG and RU are able to mediate the repair of cyclobutane pyrimidine dimers T=T and U=U, even in a

Table 5.1. T=T and U=U repair yields in the presence of OG as a function of pH. Errors are estimated at ±10%

Entry	Substrate	Irradiation time(h)	Yield(%)	
			pH7	pH9
1	**T=T**	5	0.2	0.2
2	**T=T, OG**	5	0.7	8
3	**U=U**	5	0.3	5
4	**U=U, OG**	5	1	12

bimolecular reaction. The observations are in accord with the mechanism proposed in our previous study (*1*) in which CPD is repaired reductively by accepting one electron from the photoexcited state of the purine. Unexpectedly, deamination of the OG base to form RU does not provide a more active photocatalyst, despite the lower redox potential of RU and its anionic nature, suggesting that other factors, such as the excited state lifetimes of purines and flavin mimics, may play equally important roles in the process. In contrast, OG did display the expected pH-dependent behavior, and the photorepair of CPDs was enhanced as the pH approached the pK_a value of 8.6. These studies also showed that T=T and U=U underwent repair at similar rates in the absence of a helical environment, although the overall levels are sufficiently low as to not provide an accurate assessment. Nevertheless, the results are instructive with respect to a comparison of OG and RU, and support the hypothesis that 8-oxopurine nucleosides may have played primordial roles as precursors to modern-day flavins in redox reactions of the RNA world.

Experimental

Materials. All chemicals were purchased from commercial sources and used without further purification except where otherwise stated. The 2',3',5'-tri-*O*-acetylnucleosides OG and RU were synthesized as previously described (*4-6*). [*cis,syn*]-Thymine dimer and uracil dimer were synthesized according to published procedures and purified by reversed phase HPLC (*29, 35, 36*). NMR spectra, UV spectra and/or HPLC retention times of synthesized compounds were identical with literature data. Concentrations of nucleosides and cyclobutane pyrimidine dimer were determined by UV spectrophotometry using reported extinction coefficients (*37-39*).

Photorepair of cyclobutane pyrimidine dimer (CPD). A solution containing 0.2 mM CPD (T=T or U=U) and 0.2 mM nucleoside (OG or RU) in 25 mM NaP_i buffer adjusted to the appropriate pH was irradiated in a polystyrene cuvette to cut off wavelengths below 300 nm (*40*) at ambient temperature (22 °C) with an FS40 UVB lamp (λ_{max}=313 nm, Home Phototherapy, OH, USA). In the case of thymine dimer, the irradiation mixture was analyzed by HPLC on a Varian C18 column (5 μm, 250x4.6 mm) using a linear gradient of 2% to 10% B over 20 min, then increasing B to 65% over 10 min (A: 0.1%TFA in H_2O; B: MeOH). A slightly different HPLC method with isocratic B at 1% for 15 min and then increasing to 65% B over 10 min was used to analyze the irradiation mixture of uracil dimer repair (A: H_2O; B: MeOH). In both cases, the flow rate was 0.7 mL/min, and the detector was set at 260 nm. The peaks corresponding to CPD and the repaired product were integrated and normalized against extinction coefficients to calculate the repair yield, average over 3 or more independent trials. Because the extinction coefficient of thymine dimer at 260 nm is not yet reported, this value was estimated at about 2.8×10^2 by the formula: $\varepsilon_{260} = (A_{260}/A_{220}) \times \varepsilon_{220}$.

References

1. Nguyen, K. V., and Burrows, C. J. (2011) A prebiotic role for 8-oxoguanosine as a flavin mimic in pyrimidine dimer photorepair, *J. Am. Chem.Soc. 133*, 14586-14589.

2. Yanagawa, H., Ogawa, Y., and Ueno, M. (1992) Redox ribonucleosides, *J. Biol. Chem. 267*, 13320-13326.

3. Hartman, R. F., and Rose, S. D. (1992) Efficient photosensitized pyrimidine dimer splitting by a reduced flavin requires the deprotonated flavin, *J. Am. Chem.Soc. 114*, 3559-3560.

4. Nguyen, K. V., Muller, J. G., and Burrows, C. J. (2011) Oxidation of 9-β-D-ribofuranosyl uric acid by one-electron oxidants versus singlet oxygen and its implications for the oxidation of 8-oxo-7,8-dihydroguanosine, *Tetrahedron Lett. 52*, 2176-2180.

5. Niles, J. C., Wishnok, J. S., and Tannenbaum, S. R. (2000) A novel nitration product formed during the reaction of peroxynitrite with 2',3',5'-tri-O-acetyl-7,8-dihydro-8-oxoguanosine: N-Nitro-N'-[1-(2,3,5-Tri-O-acetyl-β-D-erythro-pento-furanosyl)- 2,4-dioxoimidazolidin-5-ylidene]guanidine, *Chem. Res. Toxicol. 13*, 390-396.

6. Grünewald, C., Kwon, T., Piton, N., Förster, U., Wachtveitl, J., and Engels, J. W. (2008) RNA as scaffold for pyrene excited complexes, *Bioorg. Med. Chem 16*, 19-26.

7. Holman, M. R., Ito, T., and Rokita, S. E. (2006) Self-repair of thymine dimer in duplex DNA, *J. Am. Chem. Soc. 129*, 6-7.

8. Pan, Z., Hariharan, M., Arkin, J. D., Jalilov, A. S., McCullagh, M., Schatz, G. C., and Lewis, F. D. (2011) Electron donor–acceptor interactions with flanking purines influence the efficiency of thymine photodimerization, *J. Am. Chem. Soc.133,* 20793-20798.

9. Luo, W., Muller, J. G., Rachlin, E. M., and Burrows, C. J. (2000) Characterization of spiroiminodihydantoin as a product of one-electron oxidation of 8-oxo-7,8-dihydroguanosine, *Org. Lett. 2*, 613-617.

10. Chinnapen, D. J. F., and Sen, D. (2007) Towards elucidation of the mechanism of UV1C, a deoxyribozyme with photolyase activity, *J. Mol. Biol. 365*, 1326-1336.

11. Kruger, O., and Wille, U. (2001) Oxidative cleavage of a cyclobutane pyrimidine dimer by photochemically generated nitrate radicals ($NO_3^{\cdot}$), *Org. Lett. 3*, 1455-1458.

12. Voityuk, A. A., Michel-Beyerle, M.-E., and Roesch, N. (1996) A quantum chemical study of photoinduced DNA repair: on the splitting of pyrimidine model dimers initiated by electron transfer, *J. Am. Chem.Soc. 118*, 9750-9758.

13. Boussicault, F., Kruger, O., Robert, M., and Wille, U. (2004) Dissociative electron transfer to and from pyrimidine cyclobutane dimers: An electrochemical study, *Org. Biomolec. Chem. 2*, 2742-2750.

14. Dandliker, P. J., Holmlin, R. E., and Barton, J. K. (1997) Oxidative thymine dimer repair in the DNA helix, *Science 275*, 1465-1468.

15. Breeger, S., Hennecke, U., and Carell, T. (2004) Excess electron-transfer-based repair of a cis-syn thymine dimer in DNA is not sequence dependent, *J. Am. Chem. Soc. 126*, 1302-1303.

16. Chatgilialoglu, C., Guerra, M., Kaloudis, P., Houée-Lévin, C., Marignier, J. L., Swaminathan, V., and Carell, T. (2007) Ring opening of the cyclobutane in a thymine dimer radical anion, *Chem. Eur. J. 13*, 8979-8984.

17. Fazio, D., Trindler, C., Heil, K., Chatgilialoglu, C., and Carell, T. (2011) Investigation of excess-electron transfer in DNA double-duplex systems allows estimation of absolute excess-electron transfer and CPD cleavage rates, *Chem. Eur. J. 17*, 206-212.

18. Heil, K., Pearson, D., and Carell, T. (2011) Chemical investigation of light induced DNA bipyrimidine damage and repair, *Chem. Soc. Rev.40,* 4271-4278.

19. Schwögler, A., Burgdorf, L., and Carell, T. (2000) Self-repairing DNA based on a reductive electron transfer through the base stack, *Angew. Chem. Int. Ed. 39*, 3918-3920.

20. Epple, R., Wallenborn, E.-U., and Carell, T. (1997) Investigation of flavin-containing DNA-repair model compounds, *J. Am. Chem.Soc. 119*, 7440-7451.

21. Jorns, M. S. (1987) Photosensitized cleavage of thymine dimer with reduced flavin. A model for enzymic photorepair of DNA, *J. Am. Chem.Soc. 109*, 3133-3136.

22. Tang, W.-J., Song, Q.-H., Wang, H.-B., Yu, J.-y., and Guo, Q.-X. (2006) Efficient photosensitized splitting of the thymine dimer/oxetane unit on its modifying beta-cyclodextrin by a binding electron donor, *Org. Biomol. Chem. 4*, 2575-2580.

23. Wiest, O., Harrison, C. B., Saettel, N. J., Cibulka, R., Sax, M., and König, B. (2004) Design, synthesis, and evaluation of a biomimetic artificial photolyase model, *J. Org. Chem. 69*, 8183-8185.

24. Yeh, S. R., and Falvey, D. E. (1991) Model studies of DNA photorepair: radical anion cleavage of thymine dimers probed by nanosecond laser spectroscopy, *J. Am. Chem.Soc. 113*, 8557-8558.

25. Simic, M. G., and Jovanovic, S. V. (1989) Antioxidation mechanisms of uric acid, *J. Am. Chem.Soc. 111*, 5778-5782.

26. Steenken, S., Jovanovic, S. V., Bietti, M., and Bernhard, K. (2000) The trap depth (in DNA) of 8-Oxo-7,8-dihydro-2'-deoxyguanosine as derived from electron-transfer equilibria in aqueous solution, *J. Am. Chem.Soc. 122*, 2373-2374.

27. Forrest, H. S., Hatfield, D., and Lagowski, J. M. (1961) Uric acid riboside. Part 1. Isolation and reinvestigation of the structure. *J. Chem. Soc*, 963-968.

28. Culp, S. J., Cho, B. P., Kadlubar, F. F., and Evans, F. E. (1989) Structural and conformational analyses of 8-hydroxy-2'-deoxyguanosine, *Chem. Res. Toxicol. 2*, 416-422.

29. Rokita, S. E., and Walsh, C. T. (1984) Flavin and 5-deazaflavin photosensitized cleavage of thymine dimer: a model of in vivo light-requiring DNA repair, *J. Am. Chem.Soc. 106*, 4589-4595.

30. Crespo-Hernandez, C. E., Cohen, B., and Kohler, B. (2005) Base stacking controls excited-state dynamics in A-T DNA, *Nature 436*, 1141-1144.

31. Crespo-Hernandez, C. E., de La Harpe, K., and Kohler, B. (2008) Ground-state recovery following UV excitation is much slower in GC-DNA duplexes and hairpins than in mononucleotides, *J. Am. Chem. Soc. 130*, 10844-10845.

32. Kumar, A., and Sevilla, M. D. (2010) Proton-coupled electron transfer in DNA on formation of radiation-produced ion radicals, *Chem. Rev. 110*, 7002-7023.

33. Kim, S. T., and Sancar, A. (1991) Effect of base, pentose, and phosphodiester backbone structures on binding and repair of pyrimidine dimers by Escherichia coli DNA photolyase, *Biochemistry 30*, 8623-8630.

34. Butenandt, J., Epple, R., Wallenborn, E.-U., Eker, A. P. M., Gramlich, V., and Carell, T. (2000) A comparative repair study of thymine- and uracil-photodimers with model compounds and a photolyase repair enzyme, *Chem. Eur. J. 6*, 62-72.

35. Varghese, A. J. (1971) Photochemistry of uracil and uridine, *Biochemistry 10*, 4283-4290.

36. Wulff, D. L., and Fraenkel, G. (1961) On the nature of thymine photoproduct, *Biochim. Biophys. Acta 51*, 332-339.

37. Herbert, M. A., Leblanc, J. C., Weinblum, D., and Johns, H. E. (1969) Properties of thymine dimer, *Photochem. Photobiol. 9*, 33-43.

38. Trivedi, R., Rebar, L., Desai, K., and Stong, L. (1978) New ultraviolet (340 nm) method for assay of uric acid in serum or plasma, *Clin. Chem.* 24, 562-566.

39. Slade, P. G., Priestley, N. D., and Sugden, K. D. (2007) Spiroiminodihydantoin as an Oxo-atom transfer product of 8-Oxo-2'-deoxyguanosine oxidation by chromium(V), *Org. Lett*. 9, 4411-4414.

40. Chinnapen, D. J.-F., and Sen, D. (2004) A deoxyribozyme that harnesses light to repair thymine dimers in DNA, *Proc. Natl. Acad. Sci*. 101, 65-69.

CHAPTER 6

OXIDATION OF 9-β-D-RIBOFURANOSYL URIC ACID BY ONE-ELECTRON *VERSUS* SINGLET OXYGEN

Introduction

We showed that 9-β-D-ribofuranosyl uric acid (RU) can also function as flavin in mediating the repair of CPDs, though with less efficiency than OG. While oxidation products of OG have been extensively studied, those of uric acid ribonucleoside (RU) have not. To further understand the redox chemistry of RU, we therefore investigated the chemistry of RU oxidation by various oxidants. Moreover, we postulate that products of RU oxidation are potentially mutagenic lesions of DNA derived from OG under oxidative and deamination conditions.

8-Oxo-7,8-dihydro-2'-deoxyguanosine (OG) is an abundant product of oxidative damage in DNA (*1, 2*). OG is also characterized by its high susceptibility to further oxidation, and its secondary oxidation products have been characterized under various conditions (*3, 4*). In addition to oxidation, the exocyclic primary amino group of guanosine is known to be reactive with nitrogen electrophiles (*5*), such as nitric oxide (*6*), to form xanthosine and oxanosine as the major products both *in vitro* (*6, 7*) and *in vivo (8-11).* However, the same reaction in the case of OG to form uric acid nucleoside has not been studied. One possible reason is that the deamination reaction of OG leading to

uric acid nucleoside is even more sensitive to oxidation than OG, undergoing subsequent oxidation more rapidly than it can be detected. Thus, it was of interest to characterize the further oxidation products of uric acid nucleoside in order to gain more insight to the pathways and products of OG under conditions involving oxidation and deamination with the potential benefit of shedding light on additional products formed in peroxynitrite-mediated damage to DNA, a common outcome of inflammation (*12*). Moreover, the one-electron oxidation of uric acid nucleoside is also of interest in terms of its mechanistic aspects, because of parallels between the oxidation of uric acid (UA) alone and the hydantoin products derived from OG nucleoside oxidation (*13, 14*). Although the sugar moiety is known to have an influence on the redox properties of oxidized purines (*15, 16*), no direct comparisons have been made between oxidations of OG nucleoside and UA nucleoside (termed "RU" in this work).

Uric acid is known to be a scavenger for reactive oxygen species (ROS) *in vivo* (*17, 18*). While photophysical and biological aspects of the photosensitized oxidation of uric acid derivatives have been extensively studied (*19-24*), mechanistic aspects for the transformation to oxidation products still require more work. There are arguments, for example, in differentiating between type I and type II photooxidation (*25, 26*) or in formation and decomposition of reaction intermediates (*24-26*). In this study, some mechanistic aspects of the photosensitized oxidation of uric acid nucleoside will be presented and compared to the well-characterized photooxidation process of its analogous structure 8-oxo-7,8-dihydroguanosine (*27-29*).

Results and dicussion

The ribose form of uric acid nucleoside (9-ribofuranosyl-β-D-uric acid, RU) was chosen as the substrate to be oxidized due to its more convenient preparation compared with the 2'-deoxyribose form; in addition, the 2'-hydroxyl group should stabilize the glycosidic bond with respect to hydrolytic cleavage. The 2', 3' and 5' hydroxyl groups of RU were acylated (Ac_3RU) to facilitate the separation of oxidation products by reversed phase HPLC and to better mimic the chemistry in a DNA strand in which no free hydroxyls are present (*27*). Metal complexes (Na_2IrCl_6 or $K_3Fe(CN)_6$) were used as one-electron oxidants. Riboflavin was used as a "Type I" photosensitizer to undergo electron transfer chemistry, while Rose Bengal or methylene blue were used as "Type II" photosensitizers that predominantly generate singlet oxygen (*30, 31*).

Oxidation of a 0.3 mM solution of Ac_3RU in aqueous phosphate buffer at pH 7 by Na_2IrCl_6 (0.6 mM) led to the formation of five stable products (1-5) that were characterized by RP-HPLC (Figure 6.1). An identical result was obtained from the oxidation with $K_3Fe(CN)_6$. Products were identified on the basis of their masses from LC-ESI-MS studies and compared with known products of uric acid derivatives (*16, 25, 26, 32-35*). From that, 1 was assigned as ribosylurea, 2 and 3 as two diastereoisomers of allantoin ribonucleoside, 4 as two diastereomers of 5-carboxamido-5-hydroxyhydantoin ribonucleoside (HICA amide) and 5 as caffolide ribonucleoside (Figure 6.2).

To obtain additional support for the structural assignments of the oxidation products, we attempted to characterize reaction intermediates. For this purpose, 100-μL aliquots were taken from the reaction mixture periodically, and the product composition was monitored immediately by HPLC. Three transient peaks, TP1-TP3, were identified

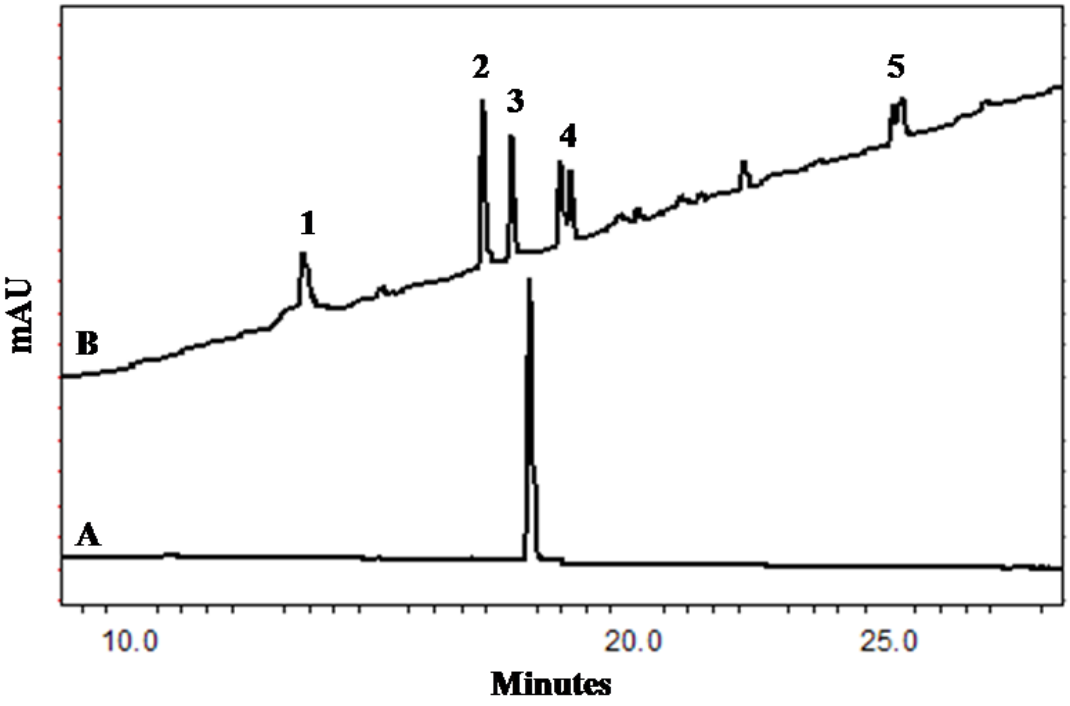

Figure 6.1. HPLC traces of (A) the starting material (B) the oxidation products of Ac_3RU by Ir(IV), monitored at 220 nm

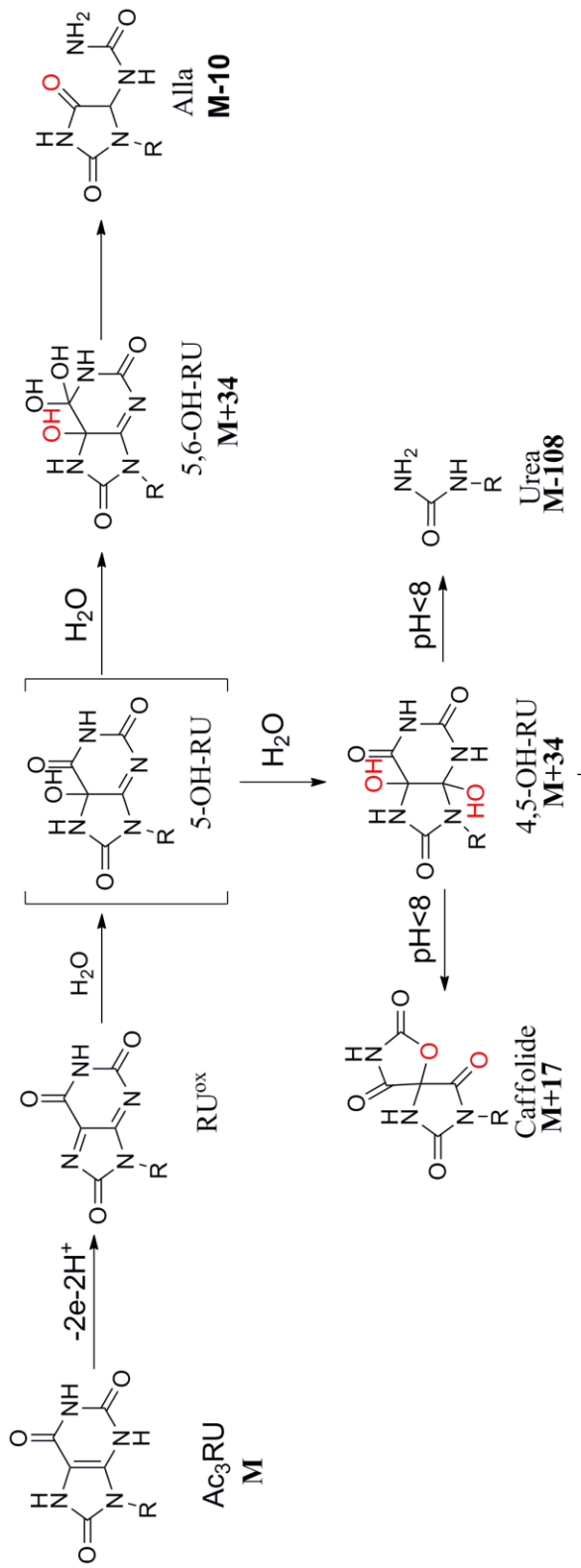

Figure 6.2. Proposed mechanism for the one-electron oxidation of Ac_3RU

with retention times at 17.1, 20.9, and 21.2 min, respectively. TP1 was very unstable under these conditions, and totally disappeared after 5 min while the two peaks corresponding to allantoin diastereomers increased. TP2 and TP3 were more stable, but completely decomposed after 2 h, and the peaks corresponding to HICA amide, urea and caffolide appeared and increased during this period of time. It was therefore reasonable to assign TP1 as a precursor to allantoin, and TP2 and TP3 as precursors of urea, caffolide and HICA amide. The LC-ESI-MS analysis showed the masses of TP2 and TP3 were the same at 460 amu (M+34) and yielded a fragment at 442 amu corresponding to the loss of a neutral water molecule. The identical mass spectra and very close retention in RP-HPLC time suggested that TP2 and TP3 were diastereoisomers. Experiments carried out in $H_2{}^{18}O$ led to a gain of 4 amu for both TP2 and TP3, corresponding to incorporation of two ^{18}O atoms from water. These data are consistent with the structure of 4,5-OH-RU, analogous to the precursors of HICA in OG oxidation by peroxynitrite (*36*) and of caffolide in the caffolide degradation pathway of uric acid (*37*).

TP1 was very unstable at pH 7 but its stability was increased when the pH was lowered. The LC-ESI-MS analysis of TP1 could be performed only at pH 3.2, and it too indicated mass of 460 amu, although it did not behave like TP2 and TP3 in yielding a 442 amu product due to dehydration. Therefore, we propose TP1 is the 5,6-dihydroxylated structure 5,6-OH-RU, a precursor to allantoin, by analogy to the enzymatic oxidation of uric acid (*38*) and to the mechanism of formation of guanidinohydantoin (Gh) from OG oxidation (*13, 39*). When experiments were conducted in $H_2{}^{18}O$, the allantoin mass increased by 2 amu while a gain of 4 amu was observed for caffolide. In the case of HICA amide, the results showed that two or three ^{18}O were incorporated, suggesting

some solvent exchangeability occurred at one more carbonyl groups. These observations help support the mechanism in Figure 6.2 for the structural rearrangements occurring from precursors to products.

The dependence of the product distribution on pH was also investigated because previous investigations indicated that OG oxidation to form hydantoin products Sp and Gh, as well as uric acid oxidation, are highly pH dependent. The oxidation of Ac_3RU was carried out at pH 5.4, 6.2, 7.0, 8.0 and 9.2. The results showed that HICA amide was formed at pH values higher than 6.2, and the amount was increased when increasing the pH. In contrast, both allantoin and caffolide formation were favored at pH 5.4-7.0 and decreased when increasing the pH.

Our experimental observation of reaction intermediates provides insights into the reaction mechanism of RU oxidation by one-electron oxidants (Figure 6.2). A common intermediate, 5-OH-RU may form first from the addition of water to C5 of a quinonoid intermediate RU^{ox}. Two electrophilic centers, C4 or C6 of 5-OH-RU were further attacked by water and led to the formation of two observable intermediates 4,5-OH-RU and 5,6-OH-RU. In the case of 5,6-OH-RU, the C6-N1 bond was broken, followed by decarboxylation leading to the formation of allantoin.

The decomposition pathways of the intermediate 4,5-OH-RU are likely more complicated. The first steps are probably the cleavage of either C4-N9 or C4-N3 bond with the assistance of the 5-OH group. When the C4-N9 bond is broken, the final product is ribosylurea after elimination of alloxan. When the C4-N3 bond is cleaved, two subsequent pathways may occur. One pathway involves hydrolysis of the amide linkage, C2-N1, which leads to HICA amide. The fact that the amide linkage is more labile under

basic conditions explains the increasing amount of HICA amide when the pH increases. Another pathway is an intramolecular process in which 4-OH participates in formation of a carbonyl; a subsequent attack of the C5-OH at C2 and elimination of NH_3 would form caffolide. This process may occur more readily if the NH_2 group could be protonated during elimination, consistent with caffolide formation being more favorable at low pH.

Our results show that the presence of the ribose moiety at the N-9 position led to the formation of more oxidation products than the uric acid heterocycle alone. The oxidation of uric acid by Ir(IV) at pH 7 gave allantoin as the only detectable product (see supporting information), while three more products (ribonucleosides of HICA amide, caffolide, and urea) were obtained in the case of uric acid nucleoside oxidation under the same conditions. The influence of N-substitution on the redox property of uric acid heterocycle has been investigated; however, the explanations were mainly based on theoretical calculations (*40*). The present mechanistic studies provided more details on understanding the difference between one-electron oxidation pathways of ribofuranosyl uric acid and the uric acid heterocyle. It is clear that 5-OH-UA and the analogous 5-OH-RU are the common intermediates of UA and RU oxidation, respectively. At pH 7, the predominant form of 5-OH-UA is the N9-deprotonated species (*38*), and the C4 is therefore unreactive with nucleophiles due to the negative charge density (Figure 6.3). It is reasonable that pathway III (Figure 6.4) is the only degradation pathway of 5-OH-UA that leads to the formation of allantoin. In contrast, 5-OH-RU is neutral, and C4 can therefore be readily attacked by water to form the 4,5-dihydroxyl intermediate that then decomposes to give urea, HICA amide and caffolide (Figure 6.1). In the oxidation of RU by Ir(IV), the formation of a spirocyclic product (pathway I, Figure 6.4), that was

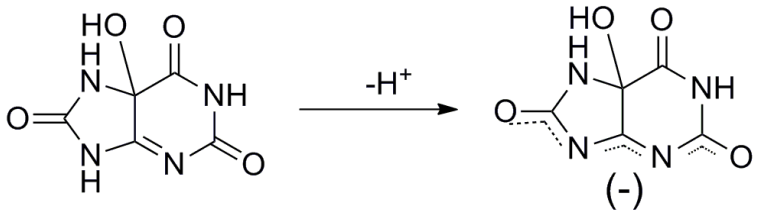

Figure 6.3. N9-deprotonation of 5-OH-UA

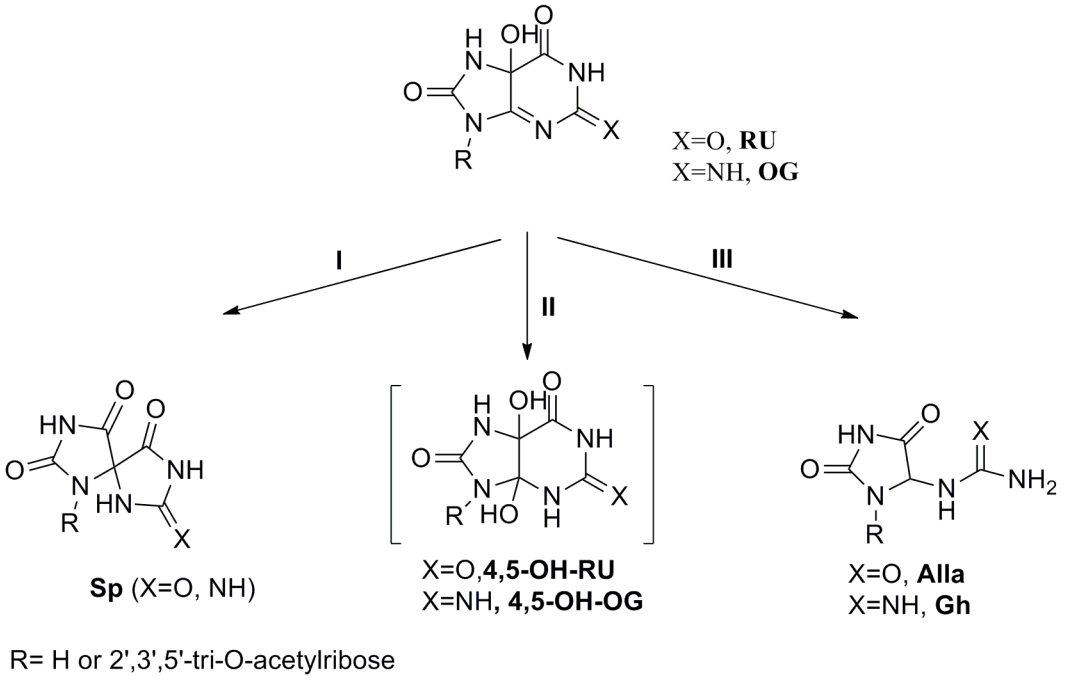

Figure 6.4. Degradation pathways of the common 5-hydroxy intermediate

observed in OG oxidation (*13*) as well as UA oxidation under more basic conditions (*41*) was not detected. Because 5-OH-OG and 5-OH-RU appear to be the initial and common intermediates in oxidation of both nucleosides, the difference in products must derive from degradation pathways of these analogous intermediates. Pathways I and II both involve nucleophilic addition to C4; however, one is an intramolecular process (I) and the other is an intermolecular one (II). The presence of a C2-carbonyl group in the case of 5-OH-RU leads to an increase in C4 reactivity toward external nucleophiles compared to 5-OH-OG. Reasonably, the more reactive C4 was easier to attack by solvent water in competition with an intramolecular acyl shift. Thus, pathway I was not observed in the oxidation of RU by one-electron oxidants.

Nevertheless, we found that the distribution of products occurring at C4 and C6 in RU oxidation shares some similarity with that of OG oxidation. In the case of OG, pathway I was known to be dominant over pathway III at high pH and high temperature (*13*). When the oxidation of RU was carried out at pH>7 or at 65°C, the amount of HICA amide was significantly increased, and the amount of allantoin decreased. This indicates that the C4 pathway is also more favorable at high pH and high temperature in RU oxidation. Interestingly, the competition between pathways I and III is also influenced by the nature of nucleophiles used to trap the quinonoid intermediate. When lysine was used as a nucleophile to compete with water to attack at C5 of RU^{ox} generating a 5-Lys-RU intermediate, the allantoin-Lys adduct was the only detectable product, whereas pathway I dominated for the reaction of OG nucleoside under these conditions. Thus, the replacement of an oxygen atom at C5 by nitrogen in the common intermediate drove its decomposition toward pathway III.

In the work described above, the oxidation reactions likely proceed by two one-electron oxidation steps with concomitant deprotonation. In order to compare the outcome of a potential 4-electron oxidant, singlet oxygen, the reactions were repeated using two different Type II photosensitizers generating $^1O_2$, Rose Bengal (RB) and methylene blue (MB). For comparison, the Type I photooxidant riboflavin (Rf) was also used. The excited state of riboflavin is a powerful one-electron oxidant, but its subsequent radical anion reacts with O_2 to further yield superoxide, $O_2^{\cdot -}$.

The HPLC traces of photooxidation of Ac_3RU mediated by Rf, MB, and RB at pH 7 are shown in Figure 6.5. Interestingly, Type I (Rf) and Type II (MB, RB) photosensitized oxidation of Ac_3RU gave the same products with only a small difference in yield. On the basis of mass and by analogy to products for from manganese porphyrin-mediated oxidation to guanosine (*42-44*) product 6 was tentatively assigned as oxidized allantoin $Alla^{ox}$ and product 7 was assigned as oxaluric acid OA. Indeed, OA was also the product of riboflavin-mediated oxidation of OG (*27*), derived from the decomposition of the unstable intermediate Gh^{ox}–an analogous structure to $Alla^{ox}$. Thus, we wondered whether OA found in this experiment was also formed from decomposition of $Alla^{ox}$. As previously described, Gh^{ox} was relatively unstable at pH 7 and converted to OA after 3h (*45*). In the present case, $Alla^{ox}$ was found to be stable at pH 7 and did not significantly decompose after two days at room temperature. This was not surprising because the $Alla^{ox}$ nucleobase can be independently synthesized, although it decomposes in very strong acidic or basic conditions(*46*). However, we found that $Alla^{ox}$ was unstable at high temperature. When heated up to 65°C for 2 h, $Alla^{ox}$ was gradually converted to OA at pH 7. Thus, the small amount of OA detected in the photosensitized oxidation of Ac_3RU

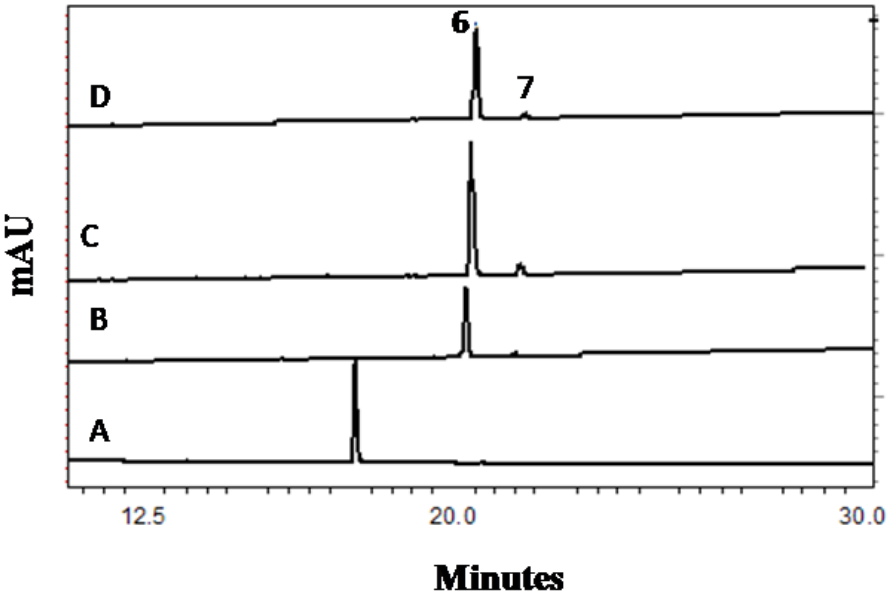

Figure 6.5. HPLC traces of (A) starting material Ac_3RU and the oxidation reactions with Riboflavin (B), Methylene Blue (C), Rose Bengal (D), monitored at 220nm.

may be evidence for the decomposition of the major product $Alla^{ox}$ when the reaction mixture was heated somewhat by the irradiation lamp.

Riboflavin-mediated oxidation involves electron transfer from the purine to Rf, and the formation of $O_2^{-\cdot}$, superoxide anion (*47*). In the case of OG, the reactive intermediates (cation radical $OG^{+\cdot}$ or neutral radical $OG^{\cdot}$) then can be trapped by either a water molecule or $O_2^{-\cdot}$ that lead to the formation of two sets of oxidation products (*27*). In the present study, the oxidation product $Alla^{ox}$ was believed to be formed via the superoxide adducted intermediate 5-OOH-RU (Figure 6.6). Interestingly, water-derived products (*48*) were not observed under the experimental conditions, which is opposite to the case of OG where the water-derived product Sp was found to be dominant at pH 7 (*27*). As described for OG, the product distribution was strongly dependent on pH. The radical cation $OG^{+\cdot}$ is much more reactive toward superoxide anion than the deprotonated form $OG^{\cdot}$, and therefore $O_2^{-\cdot}$-derived products were found to be dominant at low pH. At pH 7, RU with a pK_a of 5.4 (*49*), mostly exists as the anion RU^{-}, so that the excited state after interaction with Rf must be the neutral radical $RU^{\cdot}$. Unlike $OG^{\cdot}$, this species was exclusively trapped by anion $O_2^{-\cdot}$, not by a water molecule, and lead to the formation of 5-OOH-RU that decomposed to give $Alla^{ox}$. A possible explanation is that the presence of an oxo function at C2 of $RU^{\cdot}$ instead of an NH_2 group, as in the case of $OG^{\cdot}$, makes C5 more electropositive due to the charge delocalization. Thus, the affinity for anion $O_2^{-\cdot}$ was reasonably increased from $OG^{\cdot}$ to $RU^{\cdot}$ and $O_2^{-\cdot}$ was preferable in competing with water to react with $RU^{\cdot}$.

Photooxidation mediated by RB or MB is known to generate singlet oxygen as the reactive intermediate (*47*). Interestingly, the Type II photosensitized oxidation of

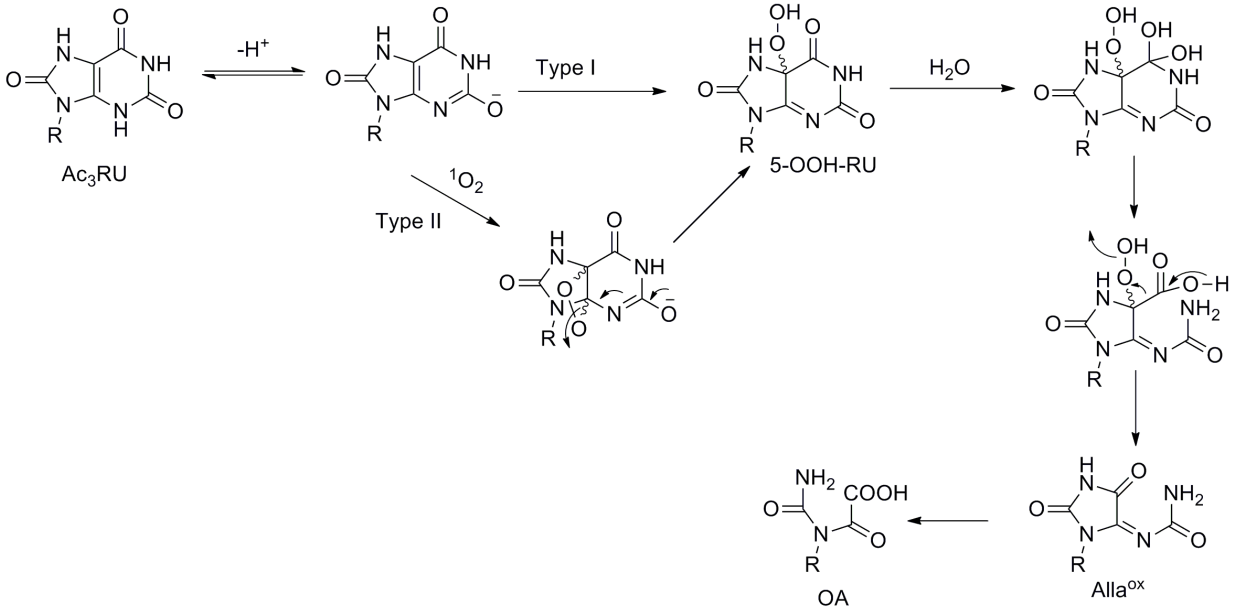

Figure 6.6. Proposed mechanism for the photosensitized oxidations of Ac_3RU

RU gave the same products as Type I oxidation. This suggests that the 5-OOH-RU intermediate must be formed at some stage. As for OG oxidation (*28*), singlet oxygen most likely adds to the C4-C5 double bond of RU to form the dioxetane intermediate. At pH 7, RU exists as the anion RU^- and the negative charge at on O2 may force the dioxetane to decompose via C4-O bond breakage to form the superoxide intermediate 5-OOH-RU (Figure 6.6). This is totally different from OG oxidation where the analogous dioxetane was preferably decomposed via the O-O and the C4-C5 bonds breakdown to generate the nine-member ring intermediate (*28*).

Conclusions

The oxidation of the nucleoside 9-β-D-ribofuranosyl uric acid has been investigated with various oxidants to understand how the pathways and products differ from those of the free base uric acid. Previously, oxidation of uric acid alone was shown to lead principally to a C5 oxidation pathway producing allantoin as the major product and spirodihydantoin as a trace product (*46*) . In this study, introduction of a ribosyl group at N9 of uric acid was found to alter the product composition. Urea, allantoin, HICA amide and caffolide were identified as the products of ribofuranosyl uric acid oxidation by one-electron oxidants at pH 7, while oxidized allantoin is the major product of the photosensitized oxidations. In comparing the various oxidation pathways of uric acid nucleoside and OG, the C4 reactivity of the 5-hydroxy common intermediates was shown to play an important role in the formation of the various degradation products. The presence of an oxo group at C2 was also found to have a dramatic effect on the reactivity of intermediates in the photosensitized oxidation pathways. These oxidation products of

uric acid nucleoside may be potentially mutagenic lesions derived from 8-oxoguanosine under oxidative conditions that include deamination. A better understanding of these lesions in the context of 8-oxoguanosine oxidation in DNA is part of our continuing investigations.

Experimental

Materials. Guanosine hydrate, 4-dimethylaminopyridine were purchased from Acros, Br_2 from Fisher Scientific, benzyl alcohol and Pd (10% on activated carbon) from Aldrich, Na from Mallinckrodt and $H_2{}^{18}O$ (>97% purity) from Icon. All other reagents were used at highest purity level commercially available. 9-β-D-ribofuranosyl uric acid was synthesized following a published procedure (*50*).

Synthesis of 2',3',5'-tri-O-acetyl-9-β-D-ribofuranosyl uric acid (Ac_3RU). To a suspension of 9-β-D-ribofuranosyl uric acid (100 mg, 0.33 mmol) in acetonitrile (5 mL) were added DMAP (3 mg, 0.025 mmol), Et_3N (0.18 mL, 1.35 mmol), and anhydride acetic acid (0.11 mL, 1.2 mmol). The reaction mixture was stirred for 1 h at room temperature and the solvent was evaporated under vacuum. The oily residue was purified by flash column chromatography to yield 127 mg (0.30 mmol, 91%) of product. ^{1}H NMR (300 MHz, DMSO-d_6) δ (ppm): 10.89 (m, 3H), 5.81 (m, 2H), 5.45 (m, 1H), 4.34-4.37 (m, 1H), 4.09-4.20 (m, 2H), 2.01-2.09 (3s, 9H). HRMS: Calcd for $C_{16}H_{18}N_4O_{10}Na$ 449.0921, found 449.0923.

Oxidation of Ac_3RU with Na_2IrCl_6 or $K_3Fe(CN)_6$ at different pHs. In a final volume of 240 μL of 75 mM NaP_i buffer, Ac_3RU (0.3 mM) was incubated with Na_2IrCl_6 (0.6 mM) or $K_3Fe(CN)_6$ (0.6 mM) at room temperature. The reaction mixture was

analyzed by reversed phase HPLC using a Varian C18 (5 μm, 250X4.6 mm) column with 5% solvent B for the first 5 min followed by a gradient to 65% solvent B in 30 min (solvent A: 0.1% TFA in water, solvent B: 0.1% TFA in acetonitrile). The flow rate was 1 mL/min and the detector was set at 220 nm.

$H_2{}^{18}O$ labeling experiment. 40μL of Ac_3RU (0.3 mM) in 75 mM NaP_i buffer and 8 μL of Na_2IrCl_6 (3 mM) were lyophilized to dryness and then redissolved in $H_2{}^{18}O$. The two solutions were mixed and analyzed by LC-ESI-MS after 2 h.

Photosensitized oxidation of Ac_3RU. A 200-μL sample of 75 mM NaP_i buffer containing Ac_3RU (0.3 mM) and Rose Bengal (RB**)** (30 μM) or methylene blue (MB) (30 μM) or riboflavin (Rf) (30 μM) was irradiated with a sunlamp (λ>500 nm) for 2 h at room temperature. The sensitizers were removed after passing down a NAP-5 column (GE healthcare), and the reaction mixture was analyzed by reversed phase HPLC. The method was 5% solvent B for the first 5 min followed by a gradient to 65% solvent B in 30 min (solvent A: 0.1% TFA in water, solvent B: 0.1% TFA in acetonitrile). The flow rate was 1 mL/min and the detector was set at 220 nm.

LC-ESI/MS analysis. Two analytical methods were used. In the first method, samples were analyzed by positive electrospray ionization (ESI) on a Micromass Quattro II tandem mass spectrometer equipped with a Zspray API source. Samples were diluted in acetonitrile and water (1:1) and 50 μL was introduced *via* a Waters Alliance 2690 Separations Module. A Waters 2487 Dual Absorbance Detector was placed in line between the Alliance 2690 Separations Module and the Zspray probe ion source. Chromatographic separation was accomplished using Phenomenex Luna C18 (3 μm, 150x2.0 mm) reversed phase column and initial solvent conditions of 95% solvent A

(0.1% TFA in water) and 5% solvent B (0.1% TFA in acetonitrile). After 5 min a linear gradient of 5% solvent B to 65% solvent B over 25 min was used. The flow rate was 0.2 mL/min, and UV spectra were recorded at 220 nm. The source and desolvation temperatures were 125 °C and 250 °C, respectively. The capillary voltage was set to 3.5 kV, sampling cone voltage to 35 V, and the extractor cone to 3V. The instrument was operated and data accumulated with Micromass Masslynx software (version 4.0).

In the second method, samples were analyzed by positive electrospray ionization (ESI) on a Waters LCT XE Premier TOF mass spectrometer equipped with a Zspray API source. Samples were diluted in acetonitrile and water (1:1) and 5 µL was introduced *via* a Waters Acquity Separations Module. A Waters Acquity PDA Detector was placed in line between the Acquity Separations Module and the Zspray probe ion source. Chromatographic separation was accomplished using Acquity UPLC BEH C18 (1.7 µm, 50X2.1mm) reversed phase column and initial solvent conditions of 95% solvent A (0.1% FA in water) and 5% solvent B (acetonitrile). After 1 min a linear gradient of 5% solvent B to 90% solvent B over 6 min was used. The flow rate was 0.6 mL/min, and UV spectra were recorded at 220 nm. The source and desolvation temperatures were 100 °C and 300 °C, respectively. The capillary voltage was set to 2.85 kV and the sampling cone voltage to 85 V. The instrument was operated and data accumulated with Micromass Masslynx software (version 4.1).

References

1. Shigenaga, M. K., Park, J.-W., Cundy, K. C., Gimeno, C. J., Ames, B. N., Lester, P., and Alexander, N. G. (1990). In vivo oxidative DNA damage: Measurement of 8-hydroxy-2'-deoxyguanosine in DNA and urine by high-performance liquid chromatography with electrochemical detection, *Methods. Enzymol. 186*, 521-530.

2. Muller, J., Duarte, V., Hickerson, R., and Burrows, C. (1998) Gel electrophoretic detection of 7,8-dihydro-8-oxoguanine and 7, 8- dihydro-8-oxoadenine via oxidation by Ir (IV), *Nucl. Acids Res. 26*, 2247-2249.

3. Neeley, W. L., and Essigmann, J. M. (2006) Mechanisms of formation, genotoxicity, and mutation of guanine oxidation products, *Chem. Res. Toxicol. 19*, 491-505.

4. Gimisis, T., and Cisma, C. (2006) Isolation, characterization, and independent synthesis of guanine oxidation products, *Eur. J. Org. Chem. 2006*, 1351-1378.

5. Burrows, C. J., and Muller, J. G. (1998) Oxidative nucleobase modifications leading to strand scission, *Chem. Rev. 98*, 1109-1152.

6. Caulfield, J. L., Wishnok, J. S., and Tannenbaum, S. R. (1998) Nitric oxide-induced deamination of cytosine and guanine in deoxynucleosides and oligonucleotides, *J. Biol. Chem. 273*, 12689-12695.

7. Suzuki, T., Yamaoka, R., Nishi, M., Ide, H., and Makino, K. (1996) Isolation and characterization of a novel product, 2'-deoxyoxanosine, from 2'-deoxyguanosine, oligodeoxynucleotide, and calf thymus DNA treated by nitrous acid and nitric oxide, *J. Am.Chem. Soc. 118*, 2515-2516.

8. Nguyen, T., Brunson, D., Crespi, C. L., Penman, B. W., Wishnok, J. S., and Tannenbaum, S. R. (1992) DNA damage and mutation in human cells exposed to nitric oxide in vitro, *Proc. Natl. Acad. Sci. 89*, 3030-3034.

9. Wink, D., Kasprzak, K., Maragos, C., Elespuru, R., Misra, M., Dunams, T., Cebula, T., Koch, W., Andrews, A., Allen, J., and et, a. (1991) DNA deaminating ability and genotoxicity of nitric oxide and its progenitors, *Science. 254*, 1001-1003.

10. Tamir, S., Burney, S., and Tannenbaum, S. R. (1996) DNA damage by nitric oxide, *Chem. Res. Toxicol. 9*, 821-827.

11. deRojas-Walker, T., Tamir, S., Ji, H., Wishnok, J. S., and Tannenbaum, S. R. (1995) Nitric oxide induces oxidative damage in addition to deamination in macrophage DNA, *Chem. Res. Toxicol. 8*, 473-477.

12. Delaney, S., Delaney, J. C., and Essigmann, J. M. (2007) Chemical and biological fingerprinting: Probing the properties of DNA lesions formed by peroxynitrite, *Chem. Res. Toxicol. 20*, 1718-1729.

13. Luo, W., Muller, J. G., Rachlin, E. M., and Burrows, C. J. (2000) Characterization of Spiroiminodihydantoin as a product of one-electron oxidation of 8-Oxo-7,8-dihydroguanosine, *Org. Lett. 2*, 613-616.

14. Yu, H., Niles, J. C., Wishnok, J. S., and Tannenbaum, S. R. (2004) Spirodihydantoin is a minor product of 5-hydroxyisourate in urate oxidation, *Org. Lett. 6*, 3417-3420.

15. Goyal, R. N., and Rastogi, A. (1997) Electrochemical and peroxidase catalysed oxidation of 9-β-D-ribofuranosyluric acid -5'-monophosphate, *J. Chem. Soc., Perkin Trans. 2.*, 2423-2429.

16. Goyal, R. N., Brajter-Toth, A., Besca, J. S., and Dryhurst, G. (1983) The electrochemical and perodidase-catalyzed redox chemistry of 9-β-D-ribofuranosyl uric acid, *J. Electroanal. Chem. 144*, 163-190.

17. Ames, B. N., Cathcart, R., Schwiers, E., and Hochstein, P. (1981) Uric acid provides an antioxidant defense in humans against oxidant- and radical-caused aging and cancer: a hypothesis, *Proc. Natl. Acad. Sci. 78*, 6858-6862.

18. Grootveld, M., and Halliwell, B. (1987) Measurement of allantoin and uric acid in human body fluids. A potential index of free-radical reactions in vivo? *Biochem. J. 243*, 803-808.

19. Montaña, M. P., Massad, W. A., Amat-Guerri, F., and García, N. A. (2008) Scavenging of riboflavin-photogenerated oxidative species by uric acid, xanthine or hypoxanthine: A kinetic study, *J. Photochem.Photobiol A: Chemistry. 193*, 103-109.

20. Newburger, J., Combs, A. B., and Hsu, T.-F. (1977) *In vitro* photodecomposition of uric acid in presence of riboflavin II, *J. Pharm. Sciences. 66*, 1561-1564.

21. Kanofsky, J. R. (1990) Quenching singlet oxygen by human plasma, *Photochem. Photobiol. 51*, 299-303.

22. Dunlap, W. C., Yamamoto, Y., Inoue, M., Kashiba-Iwatsuki, M., Yamaguchi, M., and Tomita, K. (1998) Uric acid photo-oxidation assay: in vitro comparison of sunscreening agents, *Int. J. Cosm. Sci. 20*, 1-18.

23. Murgida, D. H., Aramendía, P. F., and Erra-Balsells, R. (1998) Benzophenone-photosensitized reactions of xanthinic compounds. A mechanistic study, *Photochem. Photobiol. 67*, 487-494.

24. Murgida, D. H., Aramendía, P. F., and Balsells, R. E. (1998) Photosensitized oxidation of oxopurines by Rose Bengal, *Photochem. Photobiol. 68*, 467-473.

25. Matsuura, T., and Saito, I. (1968) Photo-induced reactions. XV. The nature of peroxide intermediates in the photosensitized oxygenation of purine derivatives, *Tetrahedron Letters 9*, 3273-3276.

26. Matsuura, T., and Saito, I. (1969) A zwitterionic peroxide intermediate in the photosensitized oxygenation of fully N-alkylated uric acids, *Tetrahedron. 25*, 549-556.

27. Luo, W., Muller, J. G., and Burrows, C. J. (2001) The pH-Dependent role of superoxide in riboflavin-catalyzed photooxidation of 8-Oxo-7,8-dihydroguanosine, *Org. Lett. 3*, 2801-2804.

28. Raoul, S., and Cadet, J. (1996) Photosensitized reaction of 8-Oxo-7,8-dihydro-2'-deoxyguanosine; Identification of 1-(2-Deoxy-b-d-erythro-pentofuranosyl) cyanuric acid as the major singlet Oxygen oxidation product, *J. Am.Chem. Soc. 118*, 1892-1898.

29. Sheu, C., and Foote, C. S. (1995) Photosensitized oxygenation of a 7,8-dihydro-8-oxoguanosine derivative. formation of dioxetane and hydroperoxide intermediates, *J. Am.Chem. Soc. 117*, 474-477.

30. Foote, C. S. (1991) Definition of type I and type II photosensitized oxidation, *Photochem. Photobiol. 54*, 659.

31. Wasserman, H. H. (1988) Recent applications of the use of singlet oxygen in the synthesis of compounds of biological interest *Studies in Org. Chem. 33*, 3-11.

32. Goyal, R. N., Brajter-Toth, A., Besca, J. S., and Dryhurst, G. (1983) The electrochemical and peroxidase-catalyzed redox chemistry of 9-β-D-ribofuranosyl uric acid, *J. Electroanal. Chem. 144*, 163-190.

33. Subramanian, P., Heeg, M. J., and Dryhurst, G. (1986) Electrochemical oxidation of 1,3,7,9-tetramethyluric acid, *J. Electroanal. Chem. 197*, 279-304.

34. Tyagi, S., and Dryhurst, G. (1987) Electrochemical oxidation of 9-β-D-ribofuranosyl uric acid in basic solution, *J. Electroanal. Chem. 223*, 119-141.

35. Goyal, R. N., and Rastogi, A. (1997) Electrochemical and peroxidase catalysed oxidation of 9-β-D-ribofuranosyluric acid 5'-monophosphate, *J. Chem. Soc., Perkin Trans. 2.*, 2423-2429.

36. Niles, J. C., Wishnok, J. S., and Tannenbaum, S. R. (2004) Mass spectrometric identification of 4-hydroxy-2,5-dioxo-imidazolidine-4-carboxylic acid during

oxidation of 8-Oxoguanosine by peroxynitrite and $KHSO_5/CoCl_2$, *Chem. Res. Toxicol. 17*, 1501-1509.

37. Poje, M., Palkovic, A., and Perina, I. (1985) Key intermediates in the caffolide pathway for degradation of uric acid, *Tetrahedron. 41*, 4681-4684.

38. Kahn, K., Serfozo, P., and Tipton, P. A. (1997) Identification of the true product of the urate oxidase reaction, *J. Am.Chem. Soc. 119*, 5435-5442.

39. Ye, Y., Muller, J. G., Luo, W., Mayne, C. L., Shallop, A. J., Jones, R. A., and Burrows, C. J. (2003) Formation of 13C-, 15N-, and 18O-labeled guanidinohydantoin from guanosine oxidation with singlet oxygen. Implications for structure and mechanism, *J. Am.Chem. Soc. 125*, 13926-13927.

40. Goyal, R. N., Thankachan, P. P., and Jain, N. (2000) Further insights into electrooxidation of N-methyl uric acids and correlation of oxidation potentials with Frontier MO energies, *Bull. Chem. Soc. Jpn. 73*, 1515-1524.

41. Modrid, N., Poje, M., and Gojmerac-Ivsi'k, A. (1994) The structure of a $C_5H_4N_40_4$ species trapped by silylation in peroxidase mediated uricolysis. A reactive ring-contraction to spirodihydantoin, *Bioorg. Med. Chem. Lett. 4*, 1685-1686.

42. Chworos, A., Coppel, Y., Dubey, I., Pratviel, G., and Meunier, B. (2001) Guanine oxidation: NMR characterization of a dehydro-guanidinohydantoin residue generated by a 2e-oxidation of d(GpT),, *J. Am. Chem. Soc. 123*, 5867-5877.

43. Vialas, C., Claparols, C., Pratviel, G., and Meunier, B. (2000) Guanine oxidation in double-stranded DNA by Mn-TMPyP/KHSO5: 5,8-Dihydroxy-7,8-dihydroguanine residue as a key precursor of imidazolone and parabanic acid derivatives, *J. Am. Chem. Soc. 122*, 2157-2167.

44. Vialas, C., Pratviel, G., Claporols, C., and Meunier, B. (1998) Efficient oxidation of 2'deoxyguanosine by Mn-TMPyP/$KHSO_5$ to imidazolone without formation of 8-oxo-dG, *J. Am. Chem. Soc. 120*, 11548-11553.

45. Luo, W., Muller, J. G., Rachlin, E. M., and Burrows, C. J. (2001) Characterization of hydantoin products from one-electron oxidation of 8-Oxo-7,8-dihydroguanosine in a nucleoside model, *Chem. Res. Toxicol. 14*, 927-938.

46. Poje, M., and Sokolic-Maravic, L. (1986) The mechanism for the conversion of uric acid into allantoin and dehydro-allantoin, *Tetrahedron. 42*, 747-751.

47. Foote, C. S. (1991) Definition of Type I and Type II photosensitized oxidations, *Photochem. Photobiol. 54*, 659-659.

48. Boussicault, F., and Robert, M. (2008) Electron transfer in DNA and in DNA-related biological processes. Electrochemical insights, *Chem. Rev. 108*, 2622-2645.

49. Forrest, H. S., Hatfield, D., and Lagowski, J. M. (1961) Uric acid riboside? Part I. Isolation and reinvestigation of the structure., *J. Chem. Soc.*, 963-968.

50. Holmes, R. E., and Robins, R. K. (1965) Purine nucleosides. IX. The synthesis of 9-β-D-ribofuranosyl uric acid and other related 8-substituted purine ribonucleosides, *J. Am.Chem. Soc. 87*, 1772-1776.